

พอลิเมอร์คอมพอสิตนำไฟฟ้าของพอลิสไตรีนและพอลิ(3,4-เอทิลีนไดออกซีไทโอฟีน)

เตรียมโดยอเล็กโทรสปีนิงและพอลิเมอไรเซชันกระตุ้นด้วยความร้อน

นายณรงค์ แก้วอ่อน

วิทยานิพนธ์นี้เป็นส่วนหนึ่งของการศึกษาตามหลักสูตรปริญญาวิทยาศาสตรมหาบัณฑิต

สาขาวิชาปิโตรเคมีและวิทยาศาสตร์พอลิเมอร์

คณะวิทยาศาสตร์ จุฬาลงกรณ์มหาวิทยาลัย

ปีการศึกษา 2552

ลิขสิทธิ์ของจุฬาลงกรณ์มหาวิทยาลัย

CONDUCTING POLYMER COMPOSITES OF POLYSTYRENE AND  
POLY(3,4-ETHYLENEDIOXYTHIOPHENE) PREPARED BY  
ELECTROSPINNING AND HEAT-ACTIVATED POLYMERIZATION

Mr. Narong Keaw-on

A Thesis Submitted in Partial Fulfillment of the Requirements  
for the Degree of Master of Science Program in Petrochemistry and Polymer Science  
Faculty of Science  
Chulalongkorn University  
Academic Year 2009  
Copyright of Chulalongkorn University

Thesis Title            CONDUCTING POLYMER COMPOSITES OF POLYSTYRENE  
AND POLY(3,4-ETHYLENEDIOXYTHIOPHENE) PREPARED  
BY ELECTROSPINNING AND HEAT-ACTIVATED  
POLYMERIZATION  
By                         Mr. Narong Keaw-on  
Field of Study         Petrochemistry and Polymer Science  
Thesis Advisor        Assistant Professor Voravee P. Hoven, Ph.D.  
Thesis Co-advisor    Assistant Professor Yongsak Sritana-anant, Ph.D.

---

Accepted by the Faculty of Science, Chulalongkorn University in Partial  
Fulfillment of the Requirements for the Master's Degree

.....Dean of the Faculty of Science  
(Professor Supot Hannongbua, Dr.rer.nat.)

THESIS COMMITTEE

.....Chairman  
(Associate Professor Supawan Tantayanon, Ph.D.)

.....Thesis Advisor  
(Assistant Professor Voravee P. Hoven, Ph.D.)

.....Thesis Co-advisor  
(Assistant Professor Yongsak Sritana-anant, Ph.D.)

.....Examiner  
(Assistant Professor Varawut Tangpasuthadol, Ph.D.)

.....External Examiner  
(Assistant Professor Chidchanok Meechaisue, Ph.D.)

ณรงค์ แก้วอ่อน: พอลิเมอร์คอมพอสิตนำไฟฟ้าของพอลิสไตรีนและพอลิ(3,4-เอทิลีนไดออกซีไทโอฟีน) เตรียมโดยอิเล็กโทรสปินนิงและพอลิเมอไรเซชันกระตุ้นด้วยความร้อน (CONDUCTING POLYMER COMPOSITES OF POLYSTYRENE AND POLY(3,4-ETHYLENEDIOXYTHIOPHENE) PREPARED BY ELECTRO SPINNING AND HEAT-ACTIVATED POLYMERIZATION)

อ. ที่ปรึกษาวิทยานิพนธ์หลัก: ผศ.ดร. วรวิทย์ โยเว่น: อ. ที่ปรึกษาวิทยานิพนธ์ร่วม: ผศ.ดร. ยงศักดิ์ ศรีธนาอนันต์, 101 หน้า

ฟิล์มพอลิเมอร์คอมพอสิตนำไฟฟ้าที่มีองค์ประกอบของพอลิ(3,4-เอทิลีนไดออกซีไทโอฟีน) เตรียมได้จากการทำปฏิกิริยาพอลิเมอไรเซชันในวัฏภาคของแข็งของ 2,5-ไดโบรโม-3,4-เอทิลีนไดออกซีไทโอฟีนในเมทริกซ์ของพอลิสไตรีนหรือซัลโฟเนตพอลิสไตรีน เริ่มจากการเตรียมแผ่นไฟเบอร์บางด้วยอิเล็กโทรสปินนิงของสารละลายผสมระหว่าง 2,5-ไดโบรโม-3,4-เอทิลีนไดออกซีไทโอฟีนและพอลิเมอร์ลงบนแผ่นกระจก หลังจากการกำจัดตัวทำละลายแล้วพอลิเมอไรเซชันในวัฏภาคของแข็งของผลึก 2,5-ไดโบรโม-3,4-เอทิลีนไดออกซีไทโอฟีนที่ฝังตัวในพอลิเมอร์เมทริกซ์เกิดขึ้นได้โดยให้ความร้อนที่ 60-80 องศาเซลเซียส ซึ่งเป็นอุณหภูมิที่ต่ำกว่าอุณหภูมิคล้ายแก้วของพอลิเมอร์และอุณหภูมิหลอมเหลวของ 2,5-ไดโบรโม-3,4-เอทิลีนไดออกซีไทโอฟีน แผ่นฟิล์มคอมพอสิตสีน้ำเงินเข้มที่มีพอลิ(3,4-เอทิลีนไดออกซีไทโอฟีน)เกิดขึ้นผ่านปฏิกิริยาการกำจัดโบรมีนและการค้ำพลัง จากการทดลองพบว่าจำเป็นต้องมีการกอดักระหว่างการให้ความร้อนเพื่อทำให้ได้การกระจายที่ดีของอนุภาคนาโนเล็กกว่าไมครอนของพอลิ(3,4-เอทิลีนไดออกซีไทโอฟีน)ในพอลิเมอร์เมทริกซ์ จากการใช้มิเตอร์วัดค่าการนำไฟฟ้าแบบสี่หัวพบว่าแผ่นฟิล์มคอมพอสิตมีค่าการนำไฟฟ้าสูงถึง 13.24 ซีเมนซ์/เซนติเมตร ซึ่งเป็นค่าที่เทียบเท่ากับค่าการนำไฟฟ้าของพอลิ(3,4-เอทิลีนไดออกซีไทโอฟีน)ที่เตรียมผ่านปฏิกิริยาพอลิเมอไรเซชันในวัฏภาคของแข็งโดยปราศจากพอลิเมอร์เมทริกซ์ นอกจากนี้ยังทำการพิสูจน์เอกลักษณ์ของพอลิ(3,4-เอทิลีนไดออกซีไทโอฟีน)ที่สังเคราะห์ได้ด้วยอิเล็กโทรสปินนิงเรโซแนนซ์สเปกโตรเมทรี, ฟลูออโรทรานส์ฟอร์มมามานสเปกโตรเมทรี, เอกซ์เรย์ดิฟแฟรกชัน, ดิฟเฟอเรนเชียลสแกนนิ่งแคลอริเมทรี และเทอร์โมกราวิเมทริกอะแนไลซิส

สาขาวิชา...ปิโตรเคมีและวิทยาศาสตร์พอลิเมอร์...ลายมือชื่อนิสิต.....  
ปีการศึกษา.....2552.....ลายมือชื่อ อ.ที่ปรึกษาวิทยานิพนธ์หลัก.....  
ลายมือชื่อ อ.ที่ปรึกษาวิทยานิพนธ์ร่วม.....

# # 5072265223: MAJOR PETROCHEMISTRY AND POLYMER SCIENCE  
 KEYWORDS: PEDOT, ELECTROSPINNING, CONDUCTING POLYMER  
 COMPOSITES, SOLID STATE POLYMERIZATION

NARONG KEAW-ON: CONDUCTING POLYMER COMPOSITES OF  
 POLYSTYRENE AND POLY(3,4-ETHYLENEDIOXYTHIOPHENE)  
 PREPARED BY ELECTROSPINNING AND HEAT-ACTIVATED  
 POLYMERIZATION. THESIS ADVISOR: ASST. PROF. VORAVEE P.  
 HOVEN, Ph.D., THESIS CO-ADVISOR: ASST. PROF. YONGSAK  
 SRITANA-ANANT, Ph.D., 101 pp

Conducting polymer composite films containing poly(3,4-ethylenedioxy thiophene) (PEDOT) was prepared by solid state polymerization (SSP) of 2,5-dibromo-3,4-ethylenedioxythiophene (DBEDOT) in the presence of polystyrene (PS) or sulfonated polystyrene (SPS) matrix. A thin fiber mat was first fabricated by electrospinning a solution mixture of polymer matrix (PS or SPS) and DBEDOT on glass slides. After the solvent was removed, the solid state polymerization of the DBEDOT crystals embedded in the polymer matrix was then induced by heating at 60-80 °C, the temperature below the glass transition temperature of the polymer matrix and the melting temperature of DBEDOT. A dark blue composite film containing PEDOT was then formed through debromination and coupling. It was found that compression during heating was necessary to produce well dispersed sub-micron PEDOT in the polymer matrix. As measured by four-point probe conductometer, the conductivity of the composite film can reach as high as 13.24 S/cm, the value equivalent to the conductivity of the pure PEDOT also generated by SSP in the absence of polymer matrix. The characteristics of the synthesized PEDOT were also determined by electron spin resonance spectrometry, fourier-transform raman spectrometry, x-ray diffraction, differential scanning calorimetry, and thermogravimetric analysis.

Field of study: Petrochemistry and Polymer Science Student's signature.....

Academic year: 2009 Advisor's signature.....

Co-advisor's signature.....

## ACKNOWLEDGEMENTS

My utmost gratitude goes to my thesis advisors, Assist. Prof. Voravee P. Hoven and Assist. Prof. Yongsak Sritana-anant, for their expertise, kindness, support, and most of all, for their patience during the course of research including completing this thesis.

I would like to thank the Center for Petroleum, Petrochemicals, and Advanced Materials from Chulalongkorn University, and Science and Technology Research Grant from the Thailand Toray Science Foundation for financial support.

I am sincerely grateful to the members of the thesis committee, Assoc. Prof. Supawan Tantayanon, Assist. Prof. Varawut Tangpasuthadol, and Assist. Prof. Chidchanok Meechaisue for their valuable comments and suggestions.

Moreover, I would like to thank Prof. Pitt Supaphol for his valuable advices especially on electrospinning. I gratefully acknowledge the members of VP group and the research groups on the fourteenth floor, Mahamakut building for their companionship and friendship. Finally, I am forever indebted to my parents and family members for their encouragement and understanding throughout the entire study.

# CONTENTS

	Page
ABSTRACT IN THAI.....	iv
ABSTRACT IN ENGLISH.....	v
ACKNOWLEDGEMENTS.....	vi
CONTENTS.....	vii
LIST OF FIGURES.....	x
LIST OF TABLES.....	xiv
LIST OF SCHEMES.....	xv
LIST OF ABBREVIATION.....	xvi
CHAPTER I INTRODUCTION.....	1
1.1 Statement of the problem.....	1
1.2 Objectives.....	2
1.3 Scope of investigation.....	2
CHAPTER II THEORY AND LITERATURE REVIEW.....	4
2.1 Conjugated polymers: organic semiconductors .....	4
2.2 Effect of doping and charge transfer.....	9
2.3 Effective conjugation length (ECL).....	13
2.4 Organic electronics.....	14
2.5 Advantages and drawbacks of organic electronics.....	16
2.6 Fabrication technologies .....	17
2.7 Poly (3,4-ethylenedioxythiophen) (PEDOT).....	18
2.8 Excellent characteristics of PEDOT .....	20
2.9 Solid state synthesis of PEDOT .....	21
2.10 Applications of PEDOT .....	23
2.11 PEDOT composites.....	25
2.12 Electrospinning process.....	29

	Page
CHAPTER III EXPERIMENTAL.....	32
3.1 Materials.....	32
3.2 Equipments.....	32
3.2.1 Nuclear Magnetic Resonance (NMR) Spectrometer .....	32
3.2.2 Fourier-Transform Infrared Spectrometer (FT-IR).....	33
3.2.3 Surface Profile Measuring System.....	33
3.2.4 Scanning Electron Microscopy (SEM).....	33
3.2.5 Differential Scanning Calorimetry (DSC).....	33
3.2.6 Thermo Gravimetric Analysis (TGA).....	33
3.2.7 X-ray Diffractometer (XRD).....	34
3.2.8 Electron Spin Resonance Spectrometer (ESR).....	34
3.2.9 Fourier-Transform Raman Spectrometer (FT-Raman).....	34
3.2.10 Four-Point Probe Conductometer (FPP).....	34
3.3 Methods.....	35
3.3.1 Synthesis of 2,5-dibromo-3,4-ethylenedioxy thiophene (DBEDOT).....	35
3.3.2 Synthesis of sulfonated polystyrene (SPS).....	35
3.3.3 Preparation of PEDOT-containing composite films.....	36
CHAPTER IV RESULTS AND DISCUSSION.....	39
4.1 Synthesis of 2,5-dibromo-3,4-ethylenedioxythiophene (DBEDOT) and sulfonated polystyrene (SPS).....	39
4.1.1 Synthesis of 2,5-dibromo-3,4-ethylenedioxy thiophene (DBEDOT).....	39
4.1.2 Synthesis of sulfonated polystyrene (SPS).....	42



	Page
4.2 Preparation of DBEDOT/polymer composite fiber mats.....	47
4.3 Preparation and conductivity of PEDOT/polymer composite films...	51
4.3.1 Effect of compression.....	51
4.3.2 Effect of temperature and DBEDOT/polymer weight ratio.....	55
4.3.3 Effect of polymer matrix, solvent, and additive....	57
4.3.4 Effect of storage time.....	59
4.4 Physical characteristics of PEDOT-containing polymer composite films.....	60
CHAPTER V CONCLUSION AND SUGGESTION.....	70
REFERENCES.....	72
APPENDICES.....	84
APPENDIX A.....	85
APPENDIX B.....	91
VITAE.....	101

## LIST OF FIGURES

Figure	Page
2.1 Conjugated polymers.....	4
2.2 Bonding in conducting conjugated polymers.....	5
2.3 Energy band gaps in materials.....	6
2.4 Chemical structures of some $\pi$ -conjugated polymers and their band gap energy .....	8
2.5 Calculated (frontier) energy levels of oligothiophenes with $n = 1-4$ and of polythiophene ( $E_g =$ band gap energy).....	9
2.6 Depictions of (a) neutral (undoped chain), (b) polaron, and (c) bipolaron.....	11
2.7 UV-VIS absorption spectra of PEDOT film on ITO during the oxidation process in 0.1 M TBAPF <sub>6</sub> -acetonitrile. The potential range is -1.0 to +0.6 V, scan rate 100 mV/s .....	13
2.8 A defect in polyacetylene and steric-induced structure twisting in poly(3-alkylthiophene).....	14
2.9 Random twisting of polythiophene.....	14
2.10 Conductivity of different materials.....	15
2.11 3,4-Ethylenedioxythiophene (EDOT) (a) and poly(3,4-ethylenedioxythiophene) (PEDOT) (b).....	19
2.12 Poly(3,4-ethylenedioxythiophene)/polystyrene sulfonic acid (PEDOT/PSS).....	24
2.13 Schematic diagram shows polymer nanofibers forming by electrospinning process.....	30
3.1 Schematic representation of electrospinning apparatus set-up.....	37
3.2 Schematic representation of the pressing of the DBEDOT/polymer fiber mats.....	38
4.1 <sup>1</sup> H-NMR spectra of EDOT and DBEDOT.....	41
4.2 Appearance of PS before (a) and after sulfonation: SPS A (b), SPS B (c), and SPS C (d).....	44

Figure	Page
4.3 <sup>1</sup> H-NMR spectra of PS, SPS A and SPS A after deuterium exchange.....	45
4.4 <sup>1</sup> H-NMR spectra of all SPS samples .....	46
4.5 FT-IR spectra of PS and SPS.....	47
4.6 SEM micrographs (at 2,000×) of as-spun PS fiber mat electrospun from 12% (w/v) PS in (a) THF, (b) mixed 1:1 (v/v) THF/DMF, and (c) DMF and as-spun SPS B fiber mat electrospun from 12% (w/v) SPS B in (d) THF, (e) mixed 1:1 THF/DMF, and (f) DMF.....	49
4.7 SEM micrographs (at 2,000×) of as-spun DBEDOT/PS composite fiber mats electrospun from a mixture containing 3:1 (w/w) DBEDOT/PS in (a) THF, (b) mixed 1:1 (v/v) THF/DMF, and (c) DMF.....	50
4.8 SEM micrographs (at 2,000×) of as-spun DBEDOT/SPS composite fiber mats electrospun from a mixture containing 3:1 (w/w) DBEDOT/SPS B in (a) DMF, (b) THF, and (c) mixed 1:1 (v/v) THF/DMF, and 3:1 DBEDOT/SPS A (w/w) in THF (d).....	51
4.9 Physical appearances of DBEDOT/PS composite fiber mats electrospun from a mixture containing 3:1 (w/w) DBEDOT/PS in DMF before SSP (a), after SSP at 70 °C for 40 h without (b) and with (c) pressing, and as a function of reaction time (d). SEM micrographs (at 2,000x) of PEDOT/PS composite film obtained after SSP at 70 °C for 40 h without (e) and with (f) pressing.....	52
4.10 SEM micrographs (at 30,000×) of PEDOT particles extracted from PEDOT/PS composite film prepared by SSP of the 3:1 (w/w) DBEDOT/PS fiber mats at 70 °C for 40 h with (a) and without (b) pressing.....	52
4.11 XRD diffractograms of (a) DBEDOT crystal, (b) controlled PEDOT, (c) electrospun PS fiber mat, (d) electrospun 3:1 (w/w) DBEDOT/PS fiber mat, PEDOT/PS composite film obtained from SSP of the 3:1 (w/w) DBEDOT/PS fiber mat electrospun from DMF solution without (e) and with (f) pressing.....	54

Figure	Page
4.12 Conductivity measured on the top and bottom side of the PEDOT/PS composite film prepared by SSP of the electrospun 3:1 (w/w) DBEDOT/PS fiber mats by heating at 70 °C for 40 h with pressing as a function of reaction time.....	55
4.13 XRD diffractograms of PEDOT/PS composite film prepared by SSP of the 3:1 (w/w) DBEDOT/PS fiber mat electrospun from DMF solution with pressing using different temperature for heat activation.....	56
4.14 Conductivity of PEDOT/PS composite film prepared by SSP of the 3:1 (w/w) DBEDOT/PS fiber mat electrospun from DMF solution with pressing as a function of storage time at ambient temperature.....	60
4.15 FT-Raman spectra of (a) PEDOT/PS, DMF, pressing, (b) PEDOT/PS, THF, pressing, (c) controlled PEDOT, (d) PEDOT/PS, DMF, non-pressing, and (e) PEDOT/SPS A, THF, pressing.....	61
4.16 FT-Raman spectra of (a) controlled PEDOT, (b) PS/PEDOT, DMF pressing, (c) PS/PEDOT, DMF, pressing, Eg, (d) PEDOT/PS, DMF, pressing, Py, (e) PS/PEDOT, DMF, non pressing, and (f) PEDOT/SPS A, THF, pressing.....	63
4.17 ESR of the PEDOT/polymer composite of PEDOT/PS, DMF, pressing (1a, 2a, 3a, and 5a), PEDOT/PS, DMF, non pressing (1b), PEDOT/PS, THF, pressing (2b, 4b), PEDOT/PS, DMF, pressing (3b), PEDOT/SPS, THF, pressing (4a), PEDOT/PS, DMF, pressing, Eg (5b), and PEDOT/PS, DMF, pressing, Py (5c).....	64
4.18 DSC thermograms of (a) PS pellet, (b) electrospun PS fiber mat, (c) as synthesized SPS A, (d) electrospun SPS A fiber mat, (e) electrospun DBEDOT/PS fiber mat, (f) PEDOT/PS composite film, non pressing, (g) controlled PEDOT, (h) PEDOT/PS composite film, pressing, and (i) PEDOT/SPS A composite film, pressing.....	67

Figure	Page
4.19 TGA thermograms of (a) PS pellet, (b) electrospun PS fiber mat, (c) as synthesized SPS A, (d) electrospun SPS A fiber mat, (e) electrospun DBEDOT/PS fiber mat, (f) PEDOT/PS composite film, non pressing, (g) controlled PEDOT, (h) PEDOT/PS composite film, pressing, and (i) PEDOT/SPS A composite film, pressing.....	69
A-1 Schematic representation of 4-point probe configuration.....	85
A-2 SEM (at 2000×) of as-spun PS fibers electrospun from 10%PS (w/v) solution in DMF (a) and THF (b).....	88
A-3 SEM (at 500×) of as-spun SPS B fibers electrospun from 12%SPS B (w/v) solution in DMF (a), mixed 1THF:1DMF (b), and THF (c).....	88
A-4 SEM (at 2000×) of PEDOT composites obtained after SSP.....	88
A-5 XRD diffractograms of raw material.....	89
A-6 XRD diffractograms of PEDOT/PS, pressing prepared by SSP of the DBEDOT/PS fiber mat by heating at 70 °C for a different period of time....	89
A-7 XRD diffractograms of PEDOT/PS, pressing prepared by SSP of the DBEDOT/PS fiber mat electrospun from different solution by heating at 70 °C for 40 h .....	89
A-8 XRD diffractograms of PEDOT/PS, pressing prepared by SSP of the DBEDOT/PS fiber mat electrospun from DMF solution by heating at 70 °C for 40 h after keeping for up to 50 days .....	90

## LIST OF TABLES

Table	Page
2.1 Conductivity data of PEDOT polymers.....	23
4.1 Solubility of DBEDOT.....	42
4.2 %DS Sulfonyl groups in SPS.....	46
4.3 Weight percentage of element of the PEDOT/PS composite film obtained by SEM analysis using EDS mode.....	53
4.4 Conductivity of the PEDOT/PS composite film prepared by SSP of the electrospun DBEDOT/PS fiber mat by heating for 40 h.....	56
4.5 Thickness and conductivity of the PEDOT/PS composite film prepared by SSP of the DBEDOT/PS fiber mat electrospun from different solution by heating at 70 °C for 40 h with pressing .....	59
4.6 Raman shift of the symmetric $C_{\alpha}=C_{\beta}$ stretching of PEDOT in the composite film.....	63
4.7 ESR data of the PEDOT/polymer composite film.....	65
A-1 Conductivity measured on the top side and the bottom side of the PEDOT/PS composite film (thickness of 55.24 $\mu\text{m}$ ) prepared by SSP of the electrospun 3:1 (w/w) DBEDOT/ PS fiber mats by heating at 70 °C for 40 h with pressing as a function of reaction time.....	86
A-2 Conductivity measured on the top side of the PEDOT composite film prepared by SSP of the electrospun 3:1 (w/w) DBEDOT/polymer matrix by heating at 70 °C for 40 h with pressing as a function of temperature, solvent, and additive.....	87

## LIST OF SCHEMES

Scheme	Page
2.1 Solid state polymerization of DBEDOT.....	22
3.1 Bromination of EDOT.....	35
3.2 Sulfonation of PS.....	35
3.3 Solid state polymerization of DBEDOT.....	38
4.1 Bromination via electrophilic aromatic substitution .....	40
4.2 Bromination mechanism via radical-based single electron transfer followed by aromatic substitution.....	40
4.3 Sulfonation of PS via electrophilic aromatic substitution.....	43
4.4 Acid-initiated coupling promotes chain growth but yields an unconjugated form of PEDOT in high substitution degree of SPS matrix.....	57
4.5 Conformation and resonance structure of PEDOT chain structure.....	62

## LIST OF ABBREVIATION

Br <sub>2</sub>	: bromine
°C	: degree celsius
CDCl <sub>3</sub>	: deuterated chloroform
CH <sub>3</sub> COOH	: acetic acid
cm	: centimeter
conc.	: concentrated
CPs	: conjugated polymers
DBEDOT	: 2,5-dibromo-3,4-ethylenedioxythiophene
DMF	: <i>N, N</i> -dimethylformamide
DSC	: differential scanning calorimetry
EDOT	: 3,4-ethylenedioxythiophene
Eg	: ethylene glycol
ESR	: electron spin resonance spectrometer
eq	: equivalent
FT-IR	: fourier-transform infrared spectrophotometer
FT-Raman	: fourier-transform raman spectrometer
g	: gram
h	: hour
HAP	: heat-activated polymerization
HOMO	: highest occupied molecular orbital
I <sub>2</sub>	: iodine
kV	: kilovoltage
LUMO	: lowest unoccupied molecular orbital
min	: minute
mL	: milliliter
mm	: millimeter
M <sub>w</sub>	: weight average molecular weight
N/A	: not available
NaHCO <sub>3</sub>	: sodium hydrogen carbonate



NBS	: <i>N</i> -bromosuccinimide
nm	: nanometer
NMR	: nuclear magnetic resonance spectroscopy
PEDOT	: poly(3,4-ethylenedioxythiophene)
ppm	: parts per million (unit of chemical shift)
PS	: polystyrene
Py	: pyridine
rpm	: revolutions per minute
S	: seimens
SEM	: scanning electron microscopy
SPS	: sulfonated polystyrene
SSP	: solid state polymerization
$T_g$	: glass transition temperature
$T_m$	: melting temperature
TGA	: thermogravimetric analysis
THF	: tetrahydrofuran
UV	: ultraviolet
w/v	: weight by volume
XRD	: x-ray diffractometer
$2\theta$	: 2 theta
$\delta$	: chemical shift

# CHAPTER I

## INTRODUCTION

### 1.1 Statement of the Problem

Poly(3,4-ethylenedioxythiophene) (PEDOT) is one of polythiophene derivatives that has received much attention in recent years due to its unique electrical properties. It combines a low oxidation potential and moderate band gap with good stability in the oxidized state. In addition to a high conductivity (500 S/cm in the electrochemical doped state), PEDOT is found to be highly transparent in thin, oxidized films. As a result, PEDOT derivatives are now utilized in several industrial applications including antistatic coatings for photographic films and hole conducting material in organic/polymer-based light-emitting diodes.

PEDOT is commercially available in the form of latex of which dispersion in aqueous is facilitated by negatively charged poly(styrene sulfonate) which also acts as a dopant. The PEDOT synthesis is conventionally confined to chemical or electrochemical oxidation of polymer solution. As a consequence, defect sites and a relatively low degree of intermolecular order limit the number of possible applications. Until recently, it has been discovered by chance that blue-black crystals of 2,5-dibromo-3,4-ethylenedioxythiophene (DBEDOT) can undergo solid state polymerization (SSP) through debromination and coupling. Without the use of initiators or catalysts, SSP could give rise to a nearly defect-free and highly ordered bromine-doped PEDOT with high conductivity (20-80 S/cm). The SSP can be accelerated by heat treatment.

Electrospinning is a simple but versatile method to produce continuous fibers having a size ranging from micrometer to nanometer. The method employs electrostatic forces to stretch a polymer jet and make superfine fibers. Numerous polymeric materials have been electrospun into continuous and uniform fibers. It has been shown that charge density of the electrified jet, surface tension, and viscoelasticity of the polymer solution play important roles both in making the production of fibers possible and in controlling the size and uniformity of the fibers.

Recent work has demonstrated a potential of the electrospinning process for introducing composite fibers of conducting polymer and insulating polymer such as polypyrrole (PPy) grown on poly(methyl methacrylate) (PMMA) fibers, PEDOT grown on PMMA or PS fibers, PPy-polyacrylonitrile (PAN) composite fibers, poly-3-hexylthiophen(P3HT)-polyethylene oxide (PEO) composite fibers, poly(*o*-toluidine)-PS composite fiber, poly(2-methoxy-5-(2'-ethylhexyloxy)-1,4-phenylene vinylene) (MEH-PPV)-PS composite fibers.

Taking advantages of DBEDOT solubility in many common organic solvents together with its competency of undergoing SSP, we attempted to produce conductive polymer composites containing PEDOT by SSP of DBEDOT embedded in a preformed insulating polymer matrix film after thermal treatment. The fabrication process based on solution casting, however, yielded the composite films with non-uniform conductivity due to the inhomogeneous distribution of the PEDOT in the matrix caused by phase incompatibility between the polar PEDOT and the non-polar matrix. Herein, we propose to use electrospinning as an alternative fabrication method. The rapid solvent evaporation and solidification of the fiber mat electrospun from the mixed solution between the desired matrix, and DBEDOT should not allow enough time for the DBEDOT to phase separate from the matrix and yield thin conductive composite fiber mat with improved PEDOT distribution and conductivity after the heat treatment.

## 1.2 Objectives

To prepare conductive polymer composites containing 3,4-polyethylenedioxythiophene (PEDOT) using electrospinning and heat-activated polymerization (HAP) of 2,5-dibromo-3,4-ethylenedioxythiophene (DBEDOT).

## 1.3 Scope of Investigation

The stepwise investigation was carried out as follows:

1. Literature survey for related research work
2. To synthesize and characterize 2,5-dibromo-3,4-ethylenedioxythiophene (DBEDOT)

3. To synthesize and characterize sulfonated polystyrene (SPS) by sulfonation of polystyrene
4. To prepare DBEDOT/polymer composite films by electrospinning of mixed solution between DBEDOT and polymer. Parameters to be investigated in this step are as follow:
  - Polymer matrix i.e. polystyrene (PS), sulfonated polystyrene (SPS)
  - Concentration of polymer matrix (10 and 12 % w/v)
  - DBEDOT: polymer weight ratio (2:1 and 3:1)
  - Solvent type (DMF, THF and mixed solvent of DMF and THF (1:1))
5. To prepare PEDOT/polymer composite films by heat-activated polymerization. Parameters to be investigated in this step are as follow:
  - Polymerization time (8, 16, 24, 32, 40, 48, and 56 h)
  - Polymerization temperature (60, 70, and 80 °C)
  - Compression during HAP
6. To determine the conductivity of the PEDOT/ polymer composite films
7. To characterize PEDOT/ polymer composite films by x-ray diffraction (XRD), FT-Raman spectroscopy, thermogravimetric analysis (TGA), and differential scanning calorimetry (DSC)
8. To characterize the PEDOT that has been extracted from the composite films by scanning electron microscope (SEM), XRD, and FT-Raman spectroscopy
9. To investigate the effect of storage time on the conductivity of the PEDOT/ polymer composite films

## CHAPTER II

### THEORY AND LITERATURE REVIEW

#### 2.1 Conjugated polymers: organic semiconductors [1-3]

Conjugated polymers (CPs) are not insulators, but are classified as organic semiconductors. Conjugated polymers contain a backbone consisting of alternating single and double bonds between carbon-carbon, carbon-sulfur, or carbon-nitrogen atoms, creating an extended  $\pi$ -network. Electron movement within this  $\pi$ -framework is the source of conductivity, with respect to electronic energy levels, hardly differs from inorganic semiconductors. Both have their electrons organized in bands rather than in discrete levels and their ground state energy bands are either completely filled or completely empty. The band structure of a conjugated polymer originates from the interaction of the  $\pi$ -orbital of the repeating units throughout the chain. Figure 2.1 shows commonly known conjugated polymers that are conductive.

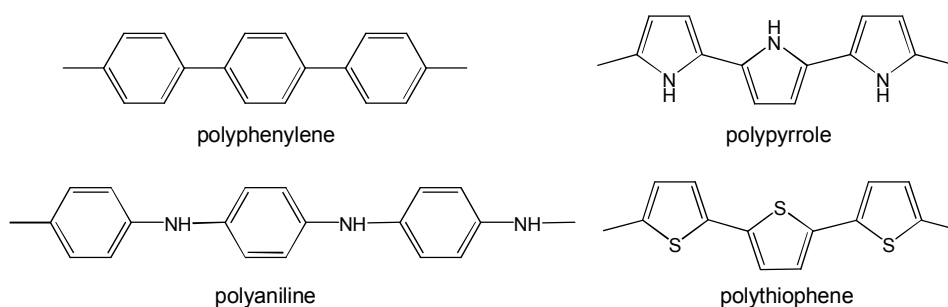


**Figure 2.1** Conjugated polymers.

Conducting and semiconducting organic materials with either electron (*n-type*) or hole transport (*p-type*) materials used in electronic applications have been rapidly developed and characterized. The bonding arrangement of the carbon atoms in the polymer backbone is the main reason for the characteristic electronic properties of tunable conductivity, electrochromism, electroluminescence and electroactivity [4].

The general character of conducting polymers is the presence of double bonds alternating with single bonds along the polymer chain, i.e. conjugated bonds. The electron configuration of the six electrons in a carbon atom (in its ground state) is  $1s^2 2s^2 2p^2$ . The electrons in the core orbital do not contribute to the chemical bonding. The s and p orbitals combine to form hybrid orbitals ( $sp^1$ ,  $sp^2$ , and  $sp^3$ ), depending upon the number of orbitals they combined, which result in triple, double, or single bond, respectively. In conjugated polymers, one 2s orbital pairs with the two 2p orbitals to form three  $sp^2$  hybrid orbitals, leaving one p orbital unhybridized. Two  $sp^2$  orbitals on each carbon atom form covalent bonds with neighboring carbon atoms; the remaining  $sp^2$  orbital normally forms a covalent bond with a hydrogen or side group. This is called  $\sigma$ -bond which has cylindrical symmetry around the internuclear axis [5]. The unhybridized  $p_z$  orbital side overlaps with the unhybridized  $p_z$  orbital on the neighboring carbon. This bond is called a  $\pi$ -bond, as is the bond arised from orbitals approaching side by side, off the internuclear axis shown in Figure 2.2. The  $sp^2$  hybrid orbitals are shown in light gray, and the unhybridized  $p_z$  orbitals in white. Electrons are represented by the dots. The two  $sp^2$  hybrid orbitals on the side extended in and out of the plane of the page.

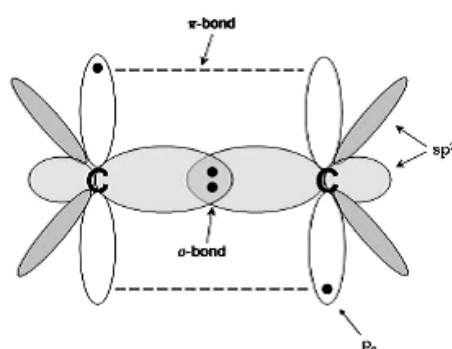


**Figure 2.2** Bonding in conducting conjugated polymers.

The electrons in the  $\pi$ -bonds are weakly bound and readily delocalized to another  $\pi$ -bond nearly as in the conjugated system. These delocalized  $\pi$ -electrons are the origin of conduction in these materials.

Analogous to semiconductors, the highest occupied band (originating from the HOMO of a single thiophene unit) is called the valence band, while the lowest unoccupied band (originating from the LUMO of a single thiophene unit) is called the conduction band. The difference in energy between these energy band levels is called the band gap energy or simply, band gap ( $E_g$ ) as shown in Figure 2.3. Generally speaking, because conducting polymers possess delocalized electrons in  $\pi$ -conjugated system along the whole polymeric chain, their conductivity is much higher than that of other polymers with no conjugated system. These latter non-conjugated polymers are usually known to be insulators.

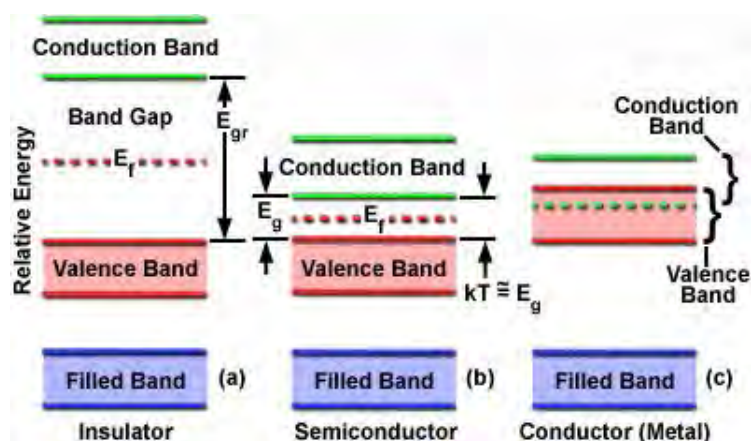


**Figure 2.3** Energy band gaps in materials.

The difference between  $\pi$ -conjugated polymers and metals is that in metals, the orbitals of the atoms overlap with the equivalent orbitals of their neighboring atoms in all directions to form molecular orbitals similar to those of isolated molecules. With  $N$  numbers of interacting atomic orbitals, there would be  $N$  molecular orbitals. In the metals or any continuous solid-state structures,  $N$  will be a very large number (typically  $10^{22}$  for  $1 \text{ cm}^3$  metal piece). With so many molecular orbitals spaced together in a given range of energies, they form an apparently continuous band of energies.

In insulators, the electrons in the valence band are separated by a large gap from the conduction band. However, in conductors like metals, the valence band

overlaps with the conduction band. And in semiconductors, there is a small enough gap between the valence and conduction bands that thermal or other excitations can bridge the gap. With such a small gap, the presence of a small percentage of a doping material can increase conductivity dramatically.

An important parameter in the band theory is the Fermi level, the top of the available electron energy levels at low temperature. The position of the Fermi level with relate to the conduction band is a crucial factor in determining electrical properties. The conductivity of the metal is due either to partly-filled valence or conduction band, or to the band gap being near zero, so that with any weak electric field the electrons easily redistribute. Electrons are excited to the higher energy bands and leave unfilled bands or “hole” at lower energy. Metals and conducting polymers exhibit opposite directions of conducting behavior as a function of temperature. For metallic materials, the conductivity increases as the temperature is lower (some of which become superconducting below certain critical temperature,  $T_c$ ) while it generally decreases with lowered temperature for polymeric semiconductors and insulators.

Since  $\pi$ -conjugated polymers allow virtually endless manipulation of their chemical structures, the control of the band gap of these semiconductors is a research issue of ongoing interest. This “band gap engineering” may give the polymer its desired electrical and optical properties. Reduction of the band gap to approximately zero is expected to afford an intrinsic conductor like metal. Examples of these  $\pi$ -conjugated polymers being intensively studied are shown in Figure 2.4.



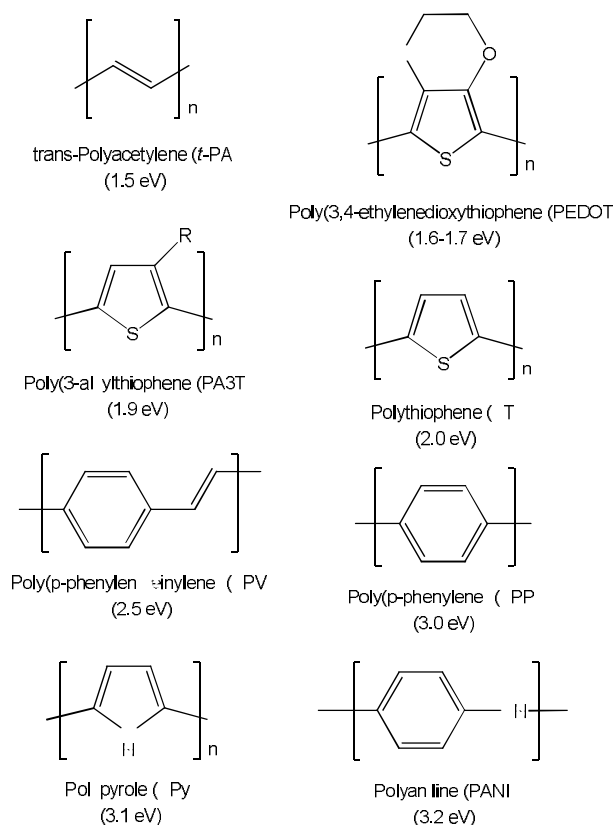


**Figure 2.4** Chemical structures of some  $\pi$ -conjugated polymers and their band gap energy [6].

Both conjugated conducting polymers and inorganic semiconductor electronic structure are very similar in nature. They have their electrons organized in bands rather than in discrete levels and their ground state energy bands are either completely filled or completely empty. The band structure of a conjugated polymer originates from the interaction of the  $\pi$ -orbitals of the repeating units throughout the chain. This is illustrated in Figure 2.5 where the calculated energy levels of oligothiophenes with  $n = 1-4$  and polythiophene are shown as a function of oligomer length. Addition of each new thiophene unit causes rehybridization of the energy levels yielding more and more sublevels until a point reached at which there are bands rather than discrete levels. The interaction between the  $\pi$ -electrons of neighboring molecules lead to a three-dimensional band structure.

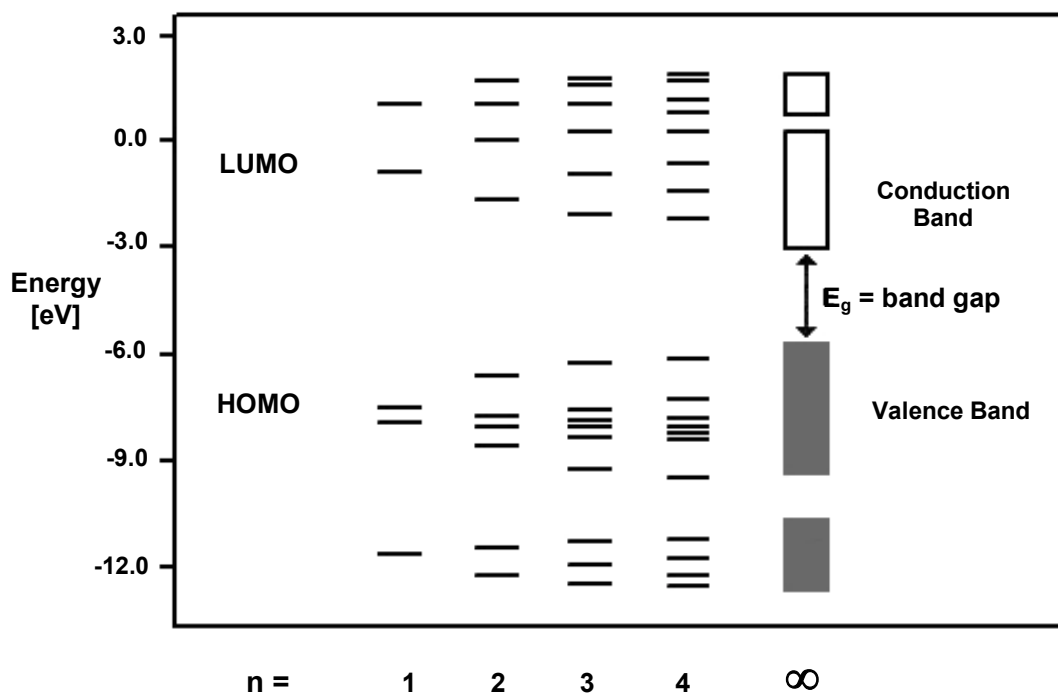


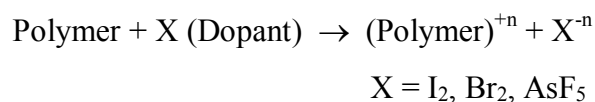
**Figure 2.5** Calculated (frontier) energy levels of oligothiophenes with  $n = 1-4$  and of polythiophene ( $E_g =$  band gap energy) [7].

## 2.2 Effect of doping and charge transfer [8]

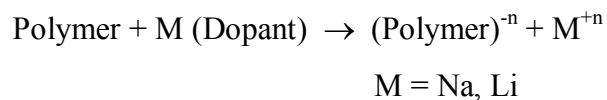
The doping is an addition of an agent into the polymer and is expected to improve the conductivity of the polymer. Reversible “doping” of conducting polymers, with associated control of the electrical conductivity over the full range from insulator to metal, can be accomplished either by chemical doping or by electrical doping. Concurrent with the doping, the electrochemical potential is moved either by a redox reaction or an acid base reaction into a region of energy where there is a high density of electronic states; charge neutrality is maintained by the introduction of counter-ions. Metallic polymers are, therefore, salts. Consequently, doped conjugated polymers are good conductors for two reasons:

1. Doping introduces carriers into the electronic structure. Since every repeating unit is a potential redox site, conjugated polymers can be doped n-type (reduced) or p-type (oxidized) to a relatively high density of charge carriers.

- *p-type*



- *n-type*



When the doping level is sufficiently high, the electronic structure evolves toward that of a metal.

2. The attraction of an electron in one unit to the nuclei in the neighboring units leads to carrier delocalization along the polymer chain and to charge carrier mobility, which is extended into three dimensions through interchain electron transfer.

Disorder, however, limits the carrier mobility and in the metallic state, limits the electrical conductivity. Indeed, research directed towards conjugated polymers with improved structural order and hence higher mobility is a focus of current activity in the field. Charge injection onto conjugated, semi-conducting macromolecular chains, or “doping”, leads to the wide variety of interesting and important phenomena which define the field. The doping can be accomplished in a number of ways; mostly either chemically or electrochemically doping.

Electron or charge transfer [9] in conjugated polymers determines whether the polymer is conductive or insulating. How the charge is transported determines the performance of the devices fabricated from the polymer. Oxidation or reduction of a conjugated polymer leads to the introduction of positive or negative charges into the polymer chain, giving rise to an increased conductivity. The term *doping* can be misleading as what occurs is best viewed as a redox process. The insulating neutral polymer is converted into a salt consisting of a polycation (or polyanion) and counterions, which are the reduced forms of the oxidizing agent (or the oxidized forms of the reducing agent). From a chemical point of view, the “doped” polymers are actually new compounds – carbocations or carbanions of the original compound.

Using solid-state physics language, however, oxidation corresponds to *p*-type doping and reduction to *n*-type doping. *P*-doping occurs with a positive applied

voltage, under which conditions the polymer chain is oxidized. Electrons move from the chain to the electrode giving rise to polarons (partially delocalized radical cations; see Figure 2.6) and bipolarons (polaron with a second electron removed) in the chain. Polarons and bipolarons may be viewed as electron holes, which can move along the chain to produce an electrical current. Anions become incorporated into the polymer matrix to compensate the positively charged polymer backbone. *N*-doping occurs when a negative applied potential is applied to the polymer, under which conditions negative charges are created in the chain as electrons move from the electrode to the polymer. Consequently, cations from the solution become incorporated into the polymer structure to compensate for the negatively charged polymer backbone. Electrons serve as charge carriers in this case.

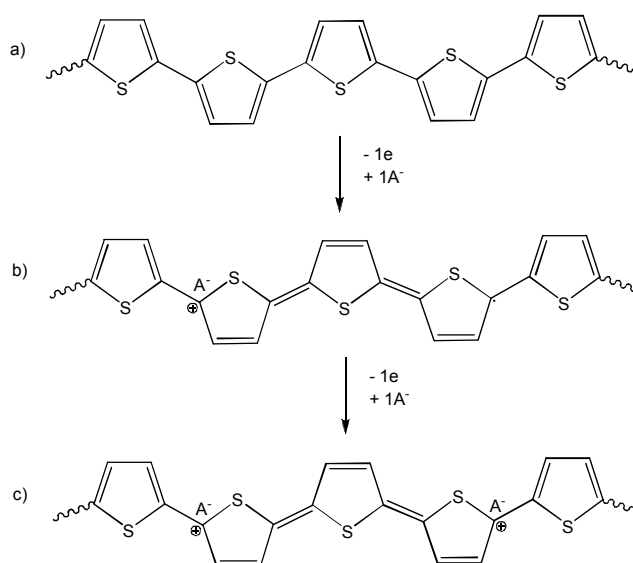


**Figure 2.6** Depictions of (a) neutral (undoped chain), (b) polaron, and (c) bipolaron.

Overall conductivity in a polymer is determined by both its intramolecular and intermolecular conductivities. Chain length plays the most important role in intramolecular conductivity. The longer the conjugated  $\pi$ -system, the greater the conductivity will be. Intermolecular conductivity is due to the same phenomenon as one finds in redox polymers (hopping). Because conjugated polymers are normally constructed of layered planar conjugated molecules, the attractive interactions

between  $\pi$ -electron clouds enhance electron hopping between layers. This has been labeled  $\pi$ -dimerization.

The *doping level* is a measure of to what degree the polymer is oxidized or reduced. The electrically conducting form is obtained when the polymer is doped. For example, polyacetylene exhibits a conductivity of  $10^{-9} \Omega^{-1}\text{cm}^{-1}$  in its undoped form while achieving conductivities of  $10^3 \Omega^{-1}\text{cm}^{-1}$  and higher in the doped form. The electrical conductivity is strongly dependent upon the polymer's doping level. Polymers may be doped either chemically or electrochemically. The doping level is normally higher for electrochemically doped polymers than for chemically doped polymers. With chemical doping, electron acceptors (*p*-doping) or electron donors (*n*-doping) need to be added to the solution in order to make the doping reaction take place. Some examples are oxygen,  $\text{I}_2$  and arsenic pentafluoride. A polymer can be doped electrochemically by simply applying an appropriate potential across the film in the presence of counterions.

In Figure 2.7, UV-VIS spectroelectrochemical curves recorded for different electrode potential are shown for regioregular poly(3,4-ethylenedioxythiophene) prepared using the method of Kvarnstrom and coworkers [10]. Cyclic voltammograms of poly(3,4-ethylenedioxythiophene) unambiguously indicate that oxidative doping of this polymer is a two-step phenomenon since two overlapping redox couples are clearly seen. This two-step oxidation is also manifested in UV-vis spectroelectrochemical studies. The spectra recorded for increasing doping levels show gradual bleaching of the  $\pi$ - $\pi^*$  transition with simultaneous growth of two peaks at 580 nm and 700 nm, usually ascribed to the formation of bipolaron sub-gap states.

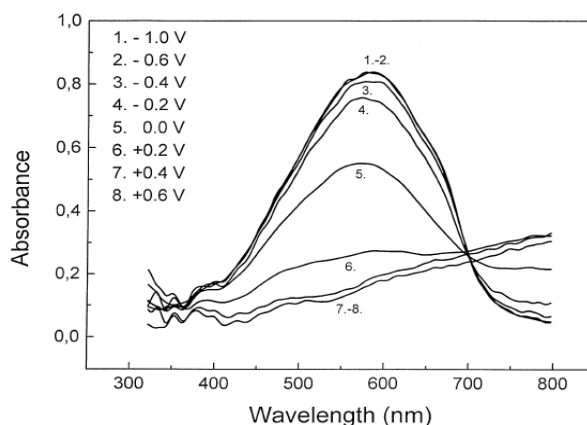


**Figure 2.7** UV-VIS absorption spectra of PEDOT film on ITO during the oxidation process in 0.1 M TBAPF<sub>6</sub>-acetonitrile. The potential range is -1.0 to +0.6 V, scan rate 100 mV/s.

### 2.3 Effective conjugation length (ECL)

Ideally, a conducting polymer would have its  $\pi$  electrons in the unsaturated bonds conjugated throughout the whole chain. This requirement usually does not hold due to the following:

- i) Formation of defects in polymer
- ii) Twisting of the planar structures out of conjugation in the polymer

Examples of the two reasons above are shown in Figure 2.8. Formation of a defect in polyacetylene as a saturated  $sp^3$ -hybridized methylene caused the disruptive effect in the flow of electrons on polymer chain. In another case, the steric incumbent between adjacent R groups on HH thienyl units in irregular poly(3-alkylthiophene) brought about the twisting of the thienyl ring planes out of coplanarity, causing an increase in the energy needed to allow the flow of electrons through the polymer chain, hence making the polymer chain less conductive.

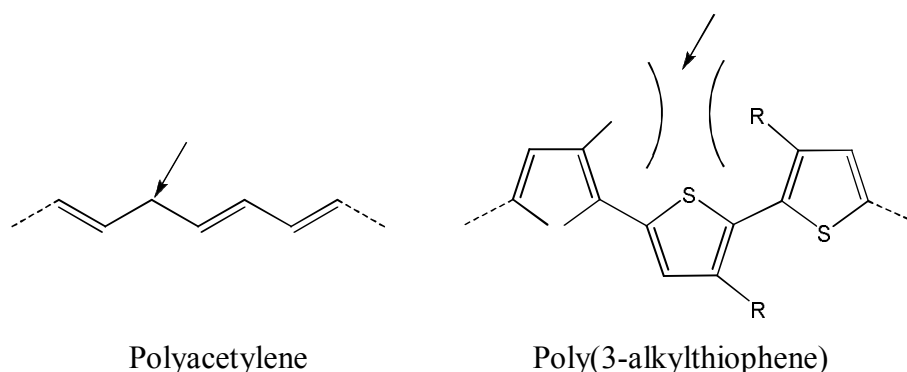


**Figure 2.8** A defect in polyacetylene and steric-induced structure twisting in poly(3-alkylthiophene).

Another possible reason would be the twisting of polymer chain, which occurs randomly at the single bonds and divided the polymer into separated sections with their own coplanarity (Figure 2.9). Twisting of polymer chain would also cause the reduction of conjugation in the polymer.

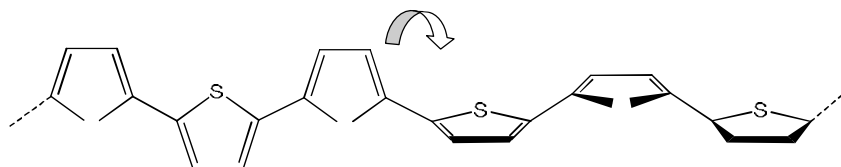


**Figure 2.9** Random twisting of polythiophene.

## 2.4 Organic electronics [11-14]

During the last few decades, much attention has been paid to the field of organic electronics. Electrical devices made out of plastic materials provide great advantages due to their special chemical and electrical behavior as compared with standard semiconductors. Organic light emitting diodes (OLEDs), plastic solar cells or organic field effect transistors (OFETs) are some of the new devices in this area. Great progress has been made to investigate, understand, improve and utilize their unique physical features. Commercial products are entering the consumer markets and show the potential of this new technology. The foundation of the field of organic

electronics was established back in the seventies with the discovery that the conductivity of polyacetylene films can be changed over several orders of magnitude by chemical doping. For their groundbreaking work in this area, MacDiarmid, Heeger and Shirakawa were awarded the Nobel Prize in Chemistry 2000. Excellent introductions into the field of organic electronics are their Nobel lectures. Intrinsic conducting plastic materials and semiconductors, both electron (n-type) and hole transport (p-type) materials with band-like structures, could now be made. Since the early work, many innovative materials in pure form have been developed and characterized for the usage in electronic applications. An overview of the conductivity of different materials from insulators to metals is shown in Figure 2.10.

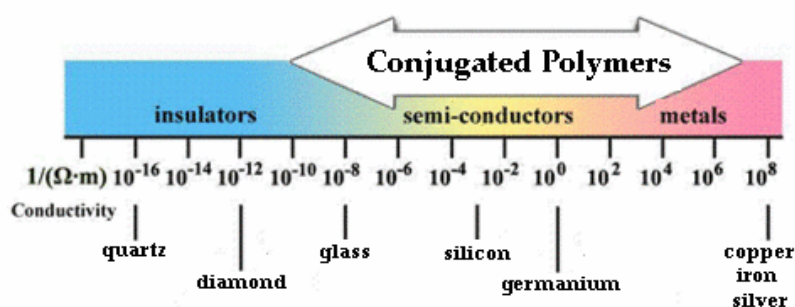


**Figure 2.10** Conductivity of different materials.

According to the attractive and tunable properties of organic conducting polymers, this facilitates the use of conducting polymers in many applications such as:

- Applications utilizing the inherent conductivity of polymer: Antistatic coating (metal and polymer), microelectronic devices, stealth material for providing a minimum radar profile for military aircrafts and naval vessels
- Electrochemical switching, energy storage and conversion, new rechargeable battery, redox supercapacitors
- Polymer photovoltaics (light- induce charge separation)
- Display technologies: Light emitting diode (LED), flat panel displays



- Electromechanical actuators: Artificial muscles, windows wipers in spacecrafts, rehabilitation gloves electronic braille screen, bionic ears for deaf patients.
- Separation technologies: Novel smart-membrane, selective molecular recognition
- Cellular communication: Growth and control of biological cell cultures
- Controlled release devices: Ideal host for the controlled release of chemical substances
- Corrosion protection: New-generation corrosion protective coatings

## **2.5 Advantages and drawbacks of organic electronics [15-24]**

Organic materials, in general, possess some unique features. Their chemical structure can be altered and adapted to the need of the application. The success of thermoplastics as a cheap and durable material used widely in our daily life is only but one example. There, the material was designed to be moldable to simplify fabrication but also to exhibit good mechanical characteristics and chemical stability. By changing part of the molecular structure, the behavior of the matter can be modified. For example, adding polar OH side groups to a molecule will result in a better solubility in water. The same approach can be used to adjust the properties of organic electronic material. The common technologies and techniques to modify the chemical structure can now be applied to adjust the electrical behavior of molecules out of this new class of organic electronic materials. Because there are an almost infinite number of combinations available, the possibilities seem to be virtually unlimited. This is an advantage of organic electronics over the established microelectronic technology. When inorganic single-crystals are used, the electrical properties are changed only by doping. The substrate material itself remains unchanged. Some examples where the versatility of organic electronic materials is used can be given out of the field of optoelectronics. For a full color display, the pixels have to emit light at different wavelengths for red, green and blue. Materials for

OLEDs have been developed for all three colors and can even be stacked on each other to achieve a higher pixel density.

Because plastics can be used as substrate material, the combination provides an opportunity to build flexible devices, something that was not possible with silicon based technology. The bases for the novel materials are known components in organic chemistry. This makes them potentially low cost, at least if the fabrication process is not too expensive and the material can be mass-produced. Since the materials are assembled out of organic building blocks, they can be made bio-compatible. Thus, they can be implanted and used *in vivo* without causing immune reactions. Organic layers are already used as coating material for *in situ* electrodes to record neural activity. More all-plastic, bio-compatible sensors are likely to be developed in the near future monitoring critical data like local blood pressure or blood sugar concentration.

With the organic origin of the novel materials, there is also a major drawback inherited. They easily degrade under environmental conditions due to humidity, oxygen and light. In fact, this is the major obstacle that has to be overcome before such products can be introduced into the consumer market. The principal limitation of organic materials is their confined lifetime. Requirements for many applications are in the range of several tens of thousands of hours. This is orders of magnitude beyond most numbers published to date. The performance of the electronic devices built with organic materials nowadays is far from competing with the established silicon technology. But the idea is not replacement but expansion of the application of electronic devices into new low cost/low performance markets. One example could be the RF-ID tag for supermarket products to simplify logistics and payment. But the field of possible applications is much wider once functional and durable devices can be mass produced. As important as the material itself are the technologies to fabricate functional devices as will be explained in the next section.

## **2.6 Fabrication technologies [25-28]**

Many of the new organic materials are soluble and can therefore be applied in liquid form. When the side groups of the building blocks of a polymeric material are modified, their solubility can be altered. This approach was successfully used for

many materials such as poly(phenylenevinylene) (PPV) derivatives. Using this material, the first organic LED based on a polymer was made by spin-casting a solution processable precursor [25]. The polymerization process was carried out after the thin film had been applied. If the electro-active molecules cannot be mixed with a solvent to form a solution, dispersions may be available which still allow the application of liquid-based processing technologies.

Different methods are used to form thin films. Spin-coating is one of them and probably the most widely used due to its simplicity. Especially in laboratory applications, this method has become a standard. The film thickness can be adjusted by setting the spin-speed and time. A drawback is the large amount of waste considering the quantity of material applied compared to the one effectively making up the thin film. Therefore, spin-coating is not often used for high volume fabrication.

Another technique is dip-coating, where the sample is submerged into the solution and pulled out again. When the solution is applied to the substrate using a mold, the term film casting is used. For large area processing, spraying is the most adequate method, since only the required material is applied. The ink-jet process is highly analogous to graphical ink-jet printing, tiny droplets of polymer solution are propelled onto the substrate in carefully controlled pattern.

All the technologies mentioned above are low temperature processes. This allows using substrates that would not withstand high temperatures such as most plastic materials. Flexible, all plastic electronic devices can be built with the novel organic conductive and semi-conductive materials and using the fabrication technologies explained above.

## **2.7 Poly(3,4-ethylenedioxythiophene) (PEDOT) [29-34]**

Poly(3,4-ethylenedioxythiophene) (PEDOT) is one of a few examples within the conjugated polymer family which is both p- and n-dopable. It is well known that upon electrochemical p-doping (or n-doping) conducting polymers undergo oxidation (or reduction) of the polymer backbone resulting not only in an increase of their electronic conductivity but also in structural transitions which give rise to spectral changes.

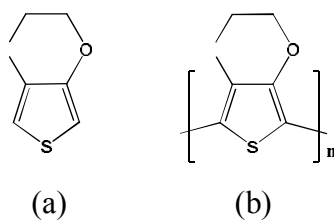


**Figure 2.11** 3,4-Ethylenedioxythiophene (EDOT) (a) and Poly(3,4-ethylenedioxythiophene) (PEDOT) (b).

PEDOT has been developed into one of the most successful materials from both fundamental and practical perspective. It possesses several advantageous properties as compared with other polythiophene derivatives: it combines a low oxidation potential and moderate band gap with good stability in the oxidized state. Also, by blocking the  $\beta$ -positions of the heterocyclic ring, the formation of  $\alpha$ - $\beta$  linkages during polymerization is prevented, resulting in a more regiochemically defined material. In addition to a high conductivity (550 S/cm in the electrochemical doped state), PEDOT is found to be highly transparent in thin, oxidized films. As a result, PEDOT derivatives are now utilized in several industrial applications including antistatic coatings for photographic films, electrode material in solid-state capacitors, substrates for electroless metal deposition in printed circuit boards, indium tin oxide (ITO) electrode-replacement material in inorganic electroluminescent lamps, and hole conducting material in organic/polymer-based light-emitting diodes (OLEDs/PLEDs).

3,4-Ethylenedioxythiophene (EDOT) is a commercially available, oxidatively polymerizable monomer which could be polymerized at relatively low applied potentials (+1.0 V vs Ag/Ag<sup>+</sup>). Jonas and Heywang [31] first polymerized EDOT to poly(3,4-ethylenedioxythiophene), (PEDOT), and found the polymer to be useful for antistatic coatings. Inganäs and co-workers [33] showed the usefulness of PEDOT as a potential material for electrochromic devices due to its ability to cycle between an opaque blue-black in the reduced (undoped) state and a transmissive sky blue in the oxidized (doped) state. Conductivities reported for PEDOT prepared electrochemically ranged from 10 to 100 S/cm. These conductivities have been found to be stable for up to 1000 h at 120 °C in a laboratory atmosphere.

## 2.8 Excellent characteristics of PEDOT [35-43]

PEDOT is one of the most promising materials for practical applications due to its following characteristics:

- Reversible doping state

PEDOT can be repeatedly doped and undoped. PEDOT is almost transparent and light blue in the oxidized state and can be easily changed into opaque and dark blue appearance in the neutral state. Thus its color changes visibly when its doped state changes and may be suitable for optical applications, such as electrochromic displays [35].

- Excellent stability

PEDOT has improved chemical and thermal stability. Thermal studies show that a continuous degradation occurs above 150 °C and complete decomposition above 390 °C [36]. Electrical conducting properties appear to remain almost unaltered after aging in environmental conditions. Its high stability is attributed to favorable ring geometry and the electron-donating effect of the oxygen atoms at the 3,4-positions stabilizing the positive charge in the polymer backbone [37].

- Regular structure

Due to the structure of the monomer, competing polymerizations through 3- and 4- positions as in thiophene are avoided. Thus, only the 2,5-couplings of the 3,4-ethylenedioxythiophene are expected. Therefore, PEDOT is expected to have fewer defects than the thiophene analogues.

- Low band-gap (High conductivity)

PEDOT has a low band gap of 1.5-1.6 eV [38]. The lower band-gap relative to polythiophene is thought to originate from the influence of the electron-donor ethylenedioxy groups on the energies of the frontier levels of the  $\pi$  system [39]. Experimental results show that after doping, PEDOT exhibits reduced absorption in the visible: the oscillator strength shifts from around 1.5 eV (lowest  $\pi$ - $\pi^*$  transition) to below 1 eV in the metallic state [40]. Thus it shows a high electrical conductivity (up to 550 S/cm) in the doped state.

- Electrochemical properties

Compared to other conducting polymers, electrochemically synthesized films of PEDOT have a low redox potential and excellent stability in their doped state [41]. Studied by cyclic voltammetry, it was found that the redox peaks at approximately 0 mV (oxidation) and -400 mV (reduction) remained almost unaffected during cycling. However, only under an applied negative potential of -700 mV were the neutral films found to be stable. Open circuit potential measurements showed that the neutral films were rapidly oxidized [42].

## 2.9 Solid state synthesis of PEDOT [44-47]

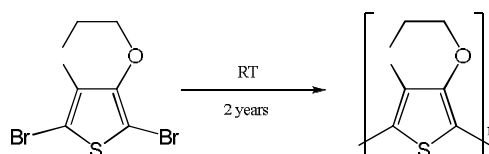
The synthesis of PEDOT can be done in several ways depending on how conductive the polymers are needed to be and what type of byproducts are contained in the polymer chain itself. There are four general ways of synthesizing PEDOT

- Oxidative chemical polymerization of the EDOT-based monomers
- Electrochemical polymerization of the EDOT-based monomers
- Transition metal-mediated coupling of dihalo derivatives of EDOT [44]
- Solid state polymerization of the DBEDOT [45]

Polymerization of PEDOT by traditional oxidative polymerization with  $\text{FeCl}_3$  in organic solvents gives an insoluble blue-black polymer powder. The limitations of traditional polymerization methods can be a serious problem for PEDOT applications as well as for in-depth investigation of molecular order in this conducting polymer. It is generally not possible to obtain a well-defined polymer structure, unless the synthesis of conducting polymers is carried out via pure chemical polymerization routes, without adding any catalysts. A possible solution for this lies in a solid-state polymerization of a structurally pre-organized crystalline monomer.

The advantages of solid-state polymerization (SSP) include low operating temperatures, which restrain side reactions and thermal degradation of the product, while requiring inexpensive equipment, and uncomplicated and environmentally sound procedures. Also by-products can be easily removed by application of vacuum or through convection caused by passing an inert gas.

In 2003, Meng et al. [45, 47] reported that the solid-state polymerization (SSP) of DBEDOT was discovered by chance as a result of prolonged storage (2 years) of the monomer at room temperature. The colorless crystalline DBEDOT, with time, transformed into a black blue material without apparent change of morphology. Surprisingly, the conductivity of this decomposition product appeared to be very high (up to 80 S/cm) for an organic solid. Even though this type of non catalytic coupling was not known in organic chemistry, indeed, the most likely explanation for the observed transformation was polymerization with formation of bromine-doped PEDOT.



**Scheme 2.1** Solid state polymerization of DBEDOT.

The room-temperature conductivity of different SSP-PEDOT samples was measured by the four point probe method (Table 2.1). The highest conductivity belongs to the polymer prepared at lowest temperature and longest reaction time, which may reflect achievement of a higher degree of order. Indeed, heating above the monomer's melting point results in dramatically reduced conductivity (0.1 S/cm), which rises up to 5.8 S/cm after doping with iodine, approaching the value of an FeCl<sub>3</sub>-synthesized PEDOT (7.6 S/cm) [47]. Not very significant, but certain increase in conductivity of SSP-PEDOT (about 2 times) was found on exposing a sample to iodine vapor.

From the experiment, they concluded that heating DBEDOT in the solid state resulted in an unprecedented self-coupling reaction and gave highly conductive and relatively well-ordered bromine-doped PEDOT. Furthermore, heating DBEDOT above its melting point led to polymer with a lower conductivity.

**Table 2.1** Conductivity data of PEDOT polymers

	$\sigma_{rt}$ (SSP-PEDOT)/ S.cm <sup>-1</sup>				$\sigma_{rt}$ (FeCl <sub>3</sub> -PEDOT)/ S.cm <sup>-1</sup>
	20	60	80	120	0-5
Reaction Temperature (°C)	20	60	80	120	0-5
Reaction time	2 years	24 h	4 h	24 h	24 h
“crystals”/ “fibers”	80	33	20	N/A	N/A
pellets as synthesized	30	18	16	0.1	N/A
pellets after I <sub>2</sub> doping	53	30	27	5.8	7.6
thin films	N/A	23	N/A	N/A	N/A
Thin films after I <sub>2</sub> doping	N/A	48	N/A	N/A	N/A

N/A = Not available

## 2.10 Applications of PEDOT [43]

Because of PEDOT has so many excellent properties, it inspires much great interest of research and a wide range of potential applications. Its low oxidation potential, moderate band gap, high conductivity and stability in the doped state makes it very attractive for many applications such as hole injection layers in OLED, solar cells, antistatic and electrostatic coatings, for metallization of insulators, and as electrodes for capacitors or photodiodes [48-50]. If the durability of the capacitors using PEDOT is enhanced, they will have a wider range of applications such as in electronic circuits for cars and man-made satellites [51]. Due to its property of being able to repeatedly doped and de-doped, it is very attractive for electrochromic applications [38, 52]. With proper choice of counter-ions, PEDOT is also of interest for applications as an electrochemical actuator [53]. PEDOT has been a successful commercial product by Bayer and AGFA with the intent of applying it to the fields of antistatic coatings and photographic films. Chemical polymerization, aqueous dispersions of PEDOT:PSS, Baytron<sup>®</sup>P, synthesized by Inganäs et al. [33], is successfully used and the fabrication volume of coated photographic film per year exceeds 108 m<sup>2</sup>. Poly(styrenesulfonate) (PSS) is used as a dopant for PEDOT. The doping process of the conjugated polymer is done by acid rather than redox-doping.



Thus, the PEDOT does not act as an electron donor but accepts protons from the sulfonate groups of the PSS dopant. Some C=C  $\pi$ -bonds of the EDOT are broken and form bonds to H<sup>+</sup> donated by the acid. As a result, there are positive charges on the PEDOT chain that will strongly attract the negative charges left on the acid. Since these happen at many points along the polymer, PEDOT and PSS become closely intertwined. An unpaired  $\pi$ -electron remains on the PEDOT chain that is highly mobile along the conjugated backbone and leads to a high conductivity. Other dopants reported in literature include tosylate and inorganic materials such as phosphomolybdate. However, PEDOT:PSS also suffers from low conductivity of less than 1 S/cm, which is lower than that of some good conducting polymers by one to two orders of magnitude. Also, it is typically laid down in an acidic water-based solution whose corrosive properties cause other problems [54]. But it has been extensively used as an antistatic coating on photographic films and as an electrode layer in flexible displays and organic light-emitting devices [55]. Further progress has been achieved through recent studies on the application of PEDOT in the electrochemical field such as actuators, capacitors, OLED, photovoltaic cells, sensors etc.

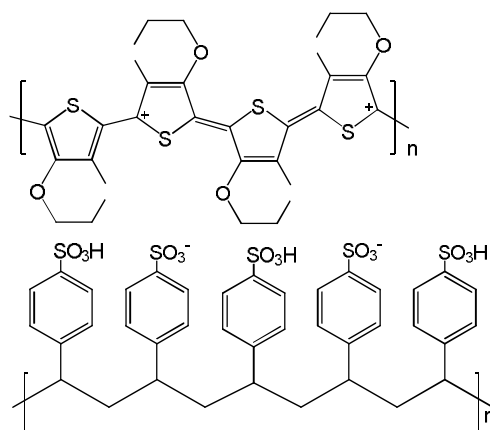


**Figure 2.12** Poly(3,4-ethylenedioxythiophene)/polystyrene sulfonic acid (PEDOT/PSS).

## 2.11 PEDOT composites

In its most basic form a composite material composed of at least two elements working together to produce material properties that are different to the properties of those elements on their own. In practice, most composites consist of a bulk material (the matrix), and a reinforcement of some kind, added primarily to increase the strength and stiffness of the matrix.

Poly(3,4-ethylenedioxythiophene) (PEDOT) and other conductive polymers are mostly prepared by oxidative polymerization using oxidizing agents such as iodine and  $\text{FeCl}_3$  or by electrochemical polymerization. These methods yielded non-processible polymers with hard, brittle, insoluble in most solvent and nonfusible even by heating up to their decomposition temperature. The PEDOT composites is the alternative to improve physical and mechanical properties of PEDOT by other components. Examples of PEDOT composites are:

- PEDOT nanocomposites (PEDOT + noble metal nanoparticles)
- PEDOT composites including carbon materials (PEDOT + carbon nanotubes)
- PEDOT composites with other polymers (PEDOT + insulating polymer or conducting polymer)

In 2009, Bai and coworkers [56] reported that conducting polymer/hydrophobic insulating polymer (CP/HIP) composite nanofibers were prepared by electrospinning and vapor deposition polymerization (VDP) with benzoyl peroxide (BPO) as oxidant. BPO is soluble in DMF and can form homogenous solutions with hydrophobic polymers such as poly(methyl methacrylate) (PMMA) and polystyrene (PS). High-quality nanofibers of PMMA or PS containing a certain amount of BPO were produced by electrospinning and used as the templates for VDP of pyrrole, 3,4-ethylenedioxythiophene (EDOT), and aniline. The formation of PPy, PEDOT and PANI were confirmed by their Raman spectra. The non-woven mats of the resulting CP/HIP composite fibers can be used as the high-sensitive sensing elements of gas sensors.

In 2009, Wang and coworkers [57] prepared PANI/poly(styrene-co-styrene sulfonate) (PS-PSS) by coating poly (styrene-co-styrene sulfonate) (PS-PSS) nanoparticles with polyaniline (PANI). PS-PSS core particles were prepared in

microemulsion system in nitrogen atmosphere and further coated with PANI by using in situ polymerization method at low temperature. It was found that the core-shell structure of PANI-coated PS-PSS can be obtained when PANI in PANI/PS-PSS copolymer varies from 2.78 to 12.5 wt%. The highest conductivity of PANI/PS-PSS pellets is 1.7 S/cm.

In 2008, Aussawasathien et al. [58] successfully prepared the camphorsulfonic acid (CSA) doped poly(o-toluidine) (POT)/PS composite fibers by electrospinning. CSA doped POT/PS composite fibers were fabricated on an interdigitated gold (Au) substrate for use as a chemical vapor sensor. The sensing device composed of CSA doped POT/PS composite fibers responded to chemical vapors in different ways, depending on the type of sensing chemicals. The resistance of the sensing device had a tendency to decrease, when exposed to a high polar solvent. In contrast, the resistance of the sensing device had a tendency to increase, when subjected to a low polar solvent. The sensing electrode could be reused several times without any change in sensing behavior or damage to the sensing materials.

In 2008, Laforgue and Robitaille [59] reported that poly(3-hexylthiophene) (P3HT)/polyethylene oxide (PEO) nanofibers were fabricated successfully by electrospinning of polymer solution. The maximum electrical conductivity found for unaligned mats was 0.16 S/cm and increased to 0.30 S/cm when the nanofibers were aligned along a preferential direction.

In 2008, Xia and Lu [60] reported that PEDOT/silk fibroin (SF) composite fibers were fabricated successfully and expediently by in situ polymerization without any modification of silk fibroin surface. SEM observation and elements analysis confirmed that PEDOT molecules had been coated successfully by such polymerization process without destroying SF in nature and the composite fibers still possessed their former fibrillar morphology and strength properties. These composite fibers exhibited better electrical and thermal properties and may have potential applications in textile, biological and other novel functional materials.

In 2007, Kusonsong [61] found that the highly conductive polymer composites of PEDOT/insulating polymer composites could be prepared by solid state polymerization (SSP) of 2,5-dibromo-3,4-ethylenedioxythiophene (DBEDOT) in the presence of either polystyrene (PS) or polybutadiene (PB) matrix. Nonetheless, the

fabrication process based on solution casting yielded the composite films with non-uniform morphology and conductivity due to the inhomogeneous distribution of the PEDOT in the matrix caused by phase incompatibility between the polar PEDOT and the non-polar matrix.

In 2007, Sun and Hagner [62] prepared the PEDOT/poly(acrylic acid) (PAA) composites by oxidative polymerization of EDOT with  $\text{FeCl}_3$  in the presence of PAA. It was found that these composites were nanowires assembled by PAA chain acted as a template. They exhibited excellent conductivity (0.56 S/cm). It provided a new water-dispersible and easily processable PEDOT dispersion. It also presented a simple self-assembly strategy for the morphology-controlled preparation of nanocomposites based on PEDOT and extended the use of polyelectrolyte as a template for designing interesting nanostructures.

In 2005, Hong and coworkers [63] prepared the PEDOT composites by in situ polymerization of EDOT on nylon 6, poly(ethylene terephthalate) (PET), and poly(trimethylene terephthalate) (PTT) fabrics using ferric p-toluenesulfonate (FepTS) as oxidant. PEDOT/nylon 6 composite fabrics showed the best electrical conductivity (0.75 S/cm, in ethanol solvent) compared to those of the other composite fabrics (0.07 S/cm for PEDOT/PET and 0.28 S/cm for PEDOT/PTT, in ethanol solvent). However, nylon 6 fabric was decomposed by EDOT radical cations and the strong acidity from the oxidant (FepTS) in contrast to PTT fabric which was a more suitable substrate for in situ polymerization of PEDOT.

In 2005, Wutticharoenmongkol and coworkers [64] have reported that PS/poly(2-methoxy-5-(2'-ethylhexyloxy)-1,4-phenylene vinylene) (MEH-PPV) blends were successfully prepared by electrospinning of PS/MEH-PPV solution in chloroform, 1,2-dichloroethane and THF. The addition of an organic salt, pyridinium formate (PF), helped improve the spinnability of the solution. Chuangchote and coworkers (2007) [65] found that the addition of PF significantly improved the electrospinnability of the PS/MEH-PPV solution.

In 2005, Sonmez and coworkers [66] found that PEDOT/poly(2-acrylamido-2-methyl-1-propane sulfonate) (PAMPS) composite films were electrochemically prepared from a mixture of water and DMF containing EDOT and polyelectrolyte, PAMPS. The conductivity of PEDOT/PAMPS free standing composite films reached

the value of 80 S/cm. The PEDOT/PAMPS exhibited a band gap of 1.65 eV, identical to PEDOT doped with small ions that could be switched rapidly between the doped and neutral state with an excellent contrast ratio of 76%. Interesting cation-exchange properties have also been demonstrated with  $\text{Ru}(\text{NH}_3)_6\text{Cl}_3$ .

In 2004, Dong and coworkers [67] reported that PANI/poly(L-lactide) (PLA) composites were performed successfully by electrospinning of PLA and in situ polymerization of aniline in PLA fiber which suspended in aniline and ammonium persulfate solution. The conductivity of PANI/PLA fibers was 0.38 S/cm.

In 2001, Lee and coworkers [68] revealed that the conducting polypyrrole (PPy)/sulfonated polycarbonate (SPC) composites were prepared by oxidative polymerization of pyrrole in the presence of SPC using  $\text{FeCl}_3$ . It was found that the conductivity of PPy/SPC composites (0.82 S/cm) was higher than that of PPy/PC composites due to the electrostatic interaction and miscibility between PPy and SPC, while the mechanical properties were similar to those of PPy/PC composites. The PPy/SPC composites were stable in the atmosphere because SPC obstructed the reaction of PPy with oxygen or moisture.

In 1999, Khan and Armes [69] found that PEDOT/PS latexes could be prepared by oxidative polymerization of EDOT in PS latexes and  $\text{Fe}(\text{OTs})_3$ . The conductivity of 0.43 S/cm was obtained at the highest PEDOT loading. At low loadings (<12 wt%) the overlayer appeared to be reasonably smooth and uniform, but increasing overlayer roughness was apparent at higher PEDOT loadings, in addition to the presence of coprecipitated PEDOT.

In this study, we have proposed the new way to overcome the inferior properties of PEDOT by blending it with another insulating polymer. Composites have been formed by directly dispersing a soluble precursor 2,5-dibromo-3,4-ethylenedioxy thiophene (DBEDOT), into an insulating polymer matrix which can form solid film by electrospinning. Thin film could be transformed into PEDOT/polymer composite by thermal treatment to induce solid state polymerization. The rapid solvent evaporation and solidification of the fiber mat electrospun from the mixed solution of the desired matrix (i.e. PS, SPS) and DBEDOT should not allow time for the DBEDOT to separate from the matrix. This would yield thin conductive composite fiber mat with improved PEDOT distribution and conductivity after the heat treatment.

## 2.12 Electrospinning process

A number of processing techniques such as drawing, template synthesis, phase separation, self-assembly, electrospinning have been used to prepare polymer nanofibers in recent years. The electrospinning process seems to be the only method which can be further developed for mass production of one-by-one continuous nanofibers from various polymers [70].

Electrospinning is a unique process that used an electrical field to create an electrically charged jet of polymer solution or melt, which dries or solidifies to leave a polymer fiber. The first patent on electrospinning process was issued to Anton Formhals in 1934 [71]. Formhals' patent claimed the novelty of capable of producing parallel filaments in continuous length, enabling the filaments to be used in textile applications. Formhals modified the existing electrostatic spinning apparatus to allow collection of continuous fibers through the used of a drum take-up. At that time, the produced fibers were still in the micrometers in diameters. Formhals's invention did not gain much attention since the concept was beyond his time and other available fiber spinning methods were more efficient and practical.

When a high voltage is applied to a polymer solution, a high electric field is generated between a polymer fluid (contained in a spinning dope reservoir with a capillary tip or a spinneret) and a metallic fiber collection ground surface. As the intensity of the electric field is increased, the hemispherical surface of the fluid at the tip of the capillary tube elongates to form a conical shape known as the Taylor cone. Further increasing the electric field, a critical value is attained with which the repulsive electrostatic force overcomes the surface tension and the charged jet of the fluid is ejected from the tip of the Taylor cone. The electrically charged jet undergoes a series of electrically included bending instabilities during its passage to the collection surface which results in the hyperstretching of the jet. This stretching process is accompanied by the rapid evaporation of the solvent molecules, further reducing the diameter of the polymer jet. The dry fibers are accumulated on the surface of the collection plate, resulting in a non-woven mesh of nano-to-micro diameter fibers. The process can be adjusted to control the fiber diameter by varying the electric field strength and polymer solution concentration, whereas the duration of

the electrospinning controls fiber deposition thickness. A schematic drawing of the electrospinning process is shown in Figure 2.13.

The properties of fiber obtained from this process depend on two types of parameters; the first is system parameters including molecular weight, molecular weight distribution, architecture of the polymer (e.g. branched or linear chain) and solution properties (viscosity, conductivity and surface tension). The second one is processing parameters including electrical field strength, flow rate, solution concentration, distance between the capillary and the collector, and ambient parameters (temperature, humidity and air velocity in the chamber) [72].

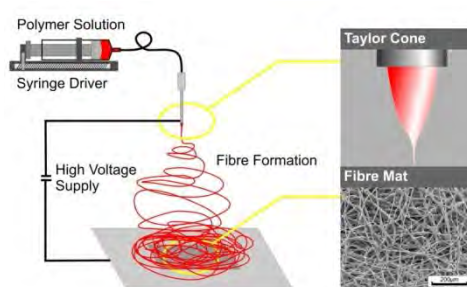


**Figure 2.13** Schematic diagram shows polymer nanofibers forming by electrospinning process.

The advantages of electrospinning process are simple equipment, requiring a short time, cost effective and producing a very high orientated fiber with very small pore sizes. Therefore, electrospun fibers from electrospinning have regained more attention probably due in part to interest in many applications such as in the field of filtration systems [73], medical prosthesis mainly grafts and vessels, tissue template [74], electromagneton shielding, protective clothing [75], composite delamination resistance [76], and chemical and biochemical sensor [77].

Jarusuwannapoom and coworkers [78] studied the effects of solvents and their properties on electrospinnability of the as-prepared PS solutions. The morphological appearance of the as-spun PS fibers were investigated qualitatively by means of a scanning electron microscope (SEM). Qualitative observation of the results obtained

suggested that the important factors determining the electrospinnability of the as-prepared PS solutions are high values of the dipole moment of the solvent and the conductivity of both the solvent and the resulting solutions, high boiling point of the solvent, not so high values of both the viscosity and the surface tension of the resulting solutions. The PS solutions in 1,2-dichloroethane, DMF, ethyl acetate, methyl ethyl ketone (MEK), and THF could produce fibers with high productivity.

Eda and coworkers [79] studied the effects of molecular weight and concentration in the electrospinning of PS. The results indicated that the degree of elongational flow, bending instability, and jet branching depended on polymer molecular weight and concentration. It was observed that jet thinning and solidification might occur at different distances from the capillary when the rheological conditions were varied. The electrospinning of SPS or PSS have not yet reported. The SPS fibers have been prepared by electrospinning of PS and treating the electrospun PS fiber mats with concentrated sulfuric acid [80].



## CHAPTER III

### EXPERIMENTAL

#### 3.1 Materials

All reagents and materials were analytical grade and used without further purification.

1. Acetone : Merck
2. Acetic acid glacial : Merck
3. Chloroform : Lab-scan
4. Dichloromethane : Fluka
5. 1,2-Dichloroethane : Lab-scan
6. 1,4-Dioxane : Merck
7. 3,4-Ethylenedioxythiophene : Aldrich
8. Ethanol : Merck
9. Ethylene glycol : Merck
10. Hexane : Fluka
11. Concentrated hydrochloric acid 37% : Merck
12. *N*-Bromosuccinimide : Merck
13. *N,N*-Dimethylformamide : Carlo Erba
14. Polystyrene ( $M_w = 3 \times 10^5$ ) : Dow Chemical
15. Pyridine : Merck
16. Sodium hydrogen carbonate : Lab-scan
17. Concentrated sulfuric acid : Merck
18. Tetrahydrofuran : Fisher Scientific

#### 3.2 Equipments

##### 3.2.1 Nuclear Magnetic Resonance (NMR) Spectrometer

$^1\text{H}$  NMR spectra were recorded in solution of  $\text{CDCl}_3$  using a Varian, model Mercury-400 nuclear magnetic resonance spectrometer (USA) operating at 400 MHz.

### **3.2.2 Fourier-Transform Infrared Spectrometer (FT-IR)**

IR spectra were collected using Perkin-Elmer FT-IR, spectrum RXI spectrometer. All samples were prepared as KBr pellets.

### **3.2.3 Surface Profile Measuring System**

The thickness of PEDOT/polymer composite films was determined by a Surface Profile Measuring System model Veeco Dektak<sup>3</sup> ST using by force 1 mg and a scanning rate of  $0.625 \mu\text{m s}^{-1}$  for  $3000 \mu\text{m}$ .

### **3.2.4 Scanning Electron Microscopy (SEM)**

The morphology of the electrospun fiber mats before and after HAP as well as the extracted PEDOT were observed with a scanning electron microscope (SEM) model JSM-6480LV. Each sample was placed on the holder with an adhesive carbon tape and coated with a thin layer of gold. The scanning electron images were obtained by using an acceleration voltage of 15 kV with a magnification of 500x and 2000x. The component element in PEDOT/polymer composite films were analyzed by energy dispersive spectroscopy (EDS) mode of Scanning Electron Microscopy.

### **3.2.5 Differential Scanning Calorimetry (DSC)**

Thermal properties, glass transition temperature ( $T_g$ ) and melting temperature ( $T_m$ ) of PEDOT/polymer composite films were investigated by Differential Scanning Calorimeter model Mettler Toledo DSC822<sup>o</sup> by heating the samples sealed in an aluminum pan from  $25 \text{ }^\circ\text{C}$  to  $300 \text{ }^\circ\text{C}$  using  $10 \text{ }^\circ\text{C}\cdot\text{min}^{-1}$  heating rate under nitrogen atmosphere ( $60 \text{ mL}\cdot\text{min}^{-1}$ ).

### **3.2.6 Thermogravimetric Analysis (TGA)**

The combustion stage and melting point of PEDOT/polymer composite films were investigated by a Mettler Toledo thermogravimetric analyzer model TGA/SDTA 851 by heating from  $30 \text{ }^\circ\text{C}$  to  $600 \text{ }^\circ\text{C}$  using  $20 \text{ }^\circ\text{C min}^{-1}$  heating rate under ambient atmosphere.

### **3.2.7 X-ray Diffractometer (XRD)**

X-ray diffractograms of standard PEDOT and extracted PEDOT from the PEDOT/polymer composite films were obtained by XRD model Rigaku D5000 using a scan range of 5.00-50.00 degree, a scan speed of 5.00 deg.min<sup>-1</sup> and a sample width of 0.020 degree.

### **3.2.8 Electron Spin Resonance Spectrometer (ESR)**

The unpaired electron or radical cation charge carriers of PEDOT in PEDOT/polymer composite films were determined by an electron spin resonance spectrometer of JEOL model JES-RE2X (X-band microwave (8.8-9.6), magnetic field range to 1.3 T, cylindrical cavity resonator (TE<sub>011</sub> mode), program ES-PRIT). The samples were analyzed by applying a microwave magnetic field between 329.0 to 344.0 mT under ambient atmosphere. 1,1-Diphenyl-2-picrylhydrazyl radicals (DPPH) was used for calibration.

### **3.2.9 Fourier-Transform Raman Spectrometer (FT-Raman)**

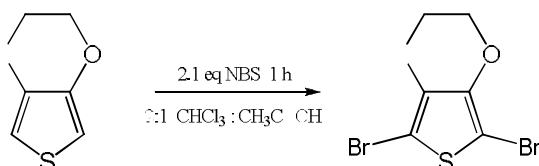
FT-Raman spectra of controlled PEDOT and the PEDOT/polymer composite films were analyzed by FT-Raman model Perkin Elmer Spectrum GX.

### **3.2.10 Four-Point Probe Conductometer**

The conductivity values of PEDOT/polymer composite films were determined by a four-point probe conductometer model KEITHLEY Semiconductor Characterization System 4200. The reported conductivity is an average value measured from four different areas using applied current between 0.1 to 1.0 mA, 0.1 mA.cycle<sup>-1</sup> applying rate under ambient atmosphere.

### 3.3 Methods

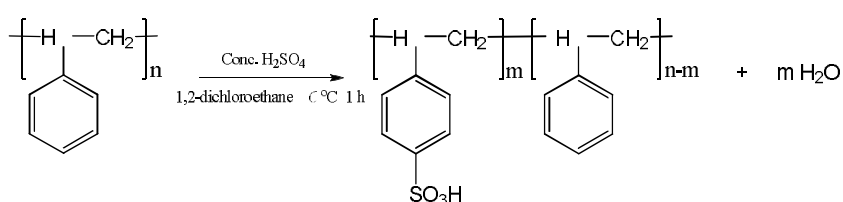
#### 3.3.1 Synthesis of 2,5-dibromo-3,4-ethylenedioxythiophene (DBEDOT)



**Scheme 3.1** Bromination of EDOT.

2,5-Dibromo-3,4-ethylenedioxythiophene (DBEDOT) was obtained via bromination of 3,4-ethylenedioxythiophene (EDOT) by slowly adding 2.1 eq *N*-bromosuccinimide (NBS) (1.50 g, 8.4 mmol) to a stirred solution of EDOT (0.57 g, 4 mmol) dissolved in a 29:1 (v/v) mixture of chloroform (29 mL) and glacial acetic acid (1 mL) for 1 h. Then the mixture was quenched and washed with saturated sodium hydrogen carbonate solution (20 mL  $\times$  3 times). The organic layer was separated and the aqueous layer was extracted with chloroform. The combined chloroform extract was dried with anhydrous magnesium sulfate. The crude mixture was purified by passing through a silica gel column, and eluted with 3:2 mixtures of hexane and dichloromethane. When approximately 2 mL of the solution mixture was left after the solvent removal by rotary evaporator, 3 mL of ethanol was added to the evaporating flask in order to induce crystallization of DBEDOT which appeared as white needle-like crystals in 95 % yield.

#### 3.3.2 Synthesis of Sulfonated Polystyrene (SPS)



**Scheme 3.2** Sulfonation of PS.

To a stirred solution of PS (3 g) in 1,2-dichloroethane (20 mL), which was prepared overnight before the reaction, was slowly added with a desired amount of conc. H<sub>2</sub>SO<sub>4</sub> (0.60, 0.90 and 1.20 mL). The mixture was heated to 60 °C under ambient atmosphere for 1 h. The sulfonation was then terminated by an addition of cool methanol (20 mL). After the solvent was removed under reduced pressure, 50 mL of saturated NaHCO<sub>3</sub> (aq) was then added to the resulting solid. The filtered solid was then washed consecutively with 10% HCl (aq) (3 × 20 mL) and water (3 × 20 mL). After being dried at 70 °C for 7 day, off-white solid powder was obtained as a product. The product was then characterized by <sup>1</sup>H-NMR and FT-IR.

### 3.3.3 Preparation of PEDOT-containing Composite Films

A mixed solution of polymer matrix (PS or SPS) and DBEDOT was prepared at ambient temperature by dissolving 0.30 g polymer matrix in 2.5 mL of a desired solvent (dimethylformamide (DMF), tetrahydrofuran (THF), and 1:1 (v/v) of DMF and THF) overnight followed by an addition of 0.90 g DBEDOT and then sonicated in an ultrasonic bath for 15 min. In the case that an additive (pyridine or ethylene glycol) was used, it was incorporated right after the addition of DBEDOT before sonication. Each of the as-prepared solutions was then placed in a 3-mL syringe having a 1.5-cm long blunt 20-gauge stainless steel hypodermic needle (i.e. outside diameter = 0.91 mm) as a nozzle which was connected with the positive electrode. The tilt angle of the syringe was set at 45° from a horizontal baseline. Fiber mats were fabricated by electrospinning the mixed solution at ambient temperature using a driving voltage of 13 kV (High voltage power supply model Gamma High Voltage Research DES30PN/M692). A grounded metal screen covered by a glass slide was used as the counter electrode and was placed 10 cm away from the tip of the needle. The schematic representation of the set-up is shown in Figure 3.1. After continuous spinning for 30 min, the as-spun polymer matrix/DBEDOT fiber mats was dried *in vacuo* at ambient temperature overnight and kept in desiccators. The fiber mat containing DBEDOT deposited was pressed against a glass slide coated with Teflon tape and clamped with paper clips (See Figure 3.2) in a closed vial and then heated in an oven at 60, 70 or 80 °C for a certain period of time to induce polymerization of DBEDOT into PEDOT (Scheme 3.3).

An average percentage yield of the PEDOT formed in the PEDOT/polymer composite film was calculated indirectly from the weight of the unreacted DBEDOT. The PEDOT/polymer composite film was first dissolved in dichloromethane. The insoluble PEDOT were removed by centrifugal wash at 5,000 rpm for 30 min with dichloromethane (5×). All fractions of supernatant collected after each washing cycle were combined and concentrated to 2-3 mL under reduced pressure by a rotary evaporator. The obtained solution containing the matrix and the unreacted DBEDOT was then purified by passing through a silica gel column using 3:2 (v/v) of hexane and dichloromethane as an eluent. The purity of the extracted DBEDOT which appeared as transparent-white crystal was verified by TLC and  $^1\text{H}$  NMR. The average percentage yield of the PEDOT formed in the composite films can be calculated using the following equation, assuming that all DBEDOT consumed was converted to PEDOT.

$$\% \text{yield} = \frac{(\text{initial weight of DBEDOT} - \text{weight of extracted DBEDOT}) \times 100\%}{(\text{initial weight of DBEDOT})} \dots\dots(3.1)$$

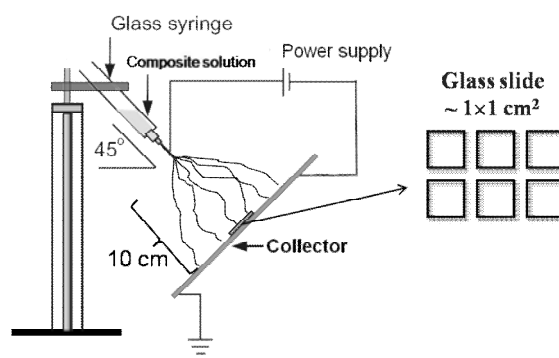


**Figure 3.1** Schematic representation of electrospinning apparatus set-up.



## **CHAPTER IV**

### **RESULTS AND DISCUSSION**

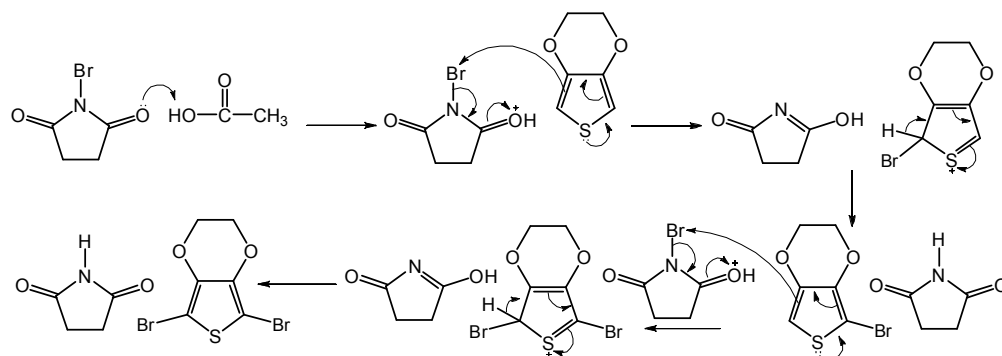
This work aims to prepare polymer composites containing 3,4-polyethylene dioxythiophene (PEDOT) by electrospinning and solid state polymerization of 2,5-dibromo-3,4-ethylenedioxythiophene (DBEDOT) activated by heating in the matrix of commercially available polymer i.e. polystyrene (PS) or sulfonated polystyrene (SPS). This chapter is divided into 3 parts. The first part involves a synthesis of DBEDOT by bromination of ethylenedioxythiophene (EDOT) and a synthesis of SPS by sulfonation of PS. The second part is dedicated to the preparation of DBEDOT/polymer composite films by electrospinning. Several parameters that can affect physical properties of the composite films were investigated including polymer matrix (PS vs SPS), polymer concentration, solvent (DMF vs THF), DBEDOT: polymer weight ratio. The last part investigates the effect of temperature, time, and compression used in the step of heat-activated polymerization on the conductivity of the composite film. Physical properties of the composites as well as the extracted PEDOT were also determined by a number of characterization techniques.

#### **4.1 Synthesis of 2,5-dibromo-3,4-ethylenedioxythiophene (DBEDOT) and sulfonated polystyrene (SPS)**

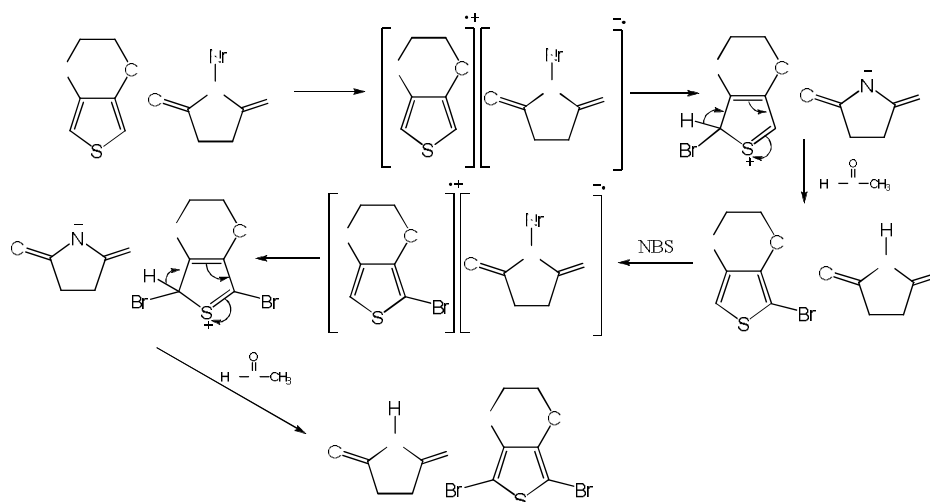
##### **4.1.1 Synthesis of 2,5-dibromo-3,4-ethylenedioxythiophene (DBEDOT)**

DBEDOT is the monomer to be used for solid state polymerization to form PEDOT. DBEDOT can be synthesized by bromination of EDOT. The mechanism of bromination of EDOT was purposed into 2 possible pathways [81,82].





**Scheme 4.1** Bromination via electrophilic aromatic substitution.



**Scheme 4.2** Bromination mechanism via radical-based single electron transfer followed by aromatic substitution.

Unlike the method described by Meng and coworkers [47], the bromination of EDOT using *N*-bromosuccinimide (NBS) in this work is a one step process. The quenching and neutralization were done simultaneously by washing the chloroform layer with saturated sodium hydrogen carbonate solution (20 mL  $\times$  3 times). The crystallization of DBEDOT product was then induced by an addition of a small amount of ethanol (3 mL) to a concentrated chloroform solution (containing  $\sim$  2 mL of chloroform) after most of chloroform was removed under reduced pressure using a

rotary evaporator. White needle-like crystals with 90% yield were recovered after purification by column chromatography and all the solvent (both chloroform and ethanol) was removed. The product was characterized by  $^1\text{H-NMR}$ .

$^1\text{H-NMR}$  spectra of the synthesized DBEDOT and EDOT are shown in Figure 4.1. The absence of a signal at 6.4 ppm suggested that the protons of EDOT at  $\alpha$  position to sulfur were substituted by bromine atoms after bromination by NBS while the proton signals of ethylene bridge at 4.27 ppm in singlet were remained [47].

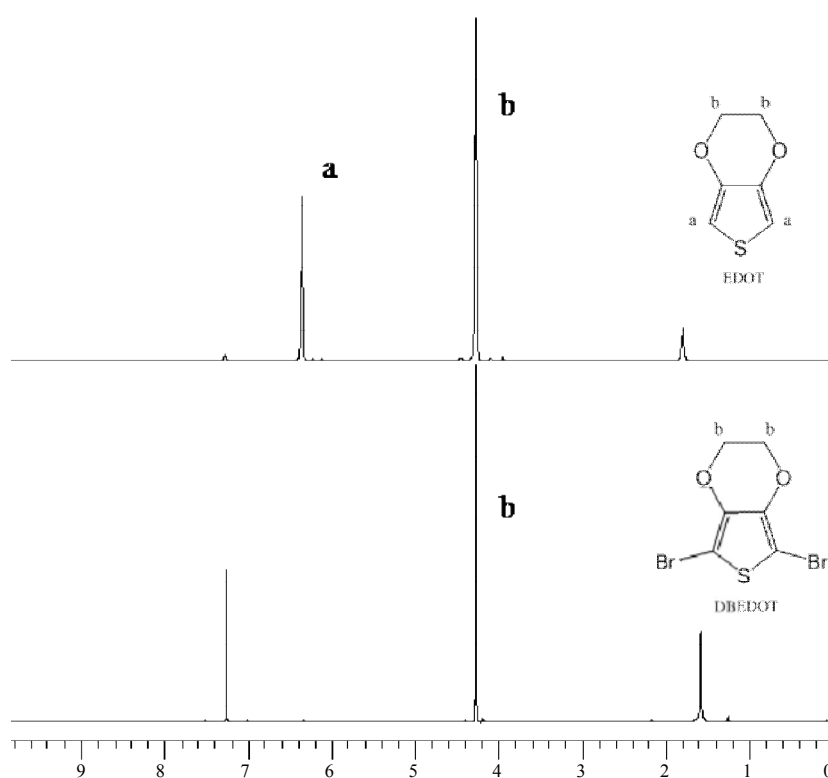


**Figure 4.1**  $^1\text{H-NMR}$  spectra of EDOT and DBEDOT.

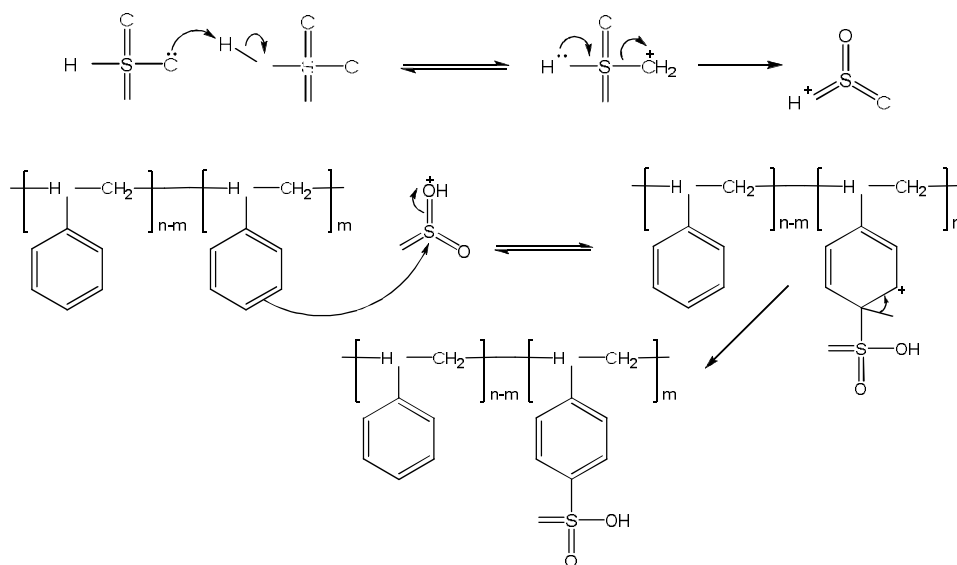
It was found that DBEDOT was highly soluble in all common organic solvents tested. The result is shown in Table 4.1 and its solution was stable when heated above solvent boiling point. DBEDOT melting temperature is about  $94^\circ\text{C}$ .

**Table 4.1** Solubility of DBEDOT

<b>Solvent</b>	<b>Observation</b>
Acetonitrile	Soluble
Butanol	Soluble (slow)
Chloroform	Soluble
Dichloromethane	Soluble
1,2-Dichloroethane	Soluble
1,4-Dioxane	Soluble
Ethanol	Soluble
Hexane	Soluble (with slightly heat)
<i>N,N</i> -Dimethylformamide	Soluble
Tetrahydrofuran	Soluble
Toluene	Soluble

#### **4.1.2 Synthesis of sulfonated polystyrene (SPS)**

H<sub>2</sub>SO<sub>4</sub> is the sulfonated reagent to be used for sulfonation of PS to form SPS. The mechanism of sulfonation on PS was based on electrophilic aromatic substitution of sulfur trioxide which can be formed by a loss of water from the sulfuric acid. Sulfur trioxide can act as a electrophile because it is a highly polar molecule with a fair amount of positive charge on the sulfur atom.



**Scheme 4.3** Sulfonation of PS via electrophilic aromatic substitution.

The  $\pi$  electrons of the aromatic C=C act as a nucleophile, attacking the electrophilic sulfur atom of sulfur trioxide, pushing charge out onto an electronegative oxygen atom. This destroys the aromaticity giving the cyclohexadienyl cation intermediate. Loss of the proton from the  $sp^3$  C bearing the sulfonyl group reforms the C=C and the aromatic system. The final stage of the reaction involves a transfer of the hydrogen from the ring to the negative oxygen or protonation of the conjugate base of the SPS by sulfuric acid produces the SPS.

Unlike the method reported by Makowski and coworkers [83], the sulfonation of PS using sulfuric acid 95-97% ( $H_2SO_4$ ) in this work is a one step process. The termination was done by adding cool methanol and then removed the solvent by rotary evaporator. The resultant solid was added by saturated sodium hydrogen carbonate aqueous solution for neutralization. The solution was filtered and protonated by washing consecutively with 10% HCl (aq) and water. The polymer was dried at  $70^\circ C$  for 7 days and thus kept in a desiccator. It was necessary to keep the SPS under dried condition since moisture can cause desulfonation. The product obtained as off-white powder (Figure 4.2) was characterized by  $^1H$ -NMR and FT-IR and subjected to solubility testing. The SPS prepared using the conc.  $H_2SO_4$  of 0.60,

0.90 and 1.20 mL (1:2.6, 1:1.7, and 1:1.3 equivalent to number of PS repeat unit) was designated as SPS A, SPS B, and SPS C, respectively.

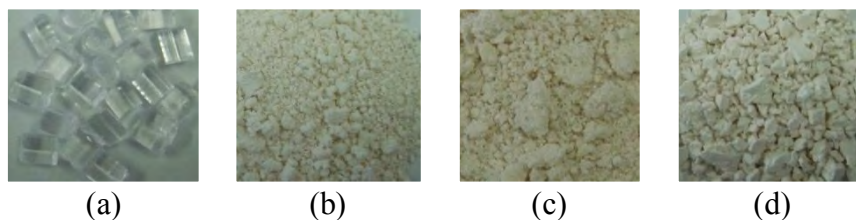


**Figure 4.2** Appearance of PS before (a) and after sulfonation: SPS A (b), SPS B (c), and SPS C (d).

$^1\text{H-NMR}$  spectra of the synthesized SPS A in comparison with PS are shown in Figure 4.3. After sulfonation, there was no change of the signals at 6.6 and 7.1 ppm which belong to the aromatic protons of PS in the spectrum of SPS A. This evidence implies that the degree of substitution was not high and the majority of PS was not reacted so that the chemical shifts of aromatic protons in the substituted repeat units cannot be distinguished from the unsubstituted one. The signal emerging at 5.3 ppm signifies the presence acidic proton of sulfonic acid [84,85]. The broadening of the signal appearing at 5.0 ppm after deuterium exchange helps verifying that the signal really came from the exchangeable acidic protons of the substituted sulfonic groups on the aromatic benzene ring of SPS. There are new signals at 2.1 and 2.2 ppm implying that the sulfonation may alter electronic environment of the methylene protons on the polymer backbone.

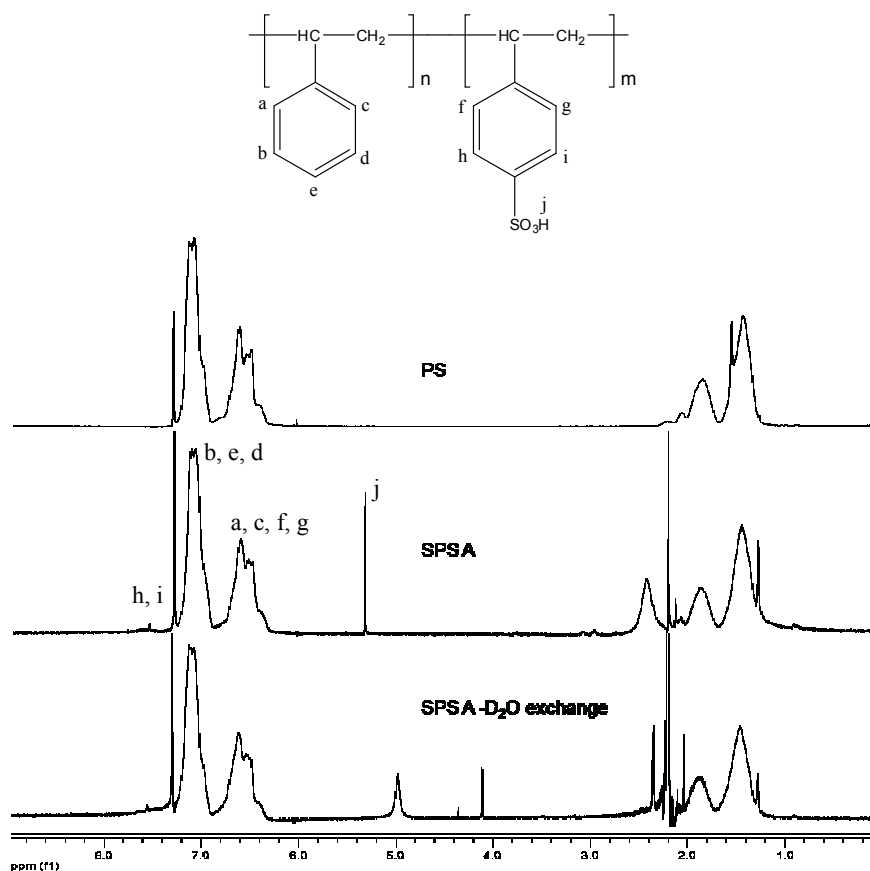
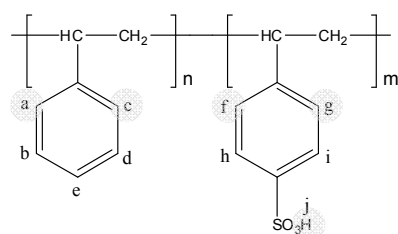


**Figure 4.3**  $^1\text{H}$ -NMR spectra of PS, SPS A, and SPS A after deuterium exchange.

Degree of sulfonyl group substitution (%DS) can be estimated from the  $^1\text{H}$ -NMR integration (Figure 4.4) using the following formula for calculation:



$$\%DS = m/(n + m) \times 100\%$$

$$\delta_{6.6} = 2m + 2n$$

$$\delta_{5.3} = m$$

$$n = (\delta_{6.6} - 2\delta_{5.3})/2$$

Where  $\delta_{5.3}$  and  $\delta_{6.6}$  are peak integration of the signals at 5.3 and 6.6 ppm, respectively.

The calculated %DS of all SPS samples are listed in Table 4.2.

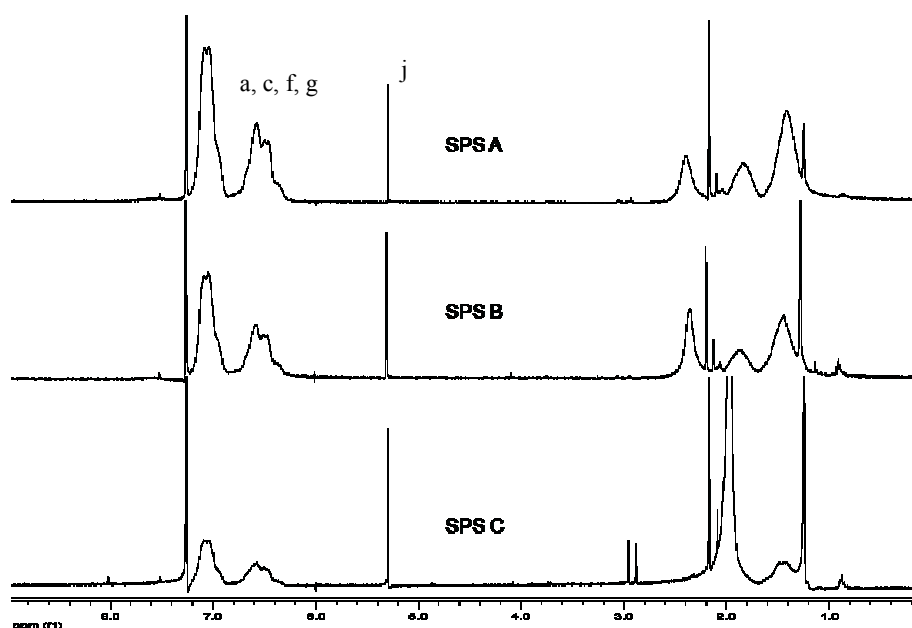


**Figure 4.4**  $^1\text{H}$ -NMR spectra of all SPS samples.

**Table 4.2** %DS of sulfonyl groups in SPS

Sample	Equivalent PS repeat unit: $\text{H}_2\text{SO}_4$	$\delta_{5.3}$	$\delta_{6.6}$	n	m	DS (%)
SPS A	2.6:1	4.20	100.00	45.80	4.20	8.40
SPS B	1.7:1	7.27	100.00	42.73	7.27	14.54
SPS C	1.3:1	16.21	100.00	33.79	16.21	32.42

FT-IR spectra of SPS are displayed in Figure 4.5. The peak assignments of SPS based on the literatures are given as follows [84,86]. The peaks at 609, 1124, and 1360  $\text{cm}^{-1}$  can be assigned to the asymmetric stretching of C–S, S–O, and S=O, respectively whereas the symmetric vibration of this bond produces the characteristic split band of absorbance at 1147 and 1184  $\text{cm}^{-1}$ . All SPS samples show a broad H-bonded O–H stretching in the region of 3127–3671  $\text{cm}^{-1}$ . The peaks due to C–H stretching at 2921 and 3020  $\text{cm}^{-1}$  were not affected by sulfonation.

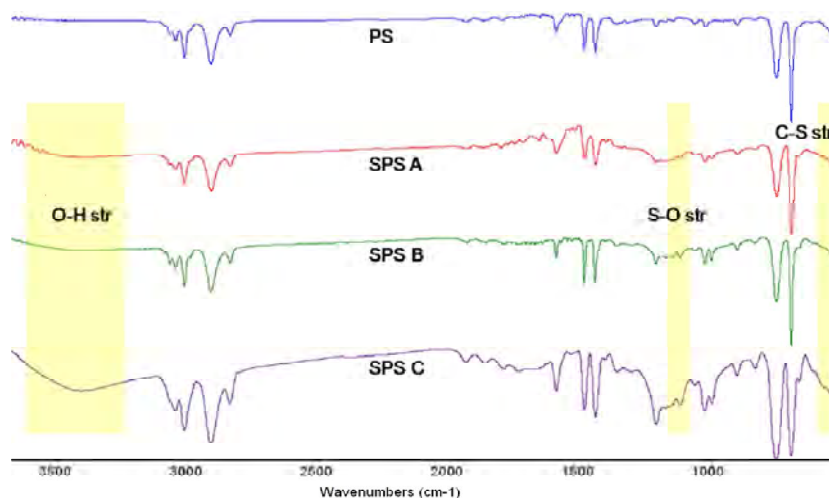


**Figure 4.5** FT-IR spectra of PS and SPS.

It was found that the solubility of SPS in DMF was much better than in THF indicating the enhanced polarity as a result of sulfonyl group incorporation taking into account about the fact that DMF is higher in polarity than THF. This characteristic is obviously opposite to the solubility of the virgin PS. The ability to solubilize in THF is inversely proportional to %DS. SPS C with the highest %DS (~30%) cannot at all dissolve in THF.

#### 4.2 Preparation of DBEDOT/polymer composite fiber mats

We have recently demonstrated that highly conductive polymer composites containing PEDOT can be obtained by SSP of DBEDOT embedded in a preformed insulating polymer matrix (i.e. PS, PB) film after appropriate thermal treatment [61]. Nonetheless, the fabrication process based on solution casting previously employed yielded the composite films with non-uniform conductivity due to the inhomogeneous distribution of the PEDOT in the matrix caused by phase incompatibility between the polar PEDOT and the non-polar matrix. Herein, we propose to use electrospinning as an alternative fabrication method. The rapid solvent evaporation and solidification of the fiber mat electrospun from the mixed solution between the desired matrix (PS or SPS) and DBEDOT should not allow enough time for the DBEDOT to phase separate



from the matrix and yield thin conductive composite film with improved PEDOT distribution and conductivity after the heat treatment.

In this research, PS was chosen as a matrix for the preparation of polymer composite mainly because it is easily spinnable. The condition of PS electrospinning has been well investigated [78,79,87], particularly with some conducting polymers including PEDOT, MEH-PPV, and poly(*o*-toluidine) [58,64,88]. The fact that its glass transition temperature and melting temperature ( $T_g = 100\text{ }^\circ\text{C}$ ,  $T_m = 256\text{ }^\circ\text{C}$ ) are above the melting temperature of DBEDOT ( $T_m = 94\text{ }^\circ\text{C}$ ) really complies with the strategy to conduct solid state polymerization by heat activation in the temperature range of 60-80  $^\circ\text{C}$ . There have also been reports suggesting that sulfonated PS (SPS) can be processed with a number of conducting polymers, namely polyaniline (PNI) and polypyrrole (PPy) [89,90]. Not only can the SPS be easily compatible with the polar conducting polymers, but it also acts as a dopant. For this reason, sulfonated analog of PS should presumably be another good matrix for the preparation of PEDOT-containing composite films.

As can be seen in Table 4.1, DBEDOT is highly soluble in most common organic solvents. In this particular study, THF and DMF were chosen as the solvents for processing mainly because both of them can dissolve both DBEDOT and the polymer matrix (PS and SPS). The dipole moment of DMF and THF are 3.82 and 1.63 Debye, respectively. In general, the concentration of polymer and type of solvent have significant impact on the morphology of the electrospun fibers: beads, fibers or a combination of beads and fibers. The polymer solution having low concentration generally leads to the formation of droplets or electrosplay [91] because the charged jet undergoes flow instability so a continuous stream of the charged jet cannot be formed. In the case of PS, it was found that the threshold polymer concentration that yielded reasonably uniform fibers and good surface coverage was 12% (w/v). Due to its lower polarity and faster rate of evaporation, THF generated fibers with a lot of beads (Figure 4.6). The beads then disappeared upon an incorporation of DMF, the solvent that is higher in polarity and has slower rate of evaporation as compared with THF. This can be observed when 1:1 (v/v) THF/DMF was used. In fact, this mixed solvent system seems to give fibers with more well-defined morphology and size distribution than DMF. Similar outcome was also observed in the case of SPS. The

morphology of fibers illustrated in Figure 4.6 (d-f) belong to SPS B, the sulfonated PS having moderate %DS (~15%).

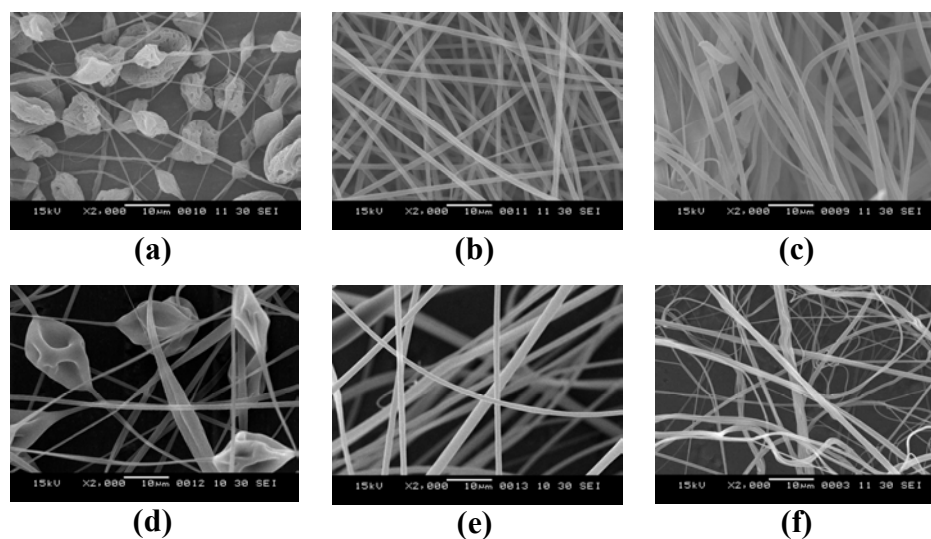


**Figure 4.6** SEM micrographs (at 2,000 $\times$ ) of as-spun PS fiber mat electrospun from 12% (w/v) PS in (a) THF, (b) mixed 1:1 (v/v) THF/DMF, and (c) DMF and as-spun SPS B fiber mat electrospun from 12% (w/v) SPS B in (d) THF, (e) mixed 1:1 THF/DMF, and (f) DMF.

Unlike the fibers electrospun from the PS solution, the fibers generated by electrospinning of the mixed solution between the PS and DBEDOT were interconnected. Apparently, the resulting fibers were less defined regardless of the solvent used for making the solution (Figure 4.7). Due to its greater polarity than THF and the mixed THF/DMF, DMF provided less fiber spreading ability and thus yielded the PS fiber mats having greater thickness (See Table 4.5 for thickness data).

On the other hand, THF seems to be a more preferable solvent for the fabrication of DBEDOT/SPS fiber mats by electrospinning than DMF and mixed 1:1 (v/v) THF/DMF. As seen in Figure 4.8, more uniform, bead-free fiber mats can be formed for both SPS A (~8 %DS) and SPS B (~15%DS). This may be explained by the fact that SPS itself is also charged. Upon using the solvent with high polarity (DMF or mixed 1:1 (v/v) THF/DMF) which should be good solvent for SPS, the charge repulsion between the polymer chains may be stronger than the attractive force

due to entanglement. As a result, the charge jet underwent flow instability leading to the formation of droplets because a continuous stream of the charged jet cannot be formed. Since SPS C having the highest %DS of 30% is not soluble in THF, it was not possible to obtain the DBEDOT/SPS C composite fiber mats with good fiber characteristics and distribution by electrospinning.

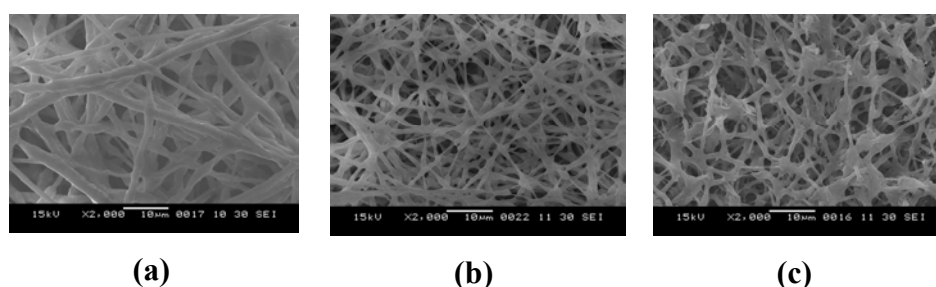


**Figure 4.7** SEM micrographs (at 2,000 $\times$ ) of as-spun DBEDOT/PS composite fiber mats electrospun from a mixture containing 3:1 (w/w) DBEDOT/PS in (a) THF, (b) mixed 1:1 (v/v) THF/DMF, and (c) DMF.

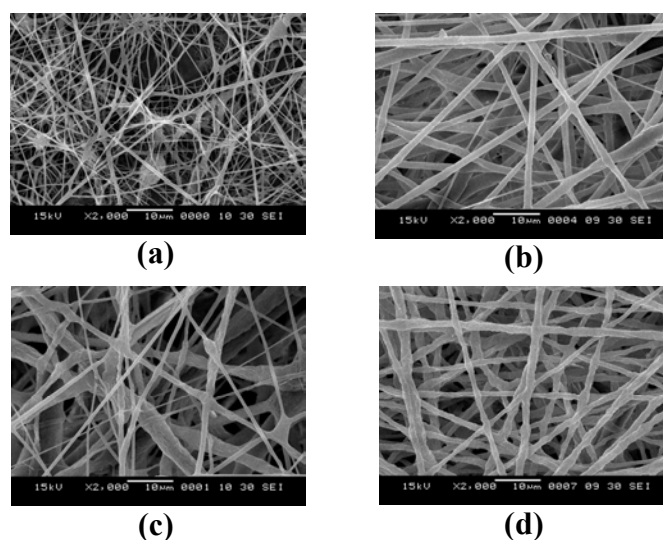


**Figure 4.8** SEM micrographs (at 2,000 $\times$ ) of as-spun DBEDOT/SPS composite fiber mats electrospun from a mixture containing 3:1 (w/w) DBEDOT/SPS B in (a) DMF, (b) THF, and (c) mixed 1:1 (v/v) THF/DMF, and 3:1 DBEDOT/SPS A (w/w) in THF (d).

### 4.3 Preparation and conductivity of PEDOT/polymer composite films

As proposed by Meng and co-workers [45,47], DBEDOT molecules in the form of crystal pack closely in parallel fashion which facilitates polymerization process in solid state. Most likely, the polymerization occurs along the stacks of the monomer and must be accompanied by significant rotation and some movement of the molecules. DBEDOT can transform to PEDOT by condensation during heat treatment. The initiation involves oxidation of DBEDOT by bromine ( $\text{Br}_2$ ) and generates DBEDOT radical carbocation as shown in Scheme 3.3. In the propagation step, this radical carbocation first reacts with another DBEDOT to form DBEDOT dimer, also in the form of radical carbocation. The elimination of bromine then yields DBEDOT dimer which will go through the propagation step and eventually forms PEDOT. The presence of bromine in the reaction, in fact, facilitates polymerization in the initiation step. Effects of several parameters on the conductivity of the resulting PEDOT containing composite films were investigated.

#### 4.3.1 Effect of compression

Upon the heat treatment, the DBEDOT/PS fiber mats completely lost the fibrous feature as visualized from SEM images shown in Figure 4.9 (e and f). As illustrated in Figure 4.9(d), the color of the DBEDOT/PS fiber mats on a glass substrate gradually changed from white to dark blue and completely turned black within 24 h upon heating at  $70^\circ\text{C}$ . The blue color can primarily be used as an indication of the SSP and the formation of PEDOT. The compression or pressing of the DBEDOT/PS fiber mats during the heat treatment was found to be critical to the effectiveness of SSP process. If the compression was applied during the heat treatment, the resulting PEDOT/PS composite film (Figure 4.9(f)) was smoother and more homogeneous than that obtained without the compression (Figure 4.9(e)) suggesting that the PEDOT can be well dispersed in the former case. The uniform distribution of the sub-micron PEDOT particles (extracted from the PEDOT/PS composite), having a diameter of  $101.05 \pm 7.79$  nm, of which morphology is shown in Figure 4.10(a), yielded the PS/PEDOT composite film with conductivity as high as 13.24 S/cm as opposed to the composite film formed in the absence of compression,

having the non-uniform PEDOT particles (Figure 4.10(a)), of which conductivity was only  $5 \times 10^{-4}$  S/cm. The low conductivity can also be explained from the fact that the compression or pressing can raise the percentage yield of the PEDOT formed in the matrix from 37% to 64%.

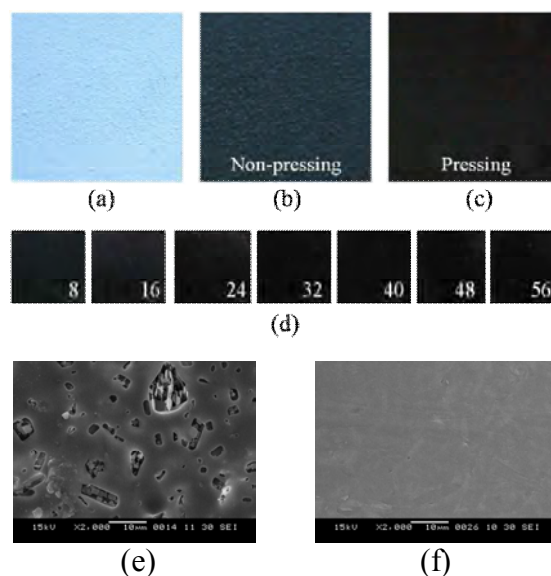


**Figure 4.9** Physical appearances of DBEDOT/PS composite fiber mats electrospun from a mixture containing 3:1 (w/w) DBEDOT/PS in DMF before SSP (a), after SSP at 70 °C for 40 h without (b) and with (c) pressing, and as a function of reaction time (d). SEM micrographs (at 2,000x) of PEDOT/PS composite film obtained after SSP at 70 °C for 40 h without (e) and with (f) pressing.

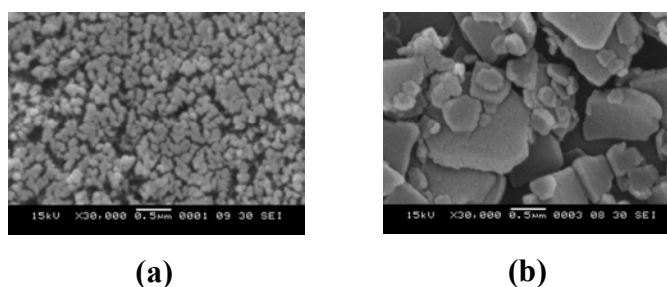


**Figure 4.10** SEM micrographs (at 30,000 $\times$ ) of PEDOT particles extracted from PEDOT/PS composite film prepared by SSP of the 3:1 (w/w) DBEDOT/PS fiber mats at 70 °C for 40 h with (a) and without (b) pressing.

The greater quantity of PEDOT in the PEDOT/PS composite film prepared by compression during heat treatment than those obtained in the absence of compression can also be realized by SEM analysis using EDS mode. According to the data shown in Table 4.3, there is much greater sulfur content especially on the surface of the PEDOT/PS composite film prepared with pressing than that prepared without pressing. This also helps explaining why the conductivity of the former is much higher than the latter because it is the surface of the composite film that came into contact with the four probes of the four-point probe conductometer during the conductivity measurement.

**Table 4.3** Weight percentage of element of the PEDOT/PS composite film obtained by SEM analysis using EDS mode

Element	%Weight	
	Without pressing	With pressing
C	57.41 ± 0.39	51.56 ± 0.21
O	16.81 ± 0.58	11.09 ± 0.8
S	1.79 ± 0.83	10.9 ± 0.57
Br	23.99 ± 1.43	26.46 ± 0.35

X-ray diffraction patterns shown in Figure 4.11 reveal the crystalline structure of the DBEDOT, PEDOT, and PS from PEDOT/PS composite films in comparison with the controlled PEDOT that was directly obtained from the heating of DBEDOT in the absence of polymer matrix. Similar to the XRD pattern of PEDOT previously reported by others [47,92], broad peak was found in the range of  $2\theta = 20-30^\circ$  for both the controlled PEDOT (Figure 4.11(b)) and PEDOT in composite film (Figure 4.11(f)) indicating the disordered structure as opposed to the crystalline structure of DBEDOT (Figure 4.11(a)) of which strong and quite sharp diffraction peaks were observed at  $2\theta \sim 6.1^\circ$ ,  $13.1^\circ$  and  $25.6^\circ$  corresponding to the (100), (200), and (020) of the orthorhombic crystal structure. The fact that the characteristic pattern of the

DBEDOT in DBEDOT/PS composite film (Figure 4.11(d)) closely resembles to that of the virgin DBEDOT (Figure 4.11(a)) strongly suggests that the electrospinning process did not alter the structure of the DBEDOT. The XRD pattern of the PEDOT/PS composite film obtained after SSP without pressing (Figure 4.11(e)) was so similar to that of DBEDOT/PS fiber mats evidently indicating that most of the DBEDOT still remained unpolymerized and was not converted to PEDOT. This is in good agreement with the conductivity result.

Results shown in Figure 4.12 demonstrate that 24 h was sufficient to bring SSP of DBEDOT to completion. This is in good agreement with the observation based on the color change. The conductivity of the PEDOT/PS composite film was not significantly increased as the heating time was extended beyond 24 h. The fact that the conductivity values measured on the bottom side can almost be superimposed on those measured on the top side implied that the PEDOT distributed evenly throughout the thickness of the composite film.

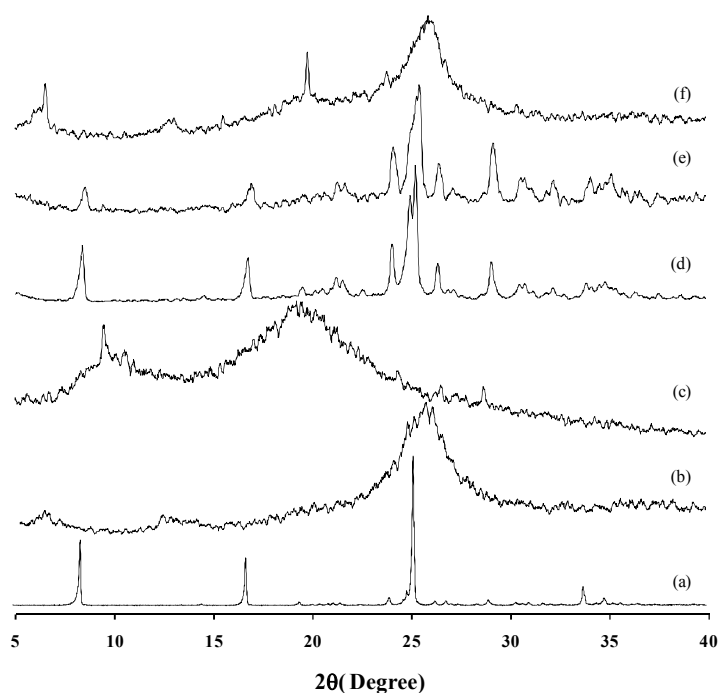


**Figure 4.11** XRD diffractograms of (a) DBEDOT crystal, (b) controlled PEDOT, (c) electrospun PS fiber mat, (d) electrospun 3:1 (w/w) DBEDOT/PS fiber mat, PEDOT/PS composite film obtained from SSP of the 3:1 (w/w) DBEDOT/PS fiber mat electrospun from DMF solution without (e) and with (f) pressing.

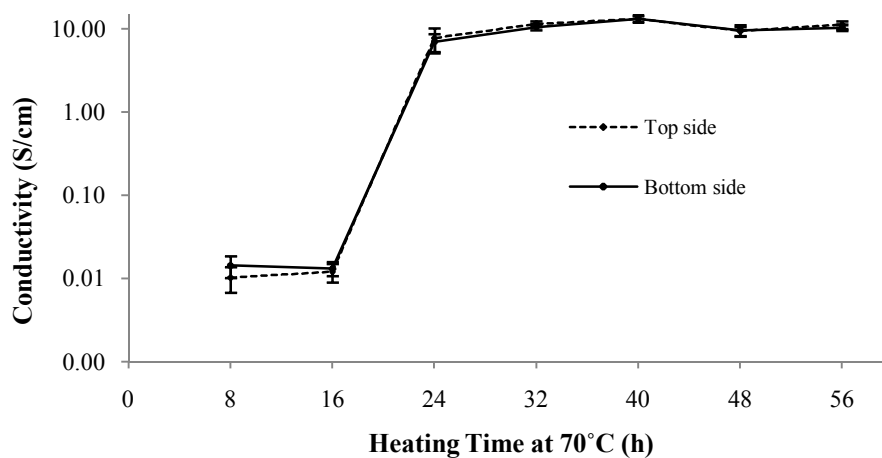


**Figure 4.12** Conductivity measured on the top and bottom side of the PEDOT/PS composite film prepared by SSP of the electrospun 3:1 (w/w) DBEDOT/ PS fiber mats by heating at 70 °C for 40 h with pressing as a function of reaction time.

#### 4.3.2 Effect of temperature and DBEDOT/polymer weight ratio

Heat activation in a temperature range of 60-80 °C was originally chosen to be used for inducing SSP mainly because it is below the melting temperatures of PS and SPS ( $T_m$  of PS and SPS > 200 °C, See DSC data in the subsequent section) and DBEDOT ( $T_m = 94$  °C). It should be emphasized that heating above 80 °C for more than 8 h was found to cause the composite film to turn transparent and melt during the heat treatment whereas the temperature below 60 °C was found to be ineffective to induce SSP. Only a small extent of polymerization was evidenced as can be realized by a slight color change of the film from white to grayish blue even after 40 h of heat treatment. Besides the observation on color change, the extent of SSP as a function of temperature using for heat activation can be quantitatively verified by the conductivity values as outlined in Table 4.4. Using the same heating time of 40 h, the 70 °C seems to be the suitable temperature for heat treatment as indicated by the highest conductivity obtained. The temperature of 60 °C was too low to effectively induce SSP whereas the temperature of 80 °C is so close to  $T_m$  of DBEDOT that the softening of the DBEDOT may occur and the polymerization was no longer in the solid state. The incomplete polymerization of DBEDOT can also be evidenced from



the presence of the characteristic crystalline peak at  $25.6^\circ$  of the PEDOT/PS composite film prepared by heat activation at  $60^\circ\text{C}$  shown in Figure 4.13.

**Table 4.4** Conductivity of the PEDOT/PS composite film prepared by SSP of the electrospun DBEDOT/PS fiber mat by heating for 40 h

DBEDOT:PS (%w/w)	Heating temperature ( $^\circ\text{C}$ )	Conductivity (S/cm)
3:1	60	3.46
	70	13.24
	80	3.04
2:1	70	3.81

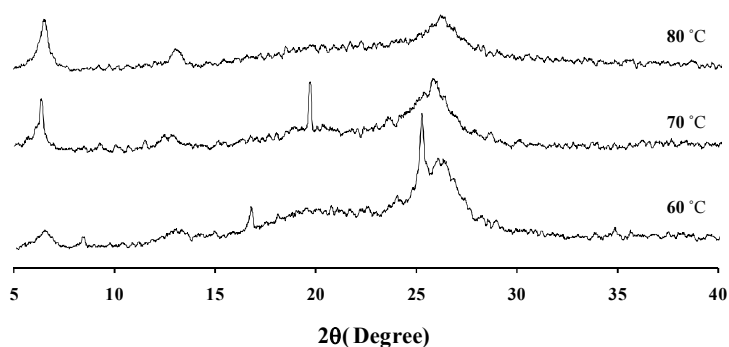


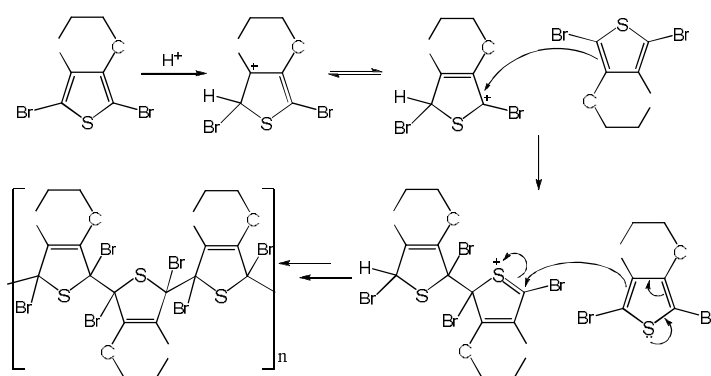
**Figure 4.13** XRD diffractograms of PEDOT/PS composite film prepared by SSP of the 3:1 (w/w) DBEDOT/PS fiber mat electrospun from DMF solution with pressing using different temperature for heat activation.

The fact that the composite film became less conductive upon decreasing the DBEDOT:PS weight ratio from 3:1 to 2:1 suggests that the conductivity of the PEDOT/PS composite film is proportional to the quantity of DBEDOT incorporated. It should be emphasized that the PEDOT/PS composite film obtained by heating the

electrospun DBEDOT/PS fiber mat having the DBEDOT:PS weight ratio of 4:1 was so brittle that it should not be desirable for practical purpose.

### 4.3.3 Effect of polymer matrix, solvent, and additive

As expected, the replacement of PS with its sulfonated counterpart, SPS, can raise the conductivity of the composite film. Upon using THF as a solvent, the conductivity of the PEDOT/SPS A composite film can reach as high as 13.88 S/cm (Table 4.5). This can be explained as a consequence of additional doping of the PEDOT by sulfonate groups of SPS A. Nevertheless, increasing the content of sulfonate groups from ~8 to ~15% did not promote the doping. The conductivity of the PEDOT/SPS B became lower (6.75 S/cm). It is believed that the excess acidity introduced from the SPS B somehow induce further chain growth of the PEDOT repeat unit and then destroy the conjugation length and deteriorate the conductivity. In fact, such speculation has been supported by the mechanism proposed in the literatures on the impact of acid on the polymerization of DBEDOT shown in Scheme 4.4 [93,94]. It should be emphasized that PS, SPS A, and SPS B exhibited similar thickness of ~20  $\mu\text{m}$  so the different conductivity should presumably depend on the nature of the matrix itself and should not have anything to do with the thickness variation.



**Scheme 4.4** Acid-initiated coupling promotes chain growth but yields an unconjugated form of PEDOT in high substitution degree of SPS matrix.

In the case of PS matrix, the greatest conductivity of the PEDOT/PS composite film was obtained when DMF was used as the solvent for making DBEDOT/ PS mixed solution for electrospinning. The fact that the DBEDOT/PS fiber mat electrospun from DMF was not as well spread out as that electrospun from the 1:1(v/v) THF/DMF and THF alone explain why the thickness of the PEDOT/PS composite film processed from DMF was the highest (See Table 4.5). The deposition of the DBEDOT in a narrow area would yield the PEDOT/PS composite film with locally high PEDOT density. As a result, the PEDOT/PS composite film obtained from the DBEDOT/PS fiber mat electrospun from DMF solution exhibited the highest conductivity. It is thus reasonable to see that the conductivity of the PEDOT/PS composite films were proportionally decreased as the solvent for electrospinning was altered from DMF to 1:1 (v/v) THF/DMF and THF. Since the boiling point of DMF (153 °C) is higher than the temperature used for the heat treatment (60-80 °C), it is also possible that there was some solvent left in the composite after the SSP. This residual polar solvent is believed to possess a screening effect between the dopant (counter ions) and charged carriers of the PEDOT main chain, which suppresses the coulomb interactions between the positively charged PEDOT and the bromine dopant [95] and subsequently promotes the charge transport within the PEDOT/PS composites. The same explanation should be applied for THF but the degree of screening should be less considering the lower boiling point and polarity of THF (66 °C, 1.63 Debye) than DMF (153 °C, 3.82 Debye).

Incorporation of some additives, for example, ethylene glycol (Eg) and pyridine (Py), did not have positive impact on the conductivity of the PEDOT/PS composite film. It is suspected that the additives introduced made the electrospun DBEDOT/PS spread much more efficiently resulting in thinner PEDOT/PS composite film. Nonetheless, the conductivity of the PEDOT/PS composite film did not correspond with the thickness. It may be difficult to take into account the thickness variation when comparing the composites having different additive. Even though the PEDOT/PS composite film having Py as the additive was almost twice thicker than that having Eg as the additive. Eg may behave as better screening molecules than Py so the composite containing Py was not as conductive as that containing Eg. It is also possible that the reducing property of the Py somewhat destroyed the bromine dopant and deteriorate the conducting property of the composite film.

**Table 4.5** Thickness and conductivity of the PEDOT/PS composite film prepared by SSP of the DBEDOT/PS fiber mat electrospun from different solution by heating at 70 °C for 40 h with pressing

<b>Matrix</b>	<b>Solvent, additive</b>	<b>Thickness (<math>\mu\text{m}</math>)</b>	<b>Conductivity (S/cm)</b>
PS	THF	19.91 $\pm$ 2.19	2.75
PS	1:1 THF/DMF	49.39 $\pm$ 1.95	5.46
PS	DMF	55.24 $\pm$ 3.44	13.24
PS	DMF, Eg	25.83 $\pm$ 0.13	6.41
PS	DMF, Py	42.61 $\pm$ 0.82	5.08
SPS A	THF	17.90 $\pm$ 0.26	13.88
SPS B	THF	18.21 $\pm$ 0.62	6.75

#### 4.3.4 Effect of storage time

As demonstrated in Figure 4.14, it was found that the conductivity kept going up upon storage. The conductivity of the stored PEDOT/PS composite film was two times higher than the as-prepared PEDOT/PS composite film. This feature implies that although the SSP can be accelerated by heat treatment, the polymerization does not come to completion with a limited amount of time. This evidently agree with what has been described by Meng et al. that the most efficient SSP occurred spontaneously and very slowly at ambient temperature [45,47]. The greater degree of polymerization is yet to be confirmed by %yield determination.

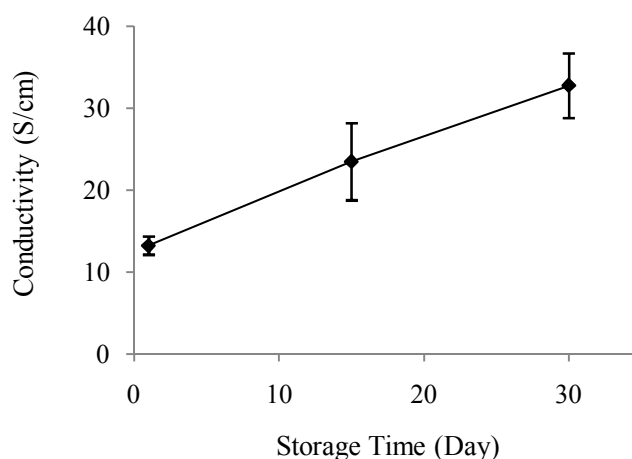


**Figure 4.14** Conductivity of PEDOT/PS composite film prepared by SSP of the 3:1 (w/w) DBEDOT/PS fiber mat electrospun from DMF solution with pressing as a function of storage time at ambient temperature.

#### 4.4 Physical characteristics of PEDOT-containing polymer composite films

The fact that the FT-Raman spectra of the composite films (Figure 4.15) exhibit the same fingerprints as those of the controlled PEDOT confirms the success of SSP in both PS and SPS matrices. The peak assignments of PEDOT based on the literatures are given as follows [96-98]. The peaks at 575 and 991  $\text{cm}^{-1}$  correspond to the ethylenedioxy ring deformation. The peaks at 700 and 1140  $\text{cm}^{-1}$  identified in the spectra are due to the symmetric stretching of the C-S-C deformation and the C-O-C deformation, respectively. The peak at 1261  $\text{cm}^{-1}$  is assigned to  $\text{C}_\alpha\text{-C}_\alpha$  inter-ring stretching while the symmetric and asymmetric  $\text{C}_\alpha\text{=C}_\beta$  stretching appear at 1433 and 1538  $\text{cm}^{-1}$ , respectively.

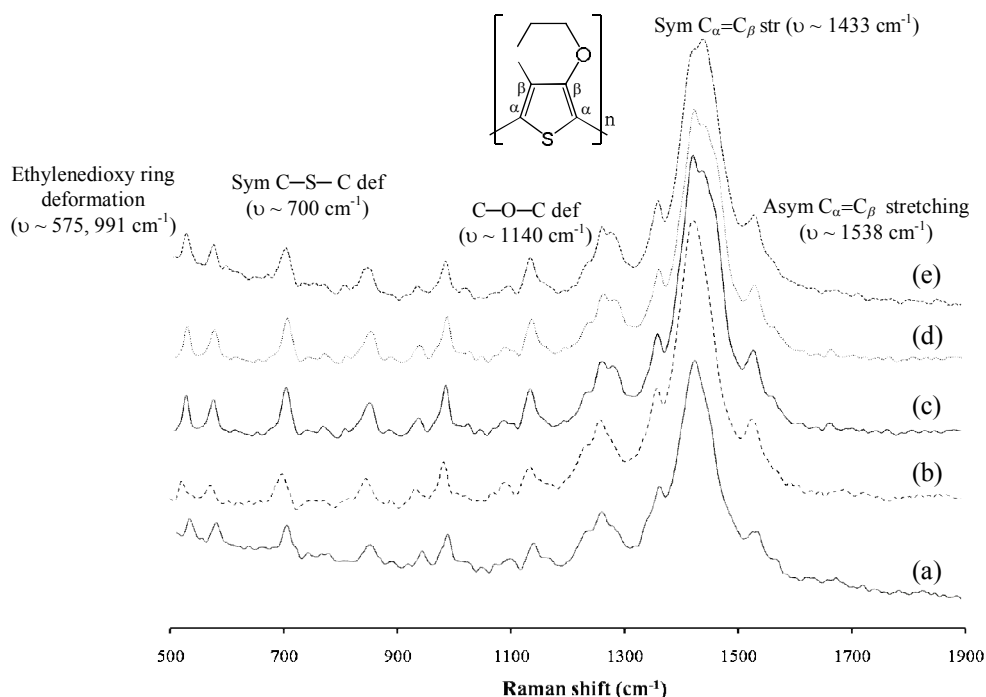
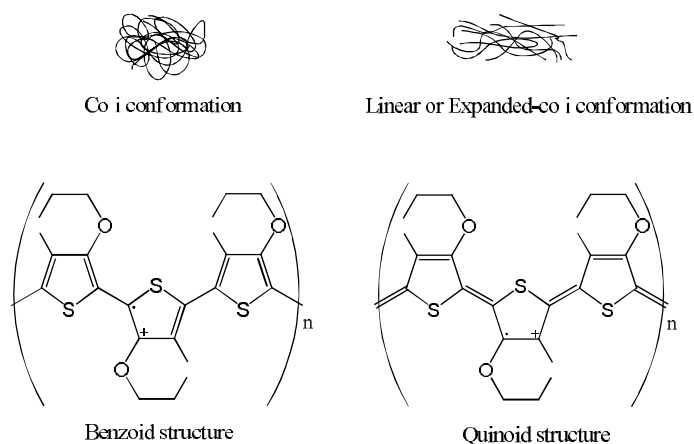


**Figure 4.15** FT-Raman spectra of (a) PEDOT/PS, DMF, pressing, (b) PEDOT/PS, THF, pressing, (c) controlled PEDOT, (d) PEDOT/PS, DMF, non-pressing, and (e) PEDOT/SPS A, THF, pressing.

The position of the band in the region of  $1400\text{-}1500 \text{ cm}^{-1}$  assigned to the symmetric stretching vibration of  $C_{\alpha}=C_{\beta}$  on the five-member ring of PEDOT can be used as an indication of PEDOT conformation and resonance structure [101-103]. When the PEDOT chains adopt coil conformation, benzoid is their favorable resonance structure (Scheme 4.5). In principle, electron transfer between the PEDOT chains having coil conformation is difficult, so that the PEDOT chains cannot be completely reduced electrochemically (difficult to dope). When the PEDOT chains are in the form of more rigid conformation, linear or expanded coil, their favorable resonance structure is quinoid which can be easily and completely doped by bromine. As a result, the quinoid structure demands less energy to vibrate so the stretching vibration of  $C_{\alpha}=C_{\beta}$  would appear at lower wavenumber than that of the benzoid structure.



**Scheme 4.5** Conformation and resonance structure of PEDOT chain structure.

From the Raman spectra specifically focusing in the region of  $1400\text{-}1500\text{ cm}^{-1}$  shown in Figure 4.16, it was found that the PEDOT chains having relatively high conductivity, namely controlled PEDOT (4.16(a)), and PEDOT/PS composite film prepared by SSP of the DBEDOT/PS fiber mat electrospun from DMF with pressing (4.16(b)) exhibit a single peak at  $\sim 1425\text{ cm}^{-1}$  (Table 4.6) with a slight shoulder on the high wavenumber side of the peak, indicating the majority of the PEDOT chains adopt the more rigid, linear or expanded coil conformation with benzoid structure. The shoulder became more obvious for the PEDOT/PS composite film having Eg as the additive (4.16(c)), of which the conductivity was less than the one without the additive. It is obvious that the composite films having relatively low conductivity exhibit two distinguishable peaks (4.16(d-f)) suggesting that the PEDOT chains are present both in the form of coil and linear/expanded coil conformation and having both quinoid and benzoid resonance structure. The lower the conductivity, the more the peak shifting towards the higher wavenumber suggesting that the benzoid is more favorable than the quinoid.

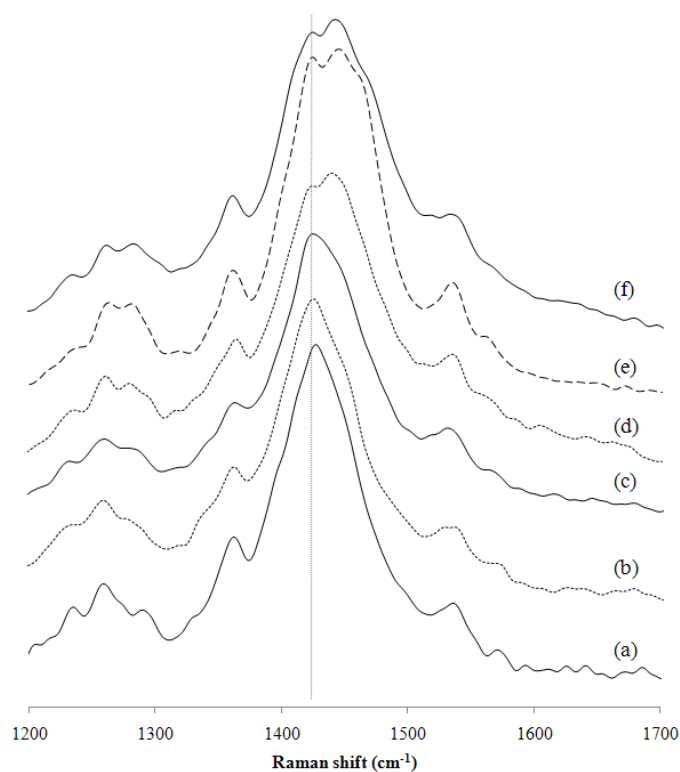


**Figure 4.16** FT-Raman spectra of (a) controlled PEDOT, (b) PS/PEDOT, DMF pressing, (c) PS/PEDOT, DMF, pressing, Eg, (d) PEDOT/PS, DMF, pressing, Py, (e) PS/PEDOT, DMF, non pressing, and (f) PEDOT/SPS A, THF, Pressing.

**Table 4.6** Raman shift of the symmetric  $C_{\alpha}=C_{\beta}$  stretching of PEDOT in the composite film

Sample	Solvent	Pressing	Additive	Conductivity (S/cm)	$C_{\alpha}=C_{\beta}$ stretching ( $\text{cm}^{-1}$ )
Controlled PEDOT	-	-	-	17.61	1426
PEDOT/PS	DMF	✓	-	13.24	1425
PEDOT/PS	DMF	✓	Eg	6.41	1424
PEDOT/PS	DMF	✓	Py	5.48	1430, 1439
PEDOT/PS	THF	✓	-	2.75	1427, 1442
PEDOT/SPS A	THF	✓	-	13.88	1431, 1442
PEDOT/PS	DMF	-	-	$5 \times 10^{-3}$	1429, 1445



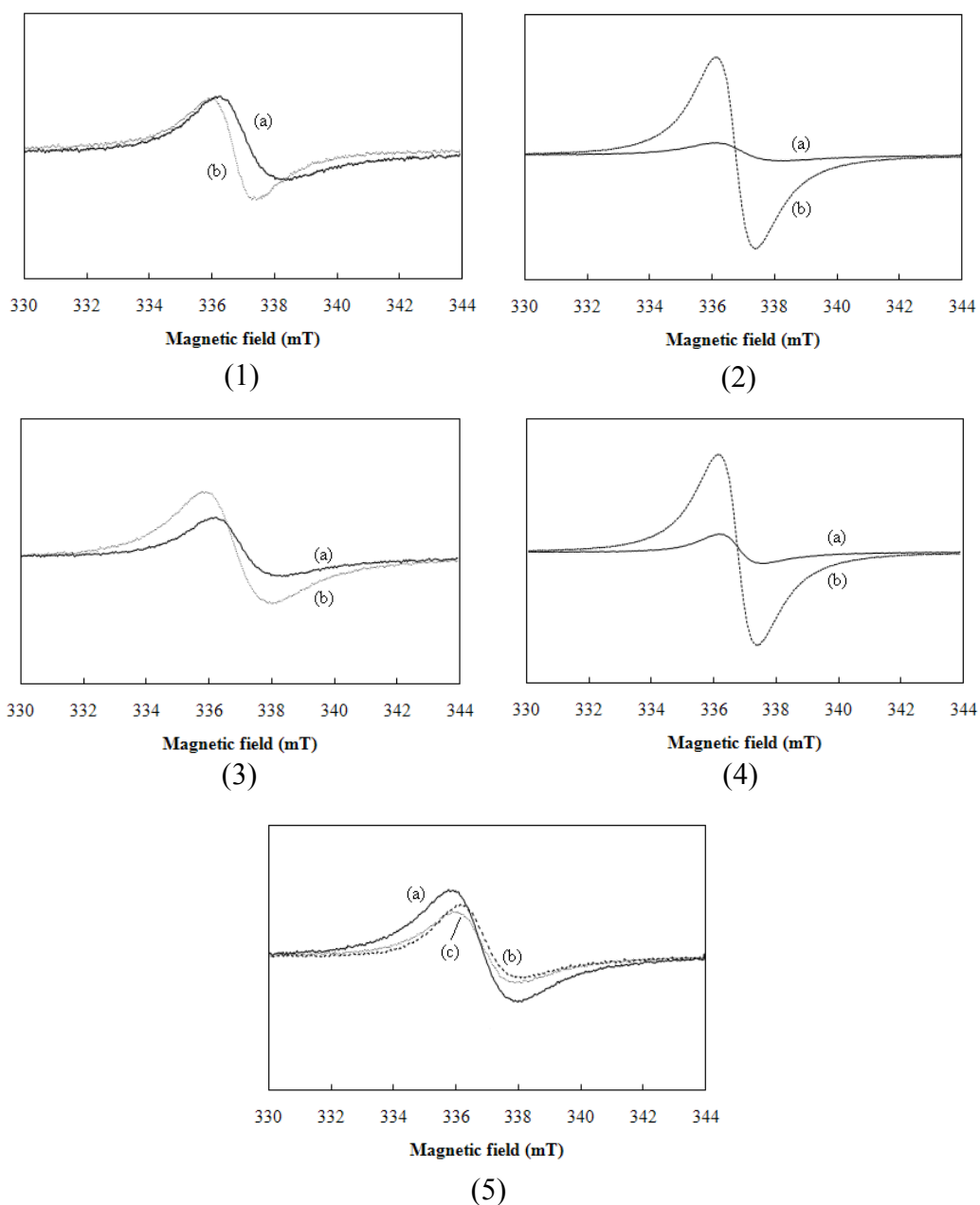


**Figure 4.17** ESR of the PEDOT/polymer composite of PEDOT/PS, DMF, pressing (1a, 2a, 3a, and 5a), PEDOT/PS, DMF, non pressing (1b), PEDOT/PS, THF, pressing (2b,4b), PEDOT/PS, DMF, pressing, fresh (3b), PEDOT/SPS, THF, Pressing (4a), PEDOT/PS, DMF, pressing, Eg (5b), and PEDOT/PS, DMF, pressing, Py (5c).

The nature of the radical cation charge carriers of PEDOT in the PEDOT/PS composite and PEDOT/SPS composite film was characterized by ESR as illustrated in Figure 4.17. The conductivity of the doped PEDOT is brought about by dication and

radical cation charge carriers [104]. A strong ESR signal was observed at  $g \approx 2.002$ - $2.005$  as outlined in Table 4.7. The ESR line width is determined by relaxation rate of the radical and is a characteristic of the degree of delocalization, the increase of ESR line width would lead to greater conductivity [99]. A polaron corresponds to a positive charge on a unit so it has a spin of  $\frac{1}{2}$  whereas a bipolaron corresponds to two positive charges delocalized over several units so it is spinless. The bipolaron would give ESR signal with less intensity but results in higher conductivity than the polaron. The transition from polarons to bipolarons is due to the conformational change of the PEDOT chains from coil to linear or expanded-coil structure so that the charge becomes more delocalized on the PEDOT chains [100]. According to the data shown in Table 4.7, it was found that the lower the conductivity of the composite film, the greater the ESR peak intensity and the narrower line width.

**Table 4.7** ESR data of the PEDOT/polymer composite film

<b>PEDOT composites</b>	<b>Pressing</b>	<b>g-factor</b>	<b>Intensity</b>	<b>line width (<math>\mu\text{T}</math>)</b>
Controlled PEDOT	-	2.005	1310	1657
PEDOT/SPS A, THF	✓	2.004	2403	1390
PEDOT/PS, DMF	✓	2.002	1473	2229
PEDOT/PS, DMF, Fresh	✓	2.004	2770	2244
PEDOT/PS, DMF, Eg	✓	2.003	1754	2226
PEDOT/PS, DMF, Py	✓	2.002	1832	2031
PEDOT/PS, THF	✓	2.004	15546	1268
PEDOT/PS, DMF	-	2.004	1814	1349

Thermal properties of the PEDOT/polymer composite film and electrospun DBEDOT/polymer fiber mat in comparison with the controlled PEDOT as well as the starting materials including PS pellets, electrospun PS fibers, as-synthesized SPS A, electrospun SPS A fibers were characterized by DSC and TGA. The electrospun DBEDOT/PS and DBEDOT/SPS A fiber mats were electrospun from the mixed solution having 3:1 (w/w) DBEDOT/polymer in DMF and THF, respectively. The condition used for SSP is heating at  $70^\circ\text{C}$  for 40 h with or without pressing. As can be

seen in Figure 4.18, upon the introduction of ~8% of sulfonyl groups to PS yielding SPS A (Figure 4.18(c)),  $T_g$  has slightly changed from that of the PS ~ 100 °C (Figure 4.18(a,b)) to 96 °C of the SPS A. Unlike the pristine PS pellets (4.18(a)), the SPS A exhibited  $T_m$  peak at 168 °C (Figure 4.18(c)) indicating the semi-crystalline morphology of this sulfonated PS [84].

The lower  $T_m$  of the SPS A than that of the PS suggested that the charge repulsions reduce the inter- and intra-chain interactions between the SPS A polymeric chains so that the SPS A demands less energy to melt. The  $T_g$  of the SPS A became considerably lower (< 100 °C) and the  $T_m$  almost disappeared after being electrospun into fibers (Figure 4.18(d)).

The endothermic peaks appearing at 94 and 195 °C in the thermogram of the DBEDOT/PS fiber mats (Figure 4.18(e)) signifies the thermal transitions of the DBEDOT which is in good agreement with the value reported by Meng and coworkers [47]. This also indicated that the thermal characteristic of the DBEDOT was not affected by the electrospinning process.

The incomplete polymerization of the DBEDOT in the DBEDOT/PS fiber mats when subjected to heat treatment without pressing can also be verified by the unchanged thermogram of the PEDOT/PS film without pressing (Figure 4.18(f)) when compared with that of the DBEDOT/PS fiber mats before heat treatment (Figure 4.18(e)). When pressing was applied, the SSP of the DBEDOT into the PEDOT was much more efficient so that the characteristic feature of the DBEDOT did not appear in the thermogram of PEDOT/PS film without pressing (Figure 4.18(h)), but exhibited two endothermic peaks appearing at lower temperature (105, 174 °C) than those of the controlled PEDOT (Figure 4.18(g)) that was synthesized by SSP of DBEDOT in the absence of polymer matrix. Besides the thermal transition previously observed at 77 °C for the electrospun SPS A fiber mats, the PEDOT/SPS A exhibited an additional endothermic peak at 114 °C (Figure 4.18(i)).

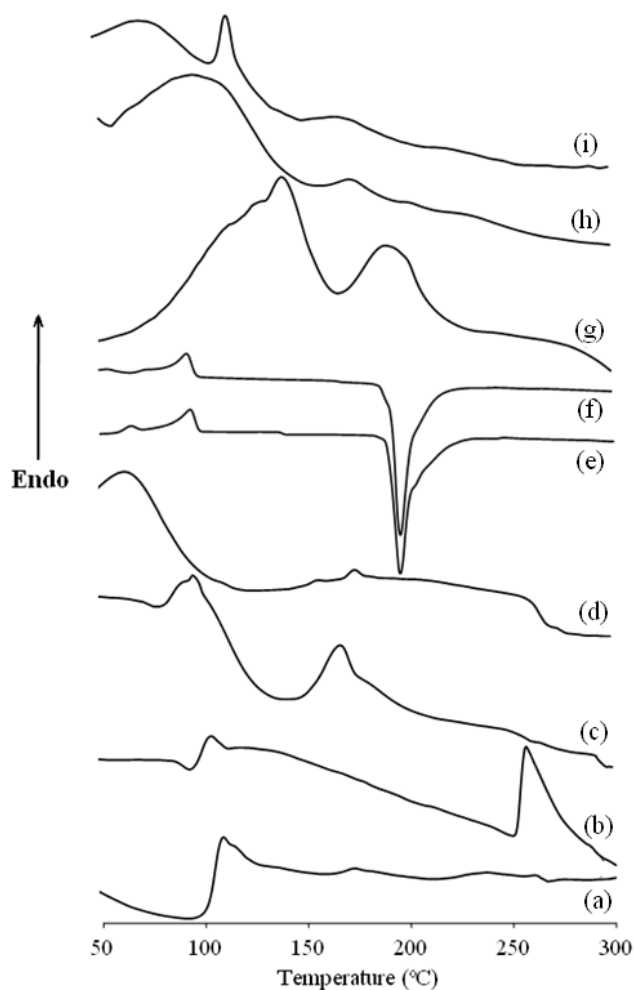


**Figure 4.18** DSC thermogram of (a) PS pellet, (b) electrospun PS fiber mat, (c) as synthesized SPS A, (d) electrospun SPS A fiber mat, (e) electrospun DBEDOT/PS fiber mat, (f) PEDOT/PS composite film, non pressing, (g) controlled PEDOT, (h) PEDOT/PS composite film, pressing, and (i) PEDOT/SPS A composite film, pressing.

Considering the thermograms shown in Figure 4.19, it was found that the major weight loss of PS and SPS A both before and after electrospinning occurring at a similar temperature in a range of 440 - 450 °C corresponds to the degradation of the PS backbone. A slight weight loss of the electrospun PS (Figure 4.19(b)) and SPS A (Figure 4.19(a)) appearing in a temperature range of 100-250 and 50-100 °C, respectively should presumably attributed to the loss of residual solvent (DMF for PS and THF for SPS A) as well as moisture. A continuous weight loss in a temperature

range of 150-320 °C of the thermograms in Figure 4.19(c) and (d) can be used as an indication of desulfonation of the SPS A [42, 61].

The fact that the PEDOT/PS composite film (Figure 4.19(f)) prepared without pressing and the electrospun DBEDOT/PS fiber mat (Figure 4.19(e)) showed 60% weight loss at the same temperature (220 °C) once again confirmed that the SSP did not go to completion without applying compression during heat treatment and the majority of the DBEDOT was still left un-polymerized. Nonetheless, this small content of PEDOT has improved the thermal stability of the PS composite. Approximately 20% of the composite weight was left even after the heating went beyond 500 °C.

The improvement of thermal stability was even greater for the PEDOT/PS (Figure 4.19(h)) and PEDOT/SPS A (Figure 4.19(i)) composite films that were prepared with pressing during the heat treatment. The weight of 45 and 35 % remained in the PEDOT/PS and PEDOT/SPS A composite films, respectively after heating above 500 °C. The degradation of the composite films in the temperature of 50-150 °C corresponds to the loss of solvent, moisture, and bromine dopant whereas the weight loss at 180-350 °C and ~420 °C can be assigned to the loss of PEDOT fragments and PS backbone, respectively. Overall, the existence of the matrix, especially PS, helped enhancing the thermal stability of the PEDOT. This feature should be desirable from practical point of view.

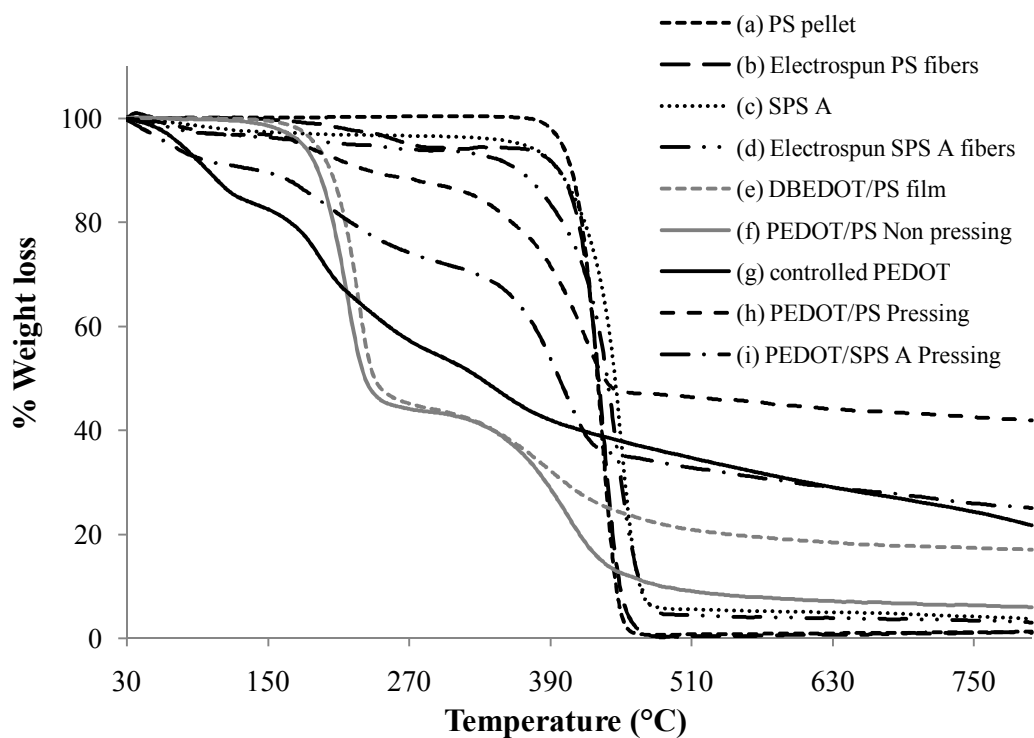


**Figure 4.19** TGA thermograms of (a) PS pellet, (b) electrospun PS fiber mat, (c) as synthesized SPS A, (d) electrospun SPS A fiber mat, (e) electrospun DBEDOT/PS fiber mat, (f) PEDOT/PS composite film, non pressing, (g) controlled PEDOT, (h) PEDOT/PS composite film, pressing, and (i) PEDOT/SPS A composite film, pressing.

## CHAPTER V

### CONCLUSION AND SUGGESTION

2,5-Dibromo-3,4-ethylenedioxythiophene (DBEDOT) was synthesized by a bromination of 3,4-ethylenedioxythiophene (EDOT) using a method modified from the published procedure. Sulfonated polystyrene (SPS) can be successfully prepared by sulfonation using conc.H<sub>2</sub>SO<sub>4</sub> as a sulfonating agent. As determined by <sup>1</sup>H NMR analysis, the sulfonation using the stoichiometric ratio of PS repeat unit to conc.H<sub>2</sub>SO<sub>4</sub> of 2.6:1, 1.7:1, and 1.3:1 yielded SPS with %DS of 8, 15, and 32 % which were labeled as SPS A, SPS B, and SPS C, respectively.

The threshold polymer concentration that resulted in reasonably uniform fibers and good surface coverage was 12% (w/v). DMF and THF were found to be the most suitable solvents for electrospinning DBEDOT/PS and DBEDOT/SPS mixed solutions, respectively. Changing the solvent and introducing some additives in the step of electrospinning, have some impact on the thickness as well as the conductivity of the PEDOT composite film after heat-activated solid state polymerization (SSP). Using electrospinning, it was possible to fabricate SPS of which %DS was not too high (SPS A and SPS B). The highly charged SPS C having 32%DS failed to form continuous jet and well defined bead-free fibrous structure.

The DBEDOT/polymer fiber mat obtained after electrospinning can be transformed into the conductive PEDOT/polymer composite film by heat activation. The optimal condition for SSP of the DBEDOT was to heat at 70 °C for at least 24 h. The compression or pressing of the electrospun DBEDOT/polymer fiber mats during the heat treatment was found necessary to efficiently induce SSP. If the compression was applied, the resulting dark blue PEDOT/polymer composite film was smoother and more homogeneous than that obtained without the compression suggesting that the PEDOT can be well dispersed in the former case. The uniform distribution of the sub-micron PEDOT particles having a diameter of ~100 nm was verified by SEM. In the case of the PEDOT/PS composite film, the conductivity can reach as high as 13.24 S/cm. The fact that the conductivity values measured on the bottom side can almost

be superimposed on those measured on the top side implied that the PEDOT distributed evenly throughout the thickness of the composite film. Without pressing during heat treatment, the majority of the DBEDOT was left un-polymerized as identified by XRD and DSC analyses.

It was found that the conductivity kept going up upon storage implying that although the SSP can be accelerated by heat treatment, the polymerization did not go to completion with a limited amount of time. The highest conductivity of 32.76 S/cm was obtained when the PEDOT/PS composite film prepared by SSP of the 3:1 (w/w) DBEDOT/PS fiber mat electrospun from DMF solution with pressing was kept for 1 month. Evidences from FT-Raman analysis indicated that at high conductive state, the PEDOT chains would preferably adopt linear or extended coil conformation and have quinoid resonance form as opposed to the coiled structure having benzoid resonance form at low conductive state. Information from ESR analysis indicated that the PEDOT chains in the PEDOT-containing composite film having relatively high conductivity are in the form of bipolaron. TGA data suggested that PEDOT in the form of polymer composite was more thermally stable than the PEDOT alone.

The percentage yield of PEDOT formed in the composite after being kept for a certain period of time is yet to be determined in order to investigate whether or not the SSP of the un-polymerized DBEDOT in the as-prepared PEDOT/polymer composite film was further induced as a function of storage time. The PEDOT particles extracted from the PEDOT/polymer composite films prepared using different heating temperature has to be characterized to determine the effect of temperature on the PEDOT particle size. Also, it is worth to investigate the thermal behavior of the DBEDOT as a function of temperature used for inducing SSP by TG/DTA.



## REFERENCES

- [1]. Roncali, J. Conjugated poly(thiophene): synthesis, functionalization, and applications. Chem. Rev. 92 (1992): 711-738.
- [2]. (a) Sirakul, T. *Synthesis of Processible Poly(3,4-Diakoxy Thiophene)*. Master's Thesis, Program of Petrochemistry and Polymer Science, Faculty of Science, Chulalongkorn University, 2006.
- (b) Bannarukkul, W. *Effect of doping agents on optical and conductive properties of poly(3-hexylthiophene)*. Master's Thesis, Program of Petrochemistry and Polymer Science, Faculty of Science, Chulalongkorn University, 2005.
- [3]. Mullekom, H. A. M. *The Chemistry of High and Low Band Gap Conjugated Polymers*. Ph.D. Dissertation, Eindhoven University of Technology, the Netherlands, 2000.
- [4]. Skotheim, T. A.; Reynolds, J. Handbook of Conducting Polymers. 3<sup>rd</sup> ed. CRC Press: Boca Raton, 2007.
- [5]. Greenham, N. C.; Friend, R. H. Semiconductor Device Physics of Conjugated Polymers, in Solid State Physics, Advances in Research and Application. Academic Press: New York, 1995.
- [6]. Forrest, S. R. The path to ubiquitous and low cost organic electronic appliances on plastic. Nature 428 (2004): 911-918.
- [7]. Heeger, A. J. Nobel Lecture: Semiconducting and metallic polymers: The Fourth Generation of Polymeric Materials. Rev. Mod. Phys. 73 (2001): 681-700.
- [8]. Heeger, A. J. Semiconducting and metallic polymers: the fourth generation of polymeric materials. Synth. Met. 125 (2002): 23-42.

- [9]. Schimmel, T.; Schwoerer, M; Naarmann, H. Mechanisms limiting the d.c. conductivity of high-conductivity polyacetylene. Synth. Met. 37 (1990): 1-6.
- [10]. Kvarnstrom, C.; Neugebauer, H.; Blomquist, S.; Ahonen, H. J.; Kankare, J.; Ivaska, A. In situ spectroelectrochemical characterization of poly(3,4-ethylenedioxythiophene). Electrochim. Acta. 44 (1999): 2739-2750.
- [11]. Chaing, C. K.; Fincher, C. R. Jr., Park, Y. W., Heeger, A. J., Shirakawa, H., Louise, E. J., Gau, S. C., McDiarmid, A. G. Electrical conductivity in doped polyacetylene. Phys. Rev. Lett. 39 (1977): 1098-1101.
- [12]. McDiarmid, A. G. Synthetic metals: A novel role for organic polymers (Nobel lecture). Angew. Chem. Int. Ed. 40 (2001): 2581-2590.
- [13]. Heeger, A. J. Semiconducting and metallic polymers: The fourth generation of polymeric materials (Nobel lecture). Angew. Chem. Int. Ed. 40 (2001): 2591-2611.
- [14]. Shirakawa, H. The discovery of polyacetylene film: The dawning of an era of conducting polymers (Nobel lecture). Angew. Chem. Int. Ed. 40 (2001): 2574-2580.
- [15]. Kanno, H., Hamada, Y., Takahashi, H. Development of OLED with high stability and luminance efficiency by co-doping methods for full color displays. IEEE J. Sel. Top. Quant. 10 (2004): 30-36.
- [16]. Forrest, S., Burrows, P., Thompson, M. The dawn of organic electronics. IEEE Spectrum 37 (2000): 29-34.
- [17]. Suzuki, M., Hatakeyama, T., Tokito, S., Sato, F. High-efficiency white phosphorescent polymer light-emitting devices. IEEE J. Sel. Top. Quant. 10 (2004): 115-120.
- [18]. Wang, X., Engel, J., Liu, C. Liquid crystal polymer (LCP) for MEMS: processes and applications. J. Micromech. Microeng. 13 (2003): 628-633.

- [19]. Cui, X.; Martin, D. C. Electrochemical deposition and characterization of poly(3,4-ethylenedioxythiophene) on neural microelectrode arrays. Sens. Actuators B: Chem. 89 (2003): 92-102.
- [20]. Jeranko, T.; Tricbutsch, H.; Sariciftci, N. S.; Hummeilen, J. C. Patterns of efficiency and degradation of composite polymer solar cells. Sol. Energy Mater. Sol. Cells. 83 (2004): 247-262.
- [21]. Scott, J. C.; Kaufman, J. H.; Brock, P. J.; Dipietro, R.; Salem, J.; Goitia, J. A. Degradation and failure of meh-ppv light-emitting diodes. J. Appl. Phys. 79 (1996): 2745-2751.
- [22]. Blom, P. W. M.; Berntsen, A. J. M.; Liedenbaum, C. T. H. F.; Schoo, H. F. M.; Croonen, Y.; Van de Weijer, P. Efficiency and stability of polymer light-emitting diodes. J. Mater. Sci. Mater. 11 (2000): 105-109.
- [23]. Yamashita, K.; Mori, T. Encapsulation of organic light-emitting diode using thermal chemical-vapour-deposition polymer film. J. Phys. D: Appl. Phys. 34 (2001): 740-743.
- [24]. Chwang, A. B.; Rothman, M. A.; Mao, S. Y.; Hewitt, R. H.; Weaver, M. S.; Silvernail, J. A.; Rajan, K.; Hack, M.; Brown, J. J.; Chu, X.; Moro, L.; Krajewski, T.; Rutherford, N. Thin film encapsulated flexible organic electroluminescent displays. Appl. Phys. Lett. 83 (2003): 413-415.
- [25]. Burroghs, J. H.; Bradley, D. D. C.; Brown, A. R.; Marks, R. N.; Mackay, K.; Friend, R. H.; Burns, P. L.; Holmes, A. B. Light-emitting diodes based on conjugated polymers. Letters to Nature 347 (1990): 539-541.
- [26]. Rogers, J. A.; Bao, Z.; Dodabalapur, A.; Makhija, A. Organic smart pixels and complementary inverter circuits formed on plastic substrates by casting and rubber stamping. IEEE. Electr. Device. L. 21 (2000): 100-103.

- [27]. Hohnholz, D.; McDiarmid, A. G. Line patterning of conducting polymers: new horizons for inexpensive, disposable electronic devices. Synth. Met. 121 (2001): 1327-1328.
- [28]. Seifert, W.; Aabrecht, H.; Mietke, S.; Kohler, T.; Werner, M. Processing and electrical characterization of intrinsic conducting polymers for electronic and MEMS application. Proceedings of SPIE 5045 (2003): 183-190.
- [29]. Groenendaal, L.; Zotti, G.; Aubert, P.-H.; Waybright, S. M.; Reynolds, J. R. Electrochemistry of poly(3,4-alkylenedioxythiophene) derivatives. Adv. Mater. 15 (2003): 855-879.
- [30]. Kwon, C. W.; Campet, G.; Kale, B. B. Structure of thin films of poly(3,4-ethylenedioxythiophene). Act. Pass. Electr. Comp. 26 (2003): 81-86.
- [31]. Jonas, F.; Schrader, L. Conductive modifications of polymers with polypyrroles and polythiophenes. Synth. Met. 41 (1991): 831-836.
- [32]. Jonas, F.; Heywang, G. Technical applications for conductive polymers. Electrochim. Acta. 39 (1994): 1345-1347
- [33]. Inganäs, O.; Salaneck, W. R.; Österholm, J. E.; Laakso, J. Thermochromic and solvatochromic effects in poly(3-hexylthiophene). Synth. Met. 22 (1988): 395-406.
- [34]. Groenendaal, L.; Jonas, F.; Freitag, D.; Pielartzik, H.; Reynolds, J. Poly(3,4-ethylenedioxythiophene) and its derivatives: Past, Present, and Future. Adv. Mater. 12 (2000): 481-494.
- [35]. Reynolds, J. R.; Kumar, A.; Reddinger, J. L.; Sankaran, B.; Sapp, S. A.; Sotzing, G. A. Unique variable-gap polyheterocycles for high-contrast dual polymer electrochromic devices. Synth. Met. 85 (1997): 1295-1298.
- [36]. Kiebooms, R.; Aleshin, A.; Hutchison, K.; Wudl, F. Thermal and electromagnetic behavior of doped poly(3,4-ethylenedioxythiophene) films. J. Phys. Chem. B. 101 (1997): 11037-11039.

- [37]. Ahonen, H. J.; Lukkari, J.; Kankare, J. n- and p-Doped Poly(3,4-ethylenedioxythiophene): Two electronically conducting states of the polymer Macromolecules. 33 (2000): 6787-6793.
- [38]. Pei, Q.; Zuccarello, G.; Ahskog, M.; Inganäs, O. Electrochromic and highly stable poly(3,4-ethylenedioxythiophene) switches between opaque blue-black and transparent sky blue. Polymer. 35 (1994): 1347-1351.
- [39]. Cornil, J.; Dos Santos, D. A.; Beljonne, D.; Bredas, J. L.; Electronic Structure of Phenylene Vinylene Oligomers: Influence of Donor/Acceptor Substitutions. J. Phys. Chem. 99 (1995): 5604-5611.
- [40]. Heywang, G.; Jonas, F. Poly(alkylenedioxythiophene)s - new, very stable conducting polymers. Adv. Mater. 4 (1992): 116-118.
- [41]. Dietrich, M.; Heinze, J.; Heywang, G.; Jonas, F. Electrochemical and spectroscopic characterization of polyalkylenedioxythiophenes. J. Electroanal. Chem. 369 (1994): 87-92.
- [42]. Kvarnstrom, C.; Neugebauer, H.; Blomquist, S.; Ahonen, H. J.; Kankare, J.; Ivaska, A.; Sariciftci, N. S. In situ FTIR spectroelectrochemical characterization of poly(3,4-ethylenedioxythiophene) films. Synth. Met. 101 (1999): 66.
- [43]. Wang, Y. Research progress on a novel conductive polymer - poly(3,4-ethylenedioxythiophene) (PEDOT). J. Phys. Conf. Ser. 152 (2009): 012023.
- [44]. Yamamoto, T.  $\pi$ -Conjugated polymers bearing electronic and optical functionalities. preparation by organometallic polycondensations, properties, and their applications. Bull. Chem. Soc. Jpn. 72 (1999): 621-638.
- [45]. Meng, H.; Perepichaka, D. F.; Wudl, F. Facial solid-state synthesis of highly conducting poly(ethylenedioxythiophene). Angew. Chem. Int. Ed. 42 (2003): 658-661.

- [46]. Vouyiouka, S. N.; Karakatsani, E. K.; Papaspyrides, C. D. Solide state polymerization. Prog. Polym. Sci. 30 (2005): 10-37.
- [47]. Meng, H.; Perepichaka, D. F.; Bendikov, M.; Wudl, F.; Pan, G. Z.; Yu, W.; Dong, W.; Brown, S. Solid-state synthesis of conducting polythiophene via an unprecedented heterocyclic coupling reaction. J. Am. Chem. Soc. 125 (2003): 15151-15162.
- [48]. Joans, F.; Krafft, W.; Muys, B.; poly(3,4-ethylenedioxythiophene)- conductive coating, technical applications and properties. Macromol. Symp. 100 (1995): 169-173.
- [49]. de Leeuw, D. M.; Kraakman, P. A.; Bongaerts, P. F. G.; Mutsaers, C. M. J.; Klaasen, D. B. M. Electroplating of conductive polymers for the metallization of insulators. Syth. Met. 66 (1994): 263-273.
- [50]. Carlberg, J. C.; Inganas, O. Poly(3,4-ethylenedioxythiophene as electrode material in electrochemical capacitors. J. Electrochem. Soc. 144 (1997): L61
- [51]. Kudoh, Y.; Akami, K.; Kusayanagi, H.; Matsuya, Y.; Chemical polymerization of 3,4-ethylenedioxythiophene in an aqueous medium containing a phenol derivative as an additive. Synth. Met. 123 (2001): 541-544.
- [52]. Sotzing, G. A.; Reddinger, J. L.; Reynolds, J. R.; Steel, P. J. Redox active electrochromic polymers from low oxidation monomers containing 3,4-ethylenedioxythiophene (EDOT). Synth. Met. 84 (1997): 199-201.
- [53]. Chen, X.; Xing, K.; Inganas, O. Electrochemically Induced Volume Changes in Poly(3,4-ethylenedioxythiophene). Chem. Mater. 8 (1996): 2439-2443.
- [54]. Ouyang, J.; Chu, C.; Chen, F.; Chen, F.; Xu, Q.; Yang, Y. High-Conductivity Poly(3,4-Ethylenedioxythiophene): Poly(styrenesulfonate) film and its application in polymer optoelectronic devices. Adv. Funct. Mater. 15 (2005): 203-208.

- [55]. Dkhissi, A.; Louwet, F.; Groenendaal, L.; Bljonne, D.; Lazzaroni, R.; Brédas, J. L. Theoretical investigation of the nature of the ground state in the low-bandgap conjugated polymer, poly(3,4-ethylenedioxythiophene). Chem. Phys. Lett. 359 (2002): 466-472.
- [56]. Bai, H.; Zhao, L.; Lu, C.; Li, C.; Shi, G. Composite nanofibers of conducting polymers and hydrophobic insulating polymers: preparation and sensing applications. Polymer 50 (2009):3292-3301.
- [57]. Wang, Y.; Shi, Y.; Xu, X.; Liu, F.; Yao, H.; Zhai, G.; Hao, J.; Li, G. Preparation of PANI-coated poly(styrene-co-styrenesulfonate) nanoparticles in microemulsion media. Colloids Surf., A 345 (2009):71-74.
- [58]. Aussawasathien, D.; Sahasithiwat, S.; Menbangpung, L. Electrospun camphorsulfonic acid doped poly(o-toluidine)-polystyrene composite fibers: Chemical vapor sensing. Synth. Met. 158 (2008): 259-263.
- [59]. Laforgue, A.; Robitaille, L. Fabrication of poly-3-hexylthiophene/polyethylene oxide nanofibers using electrospinning. Synth. Met. 158 (2008): 577-584.
- [60]. Xia, Y.; Lu, Y. Fabrication and properties of conductive conjugated polymers/silk fibroin composite fibers. Compos. Sci. Technol. 68 (2008): 1471-1479.
- [61]. Kusonsong, S. *Preparation of Conducting Polymer Composites by Solid State Polymerization of 2,5-Dibromo-3,4-ethylenedioxythiophene*. Master's thesis, Petrochemistry and Polymer Science, Faculty of Science, Chulalongkorn University, 2007.
- [62]. Sun, X.; Hagner, M. Novel Poly(acrylic acid)-mediated formation of composited, poly(3,4-ethylenedioxythiophene)-based conducting polymer nanowires. Macromolecules 40 (2007): 8537-8539.

- [63]. Hong, K.H.; Oh, K.W.; Kang, T.J. Preparation and properties of electrically conducting textiles by in situ polymerization of poly(3,4-ethylenedioxythiophene). J. Appl. Polym. Sci. 97 (2005): 1326-1332.
- [64]. Wutticharoenmongkol, P.; Supaphol, P.; Srihirin, T.; Kerdcharoen, T.; Osotchan, T. Electrospinning of polystyrene/poly(2-methoxy-5-(2'-ethylhexyloxy)-1,4-phenylene vinylene) blend. J. Polym. Sci., Part B: Polym. Phys. 43 (2005): 1881-1891
- [65]. Chuangchote, S.; Srihirin, T.; Supaphol, P. Color change of electrospun polystyrene/MEH-PPV fibers from orange to yellow through partial decomposition of MEH side group. Macromol. Rapid Commun. 28 (2007): 651-659.
- [66]. Sonmez, G.; Scgottland, P.; Reynolds, J. R. PEDOT/PAMPS: An electrically conductive polymer composite with electrochromic and cation exchange properties. Synth. Met. 155 (2005): 130-137.
- [67]. Dong, H.; Prasad, S.; Nyame, V.; Jones, W.E. Sub-micrometer conducting polyaniline tubes prepared from polymer fiber templates. Chem. Mater. 16 (2004): 371-373.
- [68]. Lee, W. J.; Kim, Y. J.; Jung, M. O.; Kim, D. H.; Cho, D. L.; Kaang, S. Preparation and properties of conducting polypyrrole-sulfonated polycarbonate composites. Synth. Met. 123 (2001): 327-333.
- [69]. Khan, M. A.; Armes, S. P. Synthesis and characterization of micrometer-sized poly(3,4-ethylenedioxythiophene)-coated polystyrene latexes. Langmuir 15 (1999): 3469-3475.
- [70]. Huang, Z. M.; Zhang, Y. Z.; Kotaki, M.; Ramakrishna, S. A review on polymer nanofibers by electrospinning and their applications in nanocomposites. Compos. Sci. Technol. 63 (2003): 2223-2253.



- [71]. Formhals, A. Process and apparatus for preparing artificial threads. US Patent No. 1,975,504; 1934.
- [72]. Doshi, J.; Reneker, D, H. Electrospinning process and applications of electrospinning. Polymer 40 (1995): 4585-4592.
- [73]. Tsai, P. P.; Schreuder-Gibson, H.; Gibson, P. Different electrostatic method for making electret filters. J. Electrostat. 54 (2002): 333-341
- [74]. Hafemann, B.; Ensslen, S.; Erdmann, C.; Niedballa, R.; Zühlke, A.; Ghofrani, K.; Kirkpatrick, C. J. Use of collagen/elastin-membrane for the tissue engineering of dermis. Burns 25 (1999): 373-384
- [75]. Gibson, P. W.; Schreuder-Gibson, H. L.; Rivin, D. .Electrospun fiber mats: Transport properties. Am. Inst. Chem. Eng. 45 (1999): 90-195.
- [76]. Saikrasun, S.; Amornsakchai, T.; Sirisinha, C.; Meesiri, W.; Bualeklimcharoen, S. Kevlar reinforcement of polyolefin-based thermoplastic lastomer. Polymer 40 (1999): 6437-6442.
- [77]. Gouma, P. I. Nanostructured polymorphic oxides for advanced chemo-sensors. Rev. Adv. Mater. Sci. 5 (2003): 147-154.
- [78]. Jarusuwannapoom, T.; Hongrojjanawiwat, W.; Jitjaicham, S.; Supaphol, P. Effect of solvents on electro-spinnability of polystyrene solutions and morphological appearance of resulting electrospun polystyrene fibers. Euro. Polym. J., 41 (2005): 409-421.
- [79]. Eda, G.; Liu, J.; Shivkumar, S. Flight path of electrospun polystyrene solutions: Effects of molecular weight and concentration. Mater. Lett. 61 (2007): 1451-1455.
- [80]. An, H.; Shin, C.; Chase, G.G. Ion exchanger using electrospun polystyrene nanofibers. J. Membr. Sci. 283 (2006): 84-87.

- [81]. Kellog, R. M.; Schaap, A. P.; Harper E. T.; Wynberg, H. Acid-Catalyzed Brominations, Deuterations, Rearrangements, and Debrominations of Thiophenes under Mild Conditions. J. Org. Chem. 32 (1968) : 2902-2909.
- [82]. Thirasart, N. *Synthesis of  $\beta$ -Substituted 2,5-Dibromothiophene and their S,S-Dioxides*. Master's thesis, Program of Petrochemistry and Polymer Science, Faculty of Science, Chulalongkorn University, 2004.
- [83]. Makowski, H. S.; Lundberg R. D.; Sighal GH. Flexible polymeric compositions comprising a normally plastic polymer sulfonated to about 10 mole % sulfonate. US Patent No. 3,870,841; 1975.
- [84]. Smitha, B.; Sridhar, S.; Khan A.A. Synthesis and characterization of proton conducting polymer membranes for fuel cells. J. Membr. Sci. 225 (2003): 63-76.
- [85]. Cong, R.; Pelton, R.; Russo, P.; Bain, A.D.; Negulescu, I.; Zhou, Z. NMR investigations of the structure of water-soluble poly (ethylene oxide) complexes with polystyrene sulfonate copolymers. Colloid. Polym. Sci. 281 (2003): 150-156.
- [86]. Cristiane R. Martins,; Giacommo Rugiri,; Marco-A. De Paoli. Synthesis in pilot plant scale and physical properties of sulfonated polystyrene. J. Braz. Chem. Soc. 14 (2003): 797-802.
- [87]. Kang, M.; Jung, R.; Kim, H-S.; Jin, H-J. Preparation of superhydrophobic polystyrene membranes by electrospinning. Colloids Surf., A 313-314 (2008): 411-414.
- [88]. Nair, S.; Hsiao, E.; Kim, S.H. Melt-welding and improved electrical conductivity of nonwoven porous nano fiber mats of poly (3,4-ethylenedioxythiophene) grown on electrospun polystyrene fiber template. Chem. Mater. 21 (2009): 115-121.
- [89]. Chen, N.; Hong, L. A study on polypyrrole - coated polystyrene sulfonic acid microspheres - a proton electrolyte. Eur. Polym. J. 37 (2001): 1027-1035.

- [90]. Fu, Y.; Weiss, R. A. In situ polymerization of aniline within lightly sulfonated polystyrene. Synth. Met. 84 (1997): 129-130.
- [91]. Pantano, C.; Gañá-Calvo, A. M.; Barero, A. Zeroth-order, Electrohydrostatic solution for electrospraying in Cone-jet mode. J. Aerosol Sci 25 (1994): 1065-1077.
- [92]. Aasmundtveit, K. E.; Samuelsen, E. J.; Inganas, O.; Pettersson, L. A. A.; Johansson, T. B.; Ferrer, S. Structural aspects of electrochemical doping and dedoping of poly (3,4-ethylenedioxythiophene). Synth. Met. 113 (2000): 93-97.
- [93]. Lock, J. P.; Im, S. G.; Gleason, K. K. Oxidative chemical vapor deposition of electrically conducting poly(3,4-ethylenedioxythiophene) films. Macromolecules 39 (2006): 5326-5329.
- [94]. Sadki, S.; Schottland, P.; Brodie, N.; Sabouraud, G.; The mechanisms of pyrrole electropolymerization. Chem. Soc. Rev. 29 (2000): 283-293.
- [95]. Kim, J. Y.; Jung, J. H.; Lee, D. E.; Joo, J. Enhancement of electrical conductivity of poly(3,4-ethylenedioxythiophene)/poly(4-styrenesulfonate) by a change of solvents. Synth. Met. 126 (2002): 311-316.
- [96]. Garreau, S.; Louarn, G.; Buisson, J. P.; Froyer, G.; Lefrant, S. In situ spectroelectrochemical raman studies of poly (3,4-ethylenedioxythiophene) (PEDT). Macromolecules 32 (1999): 6807-6812.
- [97]. Kim, T-W.; Woo, H-Y.; Jung, W-G.; Ihm, D-W.; Kim, J-Y. On the mechanism of conductivity enhancement in plasma treated poly(3,4-ethylenedioxythiophene) films. Thin Solid Films 517 (2009): 4147-4151.
- [98]. Ouyang, J.; Xu, Q.; Chu, C-W.; Yang, Y.; Li, G.; Shinar, J. On the mechanism of conductivity enhancement in poly(3,4-ethylenedioxythiophene): Poly(styrenesulfonate) film through solvent treatment. Polymer 45 (2004): 8443-8450.

- [99]. Zykwinska, A.; Domagala, W.; Czardybon, A.; Pilawa, B.; Lapkowski, M. Investigation of charge carriers in poly(3,4-butylendioxythiophene) (PBuDOT) by means of ESR spectroelectrochemistry. J. Solid. State. Eletrochem. 8 (2004): 369-375.
- [100]. Bautista, K. Four-point probe operation of polymer. The University of Texas: Dallas, 2003.
- [101]. Blythe, T.; Bloor, D. Electrical properties of polymers. Cambridge University Press: New York, 2005.
- [102]. Schuetze, A. P.; Lewis, W.; Brown, C.; Geerts, W. J. A laboratory on the four-point probe technique. Am. J. Phys. 72 (2004): 149-153.
- [103]. <http://www.purdue.edu/REM/rs/sem.htm>

## **APPENDICES**

## APPENDIX A

### Characterization Techniques

#### Conductivity measurement by four point probe technique [100-102]

Four tiny electrodes are arranged in straight line separated at exactly equal distances ( $d_1 = d_2 = d_3$ ) and touch the surface of the sample to be measured. (Figure A-1) The electrodes are further connected with an electrical circuit equipped with an Amp meter (A) and Voltmeter (V). Contacts between the four electrodes and the sample surface must be equal. During the measurement, the current (I) is applied through electrode contact 1 to 4, and difference ( $\Delta V$ ) across electrode contacts 2 and 3 is measured. The resistivity and conductivity of the sample can be calculated from the equation A-1 and A-2, respectively.

Resistivity ( $\Omega \cdot \text{cm}$ );

$$\rho = (\pi \cdot t / \ln 2)(V/I) = 4.53(R \cdot t) \quad (\text{A-1})$$

Conductivity ( $\text{S} \cdot \text{cm}^{-1}$ );

$$\sigma = 1/\rho \quad (\text{A-2})$$

Where

I is current (A)

V is voltage (Volt)

R is resistant (ohm)

t is film thickness (cm)

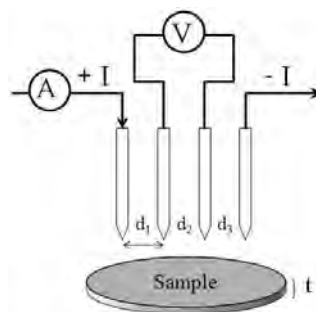


**Figure A-1** Schematic representation of 4-point probe configuration.

**Table A-1** Conductivity measured on the top side and the bottom side of the PEDOT/PS composite film (thickness of 55.24  $\mu\text{m}$ ) prepared by SSP of the electrospun 3:1 (w/w) DBEDOT/ PS fiber mats by heating 70  $^{\circ}\text{C}$  for 40 h with pressing as a function of reaction time

Time (h)	Resistant ( $\Omega$ )				Average Conductivity (S/cm)
	1	2	3	Average	
<b>Top side</b>					
8	3150.10	6126.06	4638.08	4638.08	0.010
16	2891.24	4790.06	3840.65	3840.65	0.012
24	4.21	8.07	6.14	6.14	7.716
32	3.55	4.13	3.84	3.84	11.541
40	3.07	3.63	3.35	3.35	13.241
48	4.15	5.31	4.73	4.73	9.429
56	3.52	4.42	3.97	3.97	11.217
<b>Bottom side</b>					
8	2332.86	4166.12	3249.49	3249.49	0.014
16	2769.77	4071.57	3420.67	3420.67	0.013
24	4.98	8.08	6.53	6.53	7.030
32	3.84	4.52	4.18	4.18	10.609
40	2.99	3.69	3.34	3.34	13.316
48	3.94	5.38	4.66	4.66	9.629
56	3.91	4.59	4.25	4.25	10.433

Example Conductivity calculation of 8 h Sample in table A-1

From Resistivity ( $\Omega\cdot\text{cm}$ );  $\rho = 4.53(R\cdot t)$

Conductivity ( $\text{S}\cdot\text{cm}^{-1}$ );  $\sigma = 1/\rho$

R is resistant (3150.10  $\Omega$ )

t is film thickness ( $5.5 \times 10^{-3}$  cm)

$$\rho = 4.53 \times (3150.10 \Omega \times 5.5 \times 10^{-3} \text{ cm})$$

$$= 78.48 \Omega \cdot \text{cm}$$

$$\sigma = 1/78.48 \Omega \cdot \text{cm}$$

$$\text{Conductivity} = 0.0127 \text{ S} \cdot \text{cm}^{-1}$$

**Table A-2** Conductivity measured on the top side of the PEDOT composite film prepared by SSP of the electrospun 3:1 (w/w) DBEDOT/polymer matrix by heating at 70 °C for 40 h with pressing as a function of temperature, solvent, and additive

Temperature (°C)	Solvent/ Additive	Matrix	Thickness ( $\mu\text{m}$ )	Top side resistant ( $\Omega$ )			Average Conductivity (S/cm)
				1	2	3	
60	DMF	PS	55.24	11.76	13.86	12.81	3.46
80	DMF	PS	55.24	12.34	17.24	14.79	3.04
70	DMF	PS	55.24	3.07	3.63	3.35	13.24
70	DMF:THF	PS	49.39	6.08	4.49	7.67	5.46
70	THF	PS	19.91	41.08	48.49	33.67	2.75
70	DMF, Py	PS	42.61	9.35	11.17	10.2	5.08
70	DMF, Eg	PS	25.83	12.23	13.05	14.71	6.41
70	THF	SPS A	17.90	8.43	7.81	10.31	13.88
70	THF	SPS B	18.21	17.95	18.83	17.08	6.75
70	Controlled PEDOT		100.00	1.21	1.15	1.40	17.609



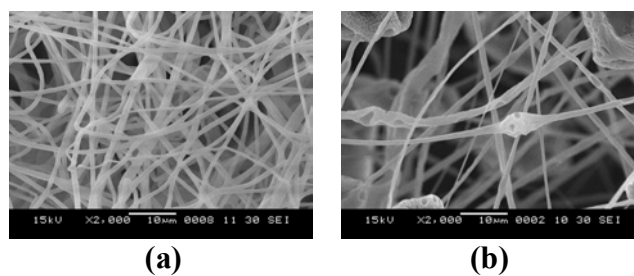


**Figure A-2** SEM (at 2000 $\times$ ) of as-spun PS fibers electrospun from 10%PS (w/v) solution in DMF (a) and THF (b).

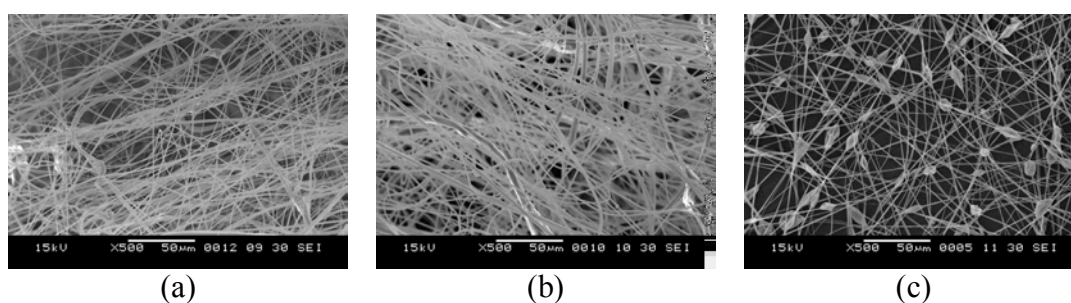


**Figure A-3** SEM (at 500 $\times$ ) of as-spun SPS B fibers electrospun from 12%SPS B (w/v) solution in DMF (a), mixed 1THF:1DMF (b), and THF (c).

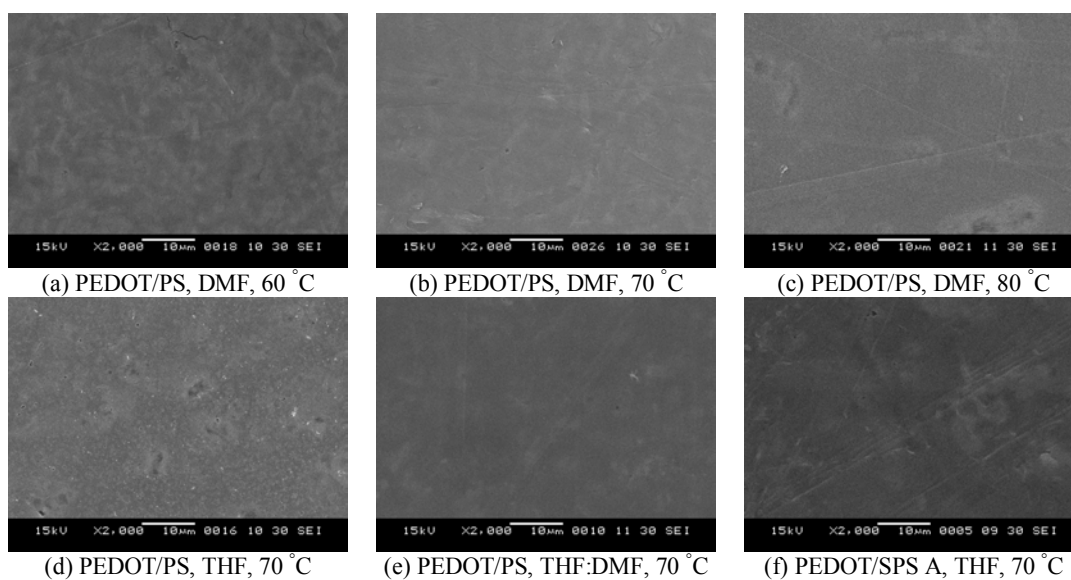


**Figure A-4** SEM (at 2000 $\times$ ) of PEDOT composites obtained after SSP.

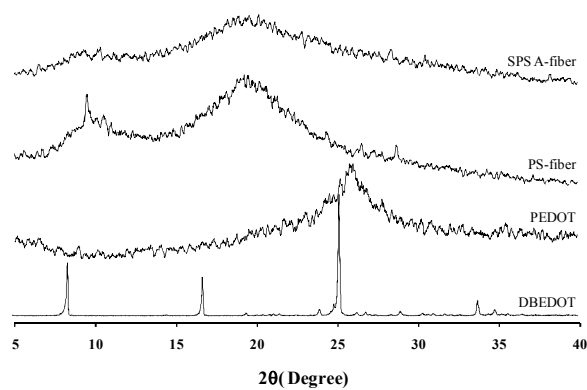


**Figure A-5** XRD diffractograms of raw material.

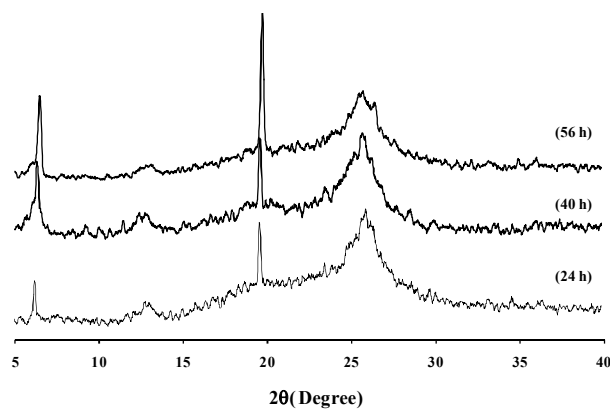


**Figure A-6** XRD diffractograms of PEDOT/PS, pressing prepared by SSP of the DBEDOT/PS fiber mat by heating at 70 °C for a different period of time.

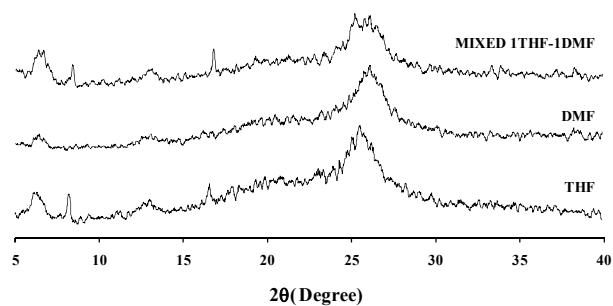


**Figure A-7** XRD diffractograms of PEDOT/PS, pressing prepared by SSP of the DBEDOT/PS fiber mat electrospun from different solution by heating at 70 °C for 40 h.

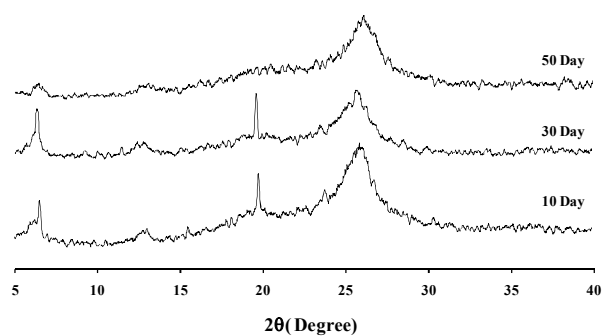


**Figure A-8** XRD diffractograms of PEDOT/PS, pressing prepared by SSP of the DBEDOT/PS fiber mat electrospun from DMF solution by heating at 70 °C for 40 h after keeping for up to 50 days.

## **APPENDIX B**

- B-1 Pure and Applied Chemistry International Conference 2009, Faculty of Science, Naresuan University, Phitsanulok, Thailand. (Abstract)
- B-2 The 2<sup>nd</sup> Polymer Graduate Conference of Thailand, Faculty of Science, Chulalongkorn University, Bangkok, Thailand. (Proceeding)

B-1


**PACCON**  
PURE AND APPLIED CHEMISTRY  
INTERNATIONAL CONFERENCE **2009**

**Abstracts**  
JANUARY 14-16, 2009  
NARESUAN UNIVERSITY, PHITSANULOK, THAILAND

**PACCON 2009**  
**ABSTRACTS**

**PURE AND APPLIED CHEMISTRY  
INTERNATIONAL CONFERENCE**

Organized by  
Sustainable Development in Chemistry Based  
on Indigenous Knowledge



S7-PO-36

### Detection of DNA-PNA Hybridization Using Quaternized Chitosan Particles in Combination with MALDI-TOF Mass Spectrometry

Jittima Meebungpraw<sup>1</sup>, Tirayut Vilavan<sup>2</sup>, Suda Kiatkamjornwong<sup>3</sup>, Voravee P. Hoven<sup>2\*</sup>

<sup>1</sup>Program of Petrochemistry and Polymer Science, Faculty of Science, Chulalongkorn University, Bangkok, 10330 Thailand

<sup>2</sup>Organic Synthesis Research Unit, Department of Chemistry, Faculty of Science, Chulalongkorn University, Bangkok, 10330 Thailand

<sup>3</sup>Department of Imaging and Printing Technology, Faculty of Science, Chulalongkorn University, Bangkok, 10330 Thailand

\*E-mail: vipavee.p@chula.ac.th, Tel: +66-22-187627 ext 102

Determination of DNA sequences are significantly important for many biotechnology-related applications ranging from medical, forensic, agriculture and food science. The concept of using a new conformationally rigid pyrrolidiny peptide nucleic acid (PNA), strong anion-exchange captures such as commercially available Q-Sepharose in combination with MALDI-TOF mass spectrometry has been proven as a simple and effective way for single nucleotide polymorphism genotyping. This research has introduced quaternized chitosan particles as alternative anion-exchange captures that may be applicable for the same purpose. The particles were prepared by homogeneous and heterogeneous reactions between chitosan and methyl iodide. Because the particles are positively charged, they can only bind ionically with the negatively charged DNA. PNA is a neutral molecule so it cannot be adsorbed by quaternized chitosan particles unless it is hybridized with the negatively charged complementary DNA to form a negatively charged DNA-PNA hybrid. The facts that the complementary PNA-DNA hybrid can be selectively captured by the positively charged quaternized chitosan particles and the particles can be easily separated from non-complementary and unhybridized PNA allow direct detection of the PNA-DNA hybridization by MALDI-TOF mass spectrometry after washing without the use of enzyme treatment or heating.

#### REFERENCES

- Boontha, B.; Nakkuntod, J.; Hirankam, N.; Chumpluk, P.; Vilaivan, T. *Anal. Chem.* **2008**.
- Vilaivan, T.; Srisuwannaket, C. *Org. Lett.* **2006**, *8*, 1897-1900.
- Hoven, V. P.; Tangpasuthadol, V.; Angkitpaiboon, Y.; Vallapa, N.; Kiatkamjornwong, S. *Carbohydr. Polym.* **2007**, *68*, 44-53.

S7-PO-37

### Structures and Mechanisms of the Mukaiyama Aldol Reactions between Metal Organic Frameworks-505 Encapsulated Formaldehyde and Silyl Enol Ether: An ONIOM Study

Sudarat Yadnum<sup>1,2</sup>, Saowapak Choomwatana<sup>1,2</sup>, Pipat Khongpracha<sup>1,2</sup>, Somkiat Nokbin<sup>1,2</sup>, Jumras Limtrakul<sup>1,2\*</sup>

<sup>1</sup>Department of Chemistry, Faculty of Science, Kasetsart University, Bangkok, 10900 Thailand

<sup>2</sup>NANOTEC Center of Excellence, National Nanotechnology Center, Kasetsart University, Bangkok, 10900 Thailand

\*E-mail: jscjrl@ku.ac.th, Tel: +662-562-5555 ext 2169

The reaction mechanism of the Mukaiyama-aldol reaction of encapsulated formaldehyde and silyl enol ether catalyzed by metal organic frameworks (MOF-505) is systematically investigated by the ONIOM (our-Own-N-layer Integrated molecular Orbital + Molecular Mechanics) approach utilizing two-layer ONIOM schemes (B3LYP/6-31G(d,p) : UFF). For comparison, the Mukaiyama-aldol reaction of silyl enol ether and formaldehyde was also studied with the bare Cu<sup>+</sup> cation as an excessive charged catalyst. Three model systems were utilized to study this reaction: (1) a non-promoted uncatalyzed model: O=CH<sub>2</sub>/H<sub>3</sub>SiOHC=CH<sub>2</sub>, (2) a formaldehyde in MOF-505: O=CH<sub>2</sub>@MOF-505/H<sub>3</sub>SiOHC=CH<sub>2</sub>; and (3) a naked Cu<sup>+</sup> cation as a catalyst: Cu(I)/O=CH<sub>2</sub>/H<sub>3</sub>SiOHC=CH<sub>2</sub>. The Mukaiyama aldol reaction of silyl enol ether with formaldehyde takes place in single concerted reaction step. It was found that metal-organic frameworks lead to an energy barrier for the reaction ΔE<sub>act</sub> of 12.0 kcal/mol. This compares to values of ΔE<sub>act</sub> of 13.7 kcal/mol for the uncatalyzed system and 6.9 kcal/mol for the reaction on the naked Cu<sup>+</sup> cation. In order to promote the Mukaiyama-aldol reaction, the metal-organic framework not only moderately reduces the reaction barrier but it also prevents a polymerization of the formaldehyde reagent.

#### REFERENCES

- Choomwattana, S.; Muihom, T.; Khongpracha, P.; Probst, M.; Limtrakul, J. *J. Phys. Chem.* **2008**, *112*, 10855-10861.
- Sangthong, W.; Probst, M.; Limtrakul, J. *J. Mol. Struct.* **2005**, *748*, 119-127.
- Muihom, T.; Namuangruk, S.; Nanok, T.; Limtrakul, J. *J. Phys. Chem. C* **2008**, *112*, 12914-12920.
- Limtrakul, J.; Nanok, T.; Jungsuttiwong, S.; Khongpracha, P.; Truong, T. N. *Chem. Phys. Lett.* **2001**, *349*, 161-166.

S7-PO-38

### Conducting Polymer Composites of Polystyrene and Poly(3,4-ethylenedioxythiophene) Prepared by Heat-Activated Polymerization of 2,5-Dibromo-3,4-ethylenedioxythiophene

Narong Keaw-on<sup>1</sup>, Sabai Kusonsong<sup>1</sup>, Yongsak Sritana-anant<sup>2</sup>, Pitt Supaphol<sup>3</sup>, Voravee P. Hoven<sup>2\*</sup>

<sup>1</sup>Program of Petrochemistry and Polymer Science, Faculty of Science, Chulalongkorn University, Bangkok, 10330 Thailand

<sup>2</sup>Organic Synthesis Research Unit, Department of Chemistry, Faculty of Science, Chulalongkorn University, Bangkok, 10330 Thailand

<sup>3</sup>Petroleum and Petrochemical College, Chulalongkorn University, Bangkok, 10330 Thailand

\*E-mail: vipavee.p@chula.ac.th, Tel: +66-22-187627 ext 102

Conducting polymer composites containing poly(3,4-ethylenedioxythiophene) (PEDOT) was prepared by heat-activated polymerization of 2,5-dibromo-3,4-ethylenedioxythiophene (DBEDOT) in the presence of polystyrene (PS). A thin film was first fabricated by drop casting or electrospinning a solution mixture of PS and DBEDOT on solid substrates. After the solvent was removed, the solid state polymerization of the DBEDOT crystals embedded in the PS matrix was then

induced by heating to 60 – 80°C, the temperature below the glass transition temperature of PS. A dark blue composite film containing PEDOT was then formed through debromination and coupling. The percentage yield of up to 85% of the PEDOT could be obtained. The presence of PEDOT in the polymer composite was verified by FT-IR spectroscopy, UV-VIS spectroscopy, Thermogravimetric analysis, and X-ray diffraction. As measured by four-point probe conductometer, the conductivity of the PEDOT/PS composite film can reach as high as 58 S/cm. It is believed that the solid state polymerization can be a new, versatile synthetic route to conducting polymer that can be done without the use of initiators or catalysts.

#### REFERENCES

1. Meng, H.; Perepichka, D. F.; Bendikov, M.; Wudl, F.; Pan, G. Z.; Yu, W.; Dong, W.; Brown, S. *J. Am. Chem. Soc.* **2003**, *125*, 15151-15162.
2. Ouyang, J.; Chu, C.; Chen, F.; Chen, F.; Xu, Q.; Yang, Y. *Adv. Funct. Mater.* **2005**, *15*, 203-208.

S7-PO-39

#### Preparation of Reverse Micellar Particles with Hydrophilic Core from Poly(vinylalcohol)

Patsara Chinwatvanich<sup>1</sup>, Supason Wanichwecharungruang<sup>2\*</sup>

<sup>1</sup>Program of Petrochemical and Polymer science, Faculty of Science, Chulalongkorn University, Bangkok, 10330 Thailand

<sup>2</sup>Department of Chemistry, Faculty of Science, Chulalongkorn University, Bangkok, 10330 Thailand

\*E-mail: pspupason@chula.ac.th, Tel: +66-2-2187634

Poly(vinylalcohol) (PV(OH)) is a hydrophilic polymer that is biocompatible, biodegradable, non-toxic and non-carcinogenic. PV(OH) is a well-accepted pharmaceutically safe polymer for both humans and the environment and has been used in various pharmaceutical, medical, cosmetic, food, and agricultural products. In the drug delivery area, PV(OH) is widely used as a stabilizer during the preparation of micro/nanoparticles in the emulsion solvent extraction/evaporation process. In this work, fabrication of reverse micellar particles from poly(vinylalcohol) (PV(OH)) is carried out. Study is focused on the relationship between processing technique and morphology of the obtained particles. Possible applications of the obtained particles are also discussed.

#### REFERENCES

1. Luadthong, C.; Wanichwecharungruang, S. P. *Euro. Polym. J.* **2008**, *44*, 1285-1295.
2. DeMerlis, C. C.; Schoneker, D. R. *Food Chem. Toxicol.* **2003**, *41*, 319.

S7-PO-40

#### Effects of Plasticizers and Heating Methods on the Properties of Esterified Cellulose Films

Panita Hongphruk, Duangdao Aht-Ong\*

Department of Materials Science, Faculty of Science, Chulalongkorn University, Bangkok, 10330 Thailand

\*E-mail: duangdao.a@chula.ac.th, Tel: +66-2-2183539

This work aimed to investigate the effects of plasticizer and heating methods on the properties of cellulose laurate film. To overcome the intrinsic drawbacks of the cellulose materials, cellulose laurate was synthesized by using waste cotton fabrics and lauroyl chloride via esterification reaction under optimum conditions of microwave energy and conventional heating methods. However, The obtainable cellulose laurate had narrow processability and was brittle than commercial synthetic polymer. Therefore, three types of plasticizer, triethyl citrate (TEC), dibutyl phthalate (DBP) and polyethylene glycol 400 (PEG400), were used as an additive at a concentration of 5%, 10%, and 15% w/w of dry cellulose laurate. The plasticized cellulose laurate film was processed by solution casting. The effects of plasticizer (i.e., type and content) and heating methods (i.e., microwave and conventional heating) on thermal and mechanical properties of plasticized cellulose laurate films were investigated. The morphology and structure of cellulose laurate were confirmed by SEM, FTIR, and <sup>1</sup>H-NMR analysis, whereas the thermal properties were characterized by TGA and DSC. The films obtained were tested for their tensile properties, and the preliminary results showed that the plasticization resulted in an increase in flexibility and ductility of cellulose laurate film, when sufficient amounts of plasticizer were used.

#### REFERENCES

1. Ratanakamnuan, U.; Aht, O. D. *Adv. Mater. Processes.* **2007**, *26-28*, 457-460.
2. Choi, J. S.; Park, W. H. *Polym. Test.* **2004**, *23*, 455-460.
3. Park, H.; Misra, M.; Drzal, L. T.; Mohanty, A. K. *Biomacromolecules.* **2004**, *5*, 2281-2288.
4. Rahman, M.; Brazel, C. S. *Prog. Polym. Sci.* **2004**, *29*, 1223-1248.
5. Edgar, K. J.; Buchanan, C. M.; Debenham, J. S.; Rundquist, P. A.; Seiler, B. D.; Shelton, M. C.; Tindall, D. *Prog. Polym. Sci.* **2001**, *26*, 1605-1688.

B-2

**Proceedings of  
The 2<sup>nd</sup> Polymer Graduate  
Conference Of Thailand**



**Organized by : Polymer Society (Thailand)**  
Chulalongkorn University

May 21–22, 2009  
Faculty of Science  
Chulalongkorn University





## Conducting Polystyrene Fiber Mats Prepared by Electrospinning and Heat-Activated Polymerization of 2,5-Dibromo-3,4-ethylenedioxythiophene

Narong Keaw-on<sup>1</sup>, Sabai Kusonsong<sup>1</sup>, Yongsak Sritana-anant<sup>2</sup>, Pitt Supaphol<sup>3</sup> and Voravee P. Hoven<sup>2\*</sup>

<sup>1</sup>Program of Petrochemistry and Polymer Science, Faculty of Science, Chulalongkorn University,

<sup>2</sup>Organic Synthesis Research Unit, Department of Chemistry, Faculty of Science, Chulalongkorn University, <sup>3</sup>Petroleum and Petrochemical College,

Chulalongkorn University, Bangkok, 10330 Thailand.

\*Tel: +66-22-187627 ext 102, Fax: +66-2218-7598, E-mail: vipavee.p@chula.ac.th

### Abstract

Conducting polymer composites containing poly(3,4-ethylenedioxythiophene) (PEDOT) was prepared by heat-activated polymerization (HAP) of 2,5-dibromo-3,4-ethylenedioxythiophene (DBEDOT) in the presence of polystyrene (PS) matrix. A thin fiber mat was first fabricated by electrospinning a solution mixture of PS and DBEDOT on glass slides coated with interdigitated gold electrode. After the solvent was removed, the solid state polymerization of the DBEDOT crystals embedded in the PS matrix was then induced by heating at 60-80 °C, the temperature below the glass transition temperature of PS. A dark blue PS composite fiber mat containing PEDOT was then formed through debromination and coupling. The presence of PEDOT in the polymer composite was verified by FT-IR spectroscopy and X-ray diffraction. As measured by digital multimeter, the conductivity of the composite fiber mat coated on interdigitated gold electrode reached as high as 45 S/cm.

**Keywords:** PEDOT, Polystyrene, Electrospinning, Conducting polymer composite, Solid state polymerization

### 1. Introduction

Poly(3,4-ethylenedioxythiophene) (PEDOT) is one of polythiophene derivatives that has received much more attention than other polythiophene derivatives in recent years for its unique electrical properties. It combines a low oxidation potential and moderate band gap with good stability in the oxidized state. In addition to a high conductivity (500 S/cm in the electrochemical doped state) [1], PEDOT is found to be highly transparent in thin, oxidized films. As a result, PEDOT derivatives are now

utilized in several industrial applications including antistatic coatings for photographic films [2] and hole conducting material in organic/polymer-based light-emitting diodes [3].

PEDOT is commercially available in the form of latex of which dispersion in aqueous is facilitated by negatively charged poly(styrene sulfonate) which also acts as a dopant [4,5]. The PEDOT synthesis is conventionally confined to chemical or electrochemical oxidation of polymer solution. As a consequence, defect sites and a relatively low degree of intermolecular order limit the number of possible applications. Until

recently, it has been discovered by chance that blue-black crystals of 2,5-dibromo-3,4-ethylenedioxythiophene (DBEDOT) can undergo solid state polymerization (SSP) through debromination and coupling. Without the use of initiators or catalysts, SSP could give rise to a nearly defect-free and highly ordered bromine-doped PEDOT with high conductivity (20-80 S/cm) [6, 7].

Taking advantages of DBEDOT solubility in many common organic solvents together with its competency of undergoing SSP, we have recently demonstrated that highly conductive polymer composites containing PEDOT can be obtained by SSP of DBEDOT embedded in a preformed insulating polymer matrix (i.e. PS, PB) film after appropriate thermal treatment [8]. Nonetheless, the fabrication process based on solution casting previously employed yielded the composite films with non-uniform conductivity due to the inhomogeneous distribution of the PEDOT in the matrix caused by phase incompatibility between the polar PEDOT and the non-polar matrix. Herein, we propose to use electrospinning as an alternative fabrication method. The rapid solvent evaporation and solidification of the fiber mat electrospun from the mixed solution between the desired matrix (PS) and DBEDOT should not allow enough time for the DBEDOT to phase separate from the matrix and yield thin conductive composite fiber mat with improved PEDOT distribution and conductivity after the heat treatment.

## 2. Experimental

Polystyrene (PS) ( $M_w \approx 300,000$  Daltons) pellets of a general purpose grade were supplied by Dow Chemical. 3,4-ethylenedioxythiophene (EDOT) and N-Bromosuccinimide (NBS) were

purchased from Sigma-Aldrich. 2,5-dibromo-3,4-ethylenedioxythiophene (DBEDOT) was synthesized by bromination of EDOT using NBS [8].

### 2.1 Electrospinning

A mixed solution of PS and DBEDOT was prepared at ambient temperature by dissolving 0.2 g PS in 2 mL dimethylformamide (DMF) overnight followed by an addition of 0.6 g DBEDOT and then sonicated in an ultrasonic bath for 15 min. Fiber mats were fabricated by electrospinning the mixed solution at ambient temperature using a driving voltage of 20 kV. A blunt 20-gauge stainless steel hypodermic needle (OD = 0.91 mm) used as a nozzle was connected with the positive electrode. A grounded metal screen covered by a glass slide, coated with interdigitated electrode (Figure 1) was used as the counter electrode and was placed 10 cm away from the tip of the needle. After continuous spinning for 30 min, the thickness of the obtained fiber mat was about 6.7  $\mu\text{m}$ , as determined by a profilometer (Dektak<sup>3H</sup> Thailand).



Figure 1. Configuration of interdigitated electrode.

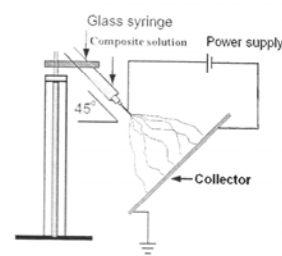
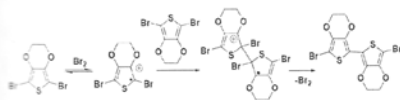


Figure 2. Schematic representation of electrospinning apparatus set-up.

### 2.2 Heat-activated Polymerization

The thin fiber mat of PS containing DBEDOT on the glass slide coated with the interdigitated electrode obtained from 2.1 was put in a closed vial and then heated in an oven to induce polymerization of DBEDOT into PEDOT (Figure 3). The resulting PEDOT/polymer composite fiber mat was then characterized by scanning electron microscope (SEM), FT-IR spectroscopy (Nicolet Impact410), and x-ray diffractometer (Rigaku D5000). Resistivity of the PEDOT/PS composite fiber mat was determined by a Keithley digital multimeter.



**Figure 3.** Mechanism of heat-activated polymerization.

### 3. Results and discussion

DMF was chosen as the solvent for fabrication because it can completely dissolve both PS and DBEDOT. The lowest concentration of PS in DMF that can generate almost bead-free fiber mat by electrospinning was 10 %w/v (Figure 4(a)).

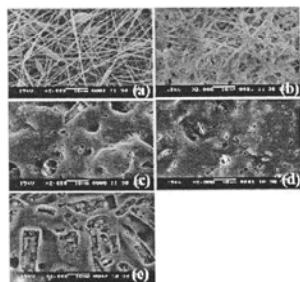


**Figure 4.** SEM images of electrospun fiber mat: pure PS (a), PS and DBEDOT (b), and PS/PEDOT composite obtained after heat treatment at 60 °C(c), 70 °C (d), 80 °C (e).

The fiber mat obtained from electrospinning the mixed solution of PS and DBEDOT (Figure 4(b)) was apparently less defined than that of the pure PS. Upon the heat treatment, the mats completely lost the fibrous feature as visualized from SEM images shown in Figure 4(c-e). As determined by the digital multimeter, the conductivity of the PEDOT/PS composite fiber mat obtained after the HAP at 80°C was greater than that obtained at the 60 and 70°C indicating the more efficient polymerization was achieved at higher temperature. The conductivity can be much improved if the pressing of the fiber mat (Figure 5) was applied during the HAP. The conductivity was raised to 45 S/cm. This value is 4 orders of magnitude higher and quite comparable to that was previously reported on the spin-cast PEDOT/PS film [8].

**Table 1.** Conductivity of PEDOT/PS fiber mats as a function of temperature using in the step of HAP

Temperature (°C)	Conductivity (S/cm)
60	$5.0 \times 10^{-6}$
70	$2.3 \times 10^{-3}$
80	$6.1 \times 10^{-3}$

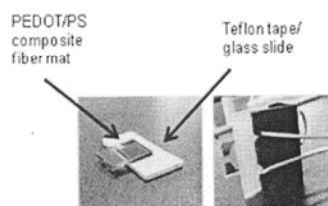


**Figure 5.** PEDOT/PS fiber mat on glass slide coated with interdigitated electrode is pressed against a glass slide covered with Teflon tape by a paper clip.

FT-IR spectroscopy was used to confirm the success of heat-activated polymerization of

DBEDOT in the composite fiber mats. FT-IR spectra of “controlled PEDOT”, which is the PEDOT prepared by a direct heating of DBEDOT crystals in the absence of the PS matrix and “extracted PEDOT”, which is the PEDOT extracted from the PEDOT/PS composite fiber mat are displayed in Figure 6. The fact that the FT-IR spectrum of the extracted PEDOT exhibits the same fingerprints as those of the controlled PEDOT confirms the success of HAP in the PS matrix. The peaks at 1511 and 1410  $\text{cm}^{-1}$  originate from the asymmetric and symmetric stretching of C=C, respectively. The peak at 901  $\text{cm}^{-1}$  (C-H bending) corresponds to the ethylenedioxy ring deformation. The peaks at 1080 and 746  $\text{cm}^{-1}$  are assigned to the C–O stretching and C–S bending, respectively.

According to Figure 7, XRD patterns of the extracted PEDOT is broader than the controlled PEDOT suggesting that the structure of the controlled PEDOT is more ordered and its crystallinity is higher in comparison with the extracted PEDOT.

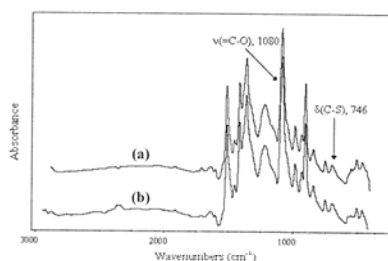


**Figure 6.** FT-IR spectra of (a) controlled PEDOT and (b) extracted PEDOT.

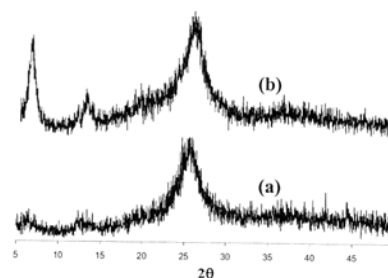


**Figure 7.** XRD patterns of (a) controlled PEDOT and (b) extracted PEDOT.

#### 4. Conclusion

Conductive PEDOT/PS composite fiber mats were successfully prepared through a combination of electrospinning and heat-activated polymerization of DBEDOT in the PS matrix. The pressing of the DBEDOT/PS fiber mat during the heat treatment was found necessary to yield the composite fiber mat with high conductivity.

#### Acknowledgements

This research is supported financially by Science and Technology Research Grant from the Thailand Toray Science Foundation. NK acknowledges a graduate scholarship from the Center for Petroleum, Petrochemicals, and Advanced Materials, Chulalongkorn University.

#### References

- [1] Aasmundtveit, K. E., Samuelsen, E. J., Inganas, O., Pettersson, L. A. A., Johansson, T. B. and Ferrer, S., *Synth. Met.* **113**, 93, (2000).
- [2] Jonas, F. and Morrison, J.T., *Synth. Met.* **85**, 1397, (1997).
- [3] Burroughs, J. H., Bradley, D. D. C., Brown, A. R., Marks, R. N., Mackay, K., Friend, R. H., Burns, P. L. and Holmes, A. B., *Letters to Nature.* **347**, 539, (1990).

- [4] Groenendaal, L., Jonas, F., Freitag, D., Pielartzik, H. and Reynolds, J., *Adv. Mater.* **12**, 481, (2000).
- [5] Jonas F. and Schrader, L., *Synth. Met.* **41**, 831, (1991).
- [6] Meng, H., Perepichka, D. F. and Wudl, F., *Angew. Chem. Int. Ed.* **42**, 658, (2003).
- [7] Meng, H., Perepichka, D. F., Bendikov, M., Wudl, F., Pan, G. Z.; Yu, W., Dong, W. and Brown, S., *J. Am. Chem. Soc.* **125**, 15151, (2003).
- [8] Kusonsong, S., Preparation of Conducting Polymer Composites by Solid State Polymerization of 2,5-Dibromo-3,4-ethylenedioxythiophene, Master's thesis, Petrochemistry and Polymer Science, Chulalongkorn University, 2007.

## VITAE

Mr. Narong Keaw-on was born on May 21, 1984 in Saraburi, Thailand. He received a bachelor degree of Science from Department of Chemistry, Faculty of Science, Ramkhamhang University, Bangkok, Thailand in 2006. He was admitted to a Master's Degree Program of Petrochemistry and Polymer Science, Faculty of Science, Chulalongkorn University and completed the program in 2009. His address is 8/1 Moo 5, Tambol Phucare, Amphor Chaloemphrakiat, Saraburi 18240.

### **Presentation in Conference:**

- |              |   |
|--------------|---|
| January 2009 | Pure and Applied Chemistry International Conference 2009, Faculty of Science, Naresuan University, Phitsanulok, Thailand.     |
| May 2009     | The 2 <sup>nd</sup> Polymer Graduate Conference of Thailand, Faculty of Science, Chulalongkorn University, Bangkok, Thailand. |